TÉCNICO LISBOA

Development of a nonlinear model predictive control application

Implementation on a Paracetamol Batch Crystallization Process

Mariana Isabel Pereira Monteiro

Thesis to obtain the Master of Science Degree in

Chemical Engineering

Advisor(s)/Supervisor(s): Prof. Dr. Carla Isabel Costa Pinheiro
Dr. Frances Elizabeth Pereira

Examination Committee

Chairperson: Prof. Dr. Sebastião Manuel Tavares da Silva Alves
Advisor: Prof. Dr. Carla Isabel Costa Pinheiro
Member of the Committee: Prof. Dr. Rui Manuel Gouveia Filipe

October 2019

Acknowledgments

I would first like to express my gratitude to Dr. Frances Pereira, not only for her guidance, but also for always making me feel part of the team. A warm thanks goes to Maria and the rest of the gDAP group, for always providing me with feedback whenever I needed. I would also like to thank Dr. Costas Pantelides for giving me the opportunity to work and learn at PSE, it was truly an amazing experience. My sincere thanks to Prof. Carla Pinheiro for her constant help and good advice throughout my thesis.

A very special thanks to all the portuguese folks down in London, for having welcomed me into their group without a blink. A special mention to Isabel and Gonçalo, who I shared my house with, they were my home away from home.

Por fim, agradeço aos meus pais e ao meu irmão, por toda a paciência, não só durante estes 6 meses mas desde sempre. Obrigada por me motivarem a fazer sempre melhor. Um obrigado especial ao Pedro por ter sempre acreditado em mim.

Abstract

This thesis presents the implementation of a Nonlinear Model Predictive Control application on a paracetamol batch crystallization process. This control strategy uses the mathematical model of the process and takes advantage of its current measurements to predict the future behaviour of some chosen Controlled Variables. The controller does this by performing an optimisation routine that minimizes the difference between the current value of the Controlled Variables and their target interval of values. In this thesis, the optimisation is described by a penalty-based objective function, in which penalties are added whenever the Controlled Variables are outside their target interval of values.

The controller was tested on a digital twin of the model, which is the real-time implementation of the controller on the process. The testing consisted in submitting the controller to different scenarios to verify whether it was able to steer the Controlled Variables into their target limits, thus, achieving their control objectives. Tested scenarios included disturbance rejection (changing Disturbance Variable impeller frequency), noise measurement (adding noise to one of the measured variables, span) and plant / model mismatch (altering one of the kinetic parameters, supersaturation order) . The controller was able to successfully steer the Controlled Variables for most cases, yielding faster results than in open-loop mode. Reaching control objectives faster than in open-loops proves to be an advantage as it can translate in ending a batch sooner, thus saving time.

Overall, the controller yielded quite satisfactory results, showing a promising future for this less commonly used control strategy.

Keywords: Nonlinear Model Predictive Control, Batch Crystallization, Digital Twin, Optimization

Resumo

A presente tese descreve a implementação de uma aplicação de controlo não-linear preditiva num modelo batch de cristalização de paracetamol. Esta estratégia de controlo consiste em usar o modelo matemático de um sistema e as suas medidas atuais para prever o trajeto futuro das suas variáveis controladas. O controlador prevê o trajeto futuro através de uma rotina de optimização, ao minimizar a diferença entre o valor atual das suas variáveis controladas e o intervalo de valores desejado para as mesmas.

O controlador foi testado num *digital-twin* do modelo, que consiste na implementação em tempo real do controlador no processo. Os testes consistiram em submeter diferentes cenários ao controlador de modo a verificar se este era ou não capaz de dirigir as variáveis controladas para os intervalos desejados, satisfazendo, assim, os objetivos de controlo. Cenários incluíram rejeição de perturbações (mudança o valor da variável de perturbação, frequência do rotor), ruído (adição de ruído a uma das variáveis medidas) e a não correspondência do modelo com a realidade (alteração de um parâmetro cinético, ordem de supersaturação). O controlador foi capaz de guiar as variáveis controladas para os seus limites desejados para a maior parte dos casos testados, obtendo, também, trajectórias mais rápidas que em cadeia aberta. Cumprir os objectivos de controlo mais rapidamente é uma vantagem dado que pode traduzir em operações batch mais breves, poupando assim tempo.

De um modo geral, o controlador apresentou resultados satisfatórios, mostrando a hipótese de um futuro promissor para esta estratégia de controlo menos implementada industrialmente.

Keywords: Controlo Não-Linear Preditivo, Cristalização Batch, Digital-twin, Optimização

Contents

List of Tables

List of Figures

Acronyms

CV Controlled Variable. iii, ix, xi, xii, 1, 3–6, 12, 13, 16, 22–34, 36, 37, 39–46, 49–60, 62–65, 67–69

DV Disturbance Variable. iii, 4, 16, 23, 29, 33, 35, 37, 41, 54, 68

gNLMPC gPROMS Nonlinear Model Predictive Controller. xi, 15–17, 36, 42, 43, 67, 68

MPC Model Predictive Control. 1, 3, 4

MV Manipulated Variable. ix, xi, xii, 1, 3, 4, 12, 13, 16, 17, 22, 25–37, 40, 42, 44, 46–48, 50–55, 57–64, 67–69

NMPC Nonlinear Model Predictive Control. iii, xi, 1, 2, 4, 5, 7, 11–13, 17, 19, 25, 67–69

PSE Process Systems Enterprise. 15

Chapter 1

Introduction

Model Predictive Control (MPC) is an important advanced control strategy developed in the 1970s, that has been growing in use ever since [1]. This usage increase lays on its ability to handle complex multi-variable systems, with multiple inputs and outputs. This strategy is based on the system's mathematical model and takes advantage of its current measurements to predict its future behaviour. It does so by performing an optimisation routine, which consists in minimising the difference between the current values of the Controlled Variables (CV) and the target ones [1,2]. This optimisation is described by an objective function that not only includes the process' measurements, but also its constraints. The result of this routine is the optimal control action that will lead to the CVs to their desired value. This control action takes form of a Manipulated Variable (MV) input.

When the model can be described linearly, linear MPC shows positive results, in both the refining and the chemicals area [3,4]. Nonetheless, it does not yield satisfactory results when the process is very nonlinear. To address this problem, Nonlinear Model Predictive Control (NMPC) has started to grow.

Nonlinear Model Predictive Control is based on the same concept as its linear counterpart. However, it has a higher degree of complexity since the optimisation problem is nonlinear, which is what prevents it from being more commonly used in industry [2,5]. Despite the challenge, there are some processes, in both polymerization and crystallization fields, which simply cannot be linearized, and, as such, linear MPC cannot be used [6–10]. For them, NMPC may be a suitable alternative.

1.1 Motivation

Implementing a NMPC strategy is rather burdensome [11], thus, only complex processes will benefit from such a difficult approach. Crystallization may just be one of those cases. Crystallization is a very common practice in the pharmaceutical industry as a separation and purification process. It is characterized by its high degree of nonlinearities given that crystals suffer very complex mechanisms, such as nucleation, agglomeration and growth. Furthermore, a lack of correct measurements in real time prevents these processes from being well controlled by more traditional approaches. It is not possible to measure properties like crystal mass and dispersity frequently throughout an operation, as sensors are still not sophisticated enough to do so. Hence, in this thesis, a Nonlinear Model Predictive Control strategy was implemented on a paracetamol batch crystallization model.

1.2 Thesis Outline

In chapter 2, a literature review on NMPC, its formulation and current applications is presented. Additionally, some basic crystallisation concepts and control schemes typically applied to crystallisation processes are described. Chapter 3 describes the modelling and simulation tools used for this work. In chapter 4, a description of the crystallisation model used is presented. It also lays out how the control scheme was designed. In chapter 5, the optimisation problem is explained, as well as how the system responds to an optimal control formulation. Chapter 6 describes the concept of emulation and how it was created. It also includes how the emulation was tested. In chapter 7 the system's responses to a set of tests are presented. In the last chapter, some conclusions and future suggestions of this work are stated.

Chapter 2

Literature Review

MPC is an advanced process control technique which consists in using the mathematical model of the system and its current measurements to calculate the optimal control action that satisfies the system's control objectives [1]. These control objectives are defined as certain setpoints for specific variables, called CVs. The controller compares the current values of the CVs and the actual ones, and optimizes what control action will minimize this difference [12]. That control action is implemented in the form of MVs setpoints. This strategy is said to be "predictive" as the controller decides the control action to implement, based on the predicted behaviour of the CVs. The concept behind this strategy is described by the following figure:

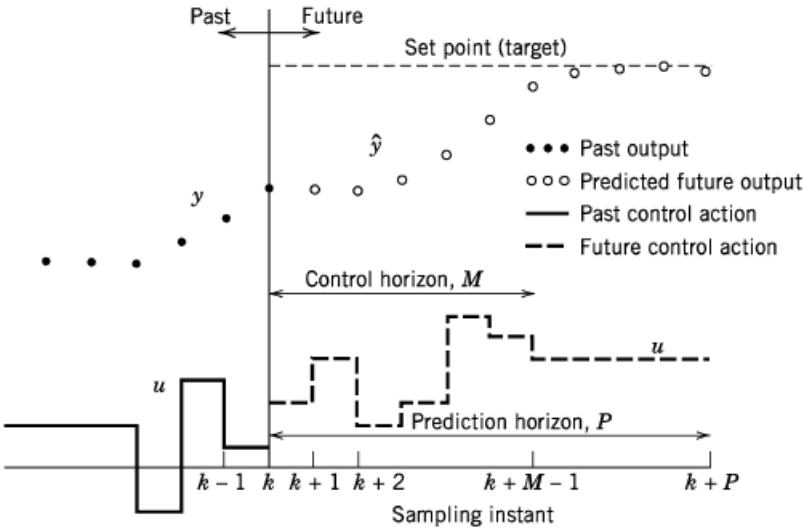

Figure 2.1: Model Predictive Control Concept [1]

y represents the past measurements of the CVs, and ŷ the predicted measurements by the controller. The target set point refers to the CVs' desired value. The past control action line u represents the past control action that has been implemented by the controller, and the dashed line u the future control action to be implemented. Different MVs set points will be given, over a control or optimisation horizon, M. The MVs will remain constant until the end of the prediction horizon, P, since the CVs have reached their desired value.

Ideally, the controller would be able to predict the exact behaviour of the CVs, after having implemented a certain control action. However, in reality, due to plant / model mismatch and to unmeasured disturbances, the predicted measurements are not equal to the actual ones [1, 13]. This

mismatch may be due to sensor/actuator delays or misreadings. To tackle this problem, the controller operates in feedback cycles. After a certain period of time, the controller takes new measurements and compares the measurements of the CVs with the values it had predicted. As they do not match, the controller performs a new optimisation to take into account this new value, and corrects what it had implemented. Hence, in practice, only the first element of the optimal control sequence is applied to the system, before the calculation sequence restarts: this strategy is called the receding horizon control, and it is very advantageous as it takes into account the most recent measurements of the state [1, 14]. For variables whose measurement is not possible frequently, state estimation calculations are used.

Both the control and the prediction horizon must be carefully chosen as they influence the controller's response. The longer they are, the more time the controller has to steer its CVs into the desired setpoints. On the other hand, the shorter the horizons, the less time the controller has to satisfy its control objectives - the more abrupt the control action must be. The duration of the cycle is also an important matter as each cycle each control move should be long enough to include relevant system's dynamics, but not so long as to miss some [12].

There are three difference types of variables: MVs, CVs and Disturbance Variables (DVs). MVs are the process variables which are allowed to be adjusted, in order to achieve the desired CV values. CVs are the process outputs, and the desired value for them is called target setpoint. The last type of variable is DV, which are variables that affect CVs, but unlike MVs, they cannot be adjusted [1].

Linear MPC is widely used in several industries since the 1970's, most of which in the refining and chemicals area [3], and it is now considered a mature technology [4]. Some of the reasons for this success include the fact that MPC allows for direct implementation of the model in the control calculation, taking into account the process input, state and output constraints [2]. Nonetheless, in processes whose model may not be well described in a linear form, linear MPC fails to achieve satisfactory results. Hence, NMPC has began to gain some attention.

2.1 Nonlinear Model Predictive Control

In NMPC, the predicted state of the system is expressed by a nonlinear function, resulting in a nonlinear optimization problem, regardless of whether the cost function is linear, quadratic or non-quadratic. This control strategy has failed to grow industrially when compared with its linear counterpart due to computational challenges, given by the non-convexity of the optimization problem [2, 5]. Furthermore, NMPC is perceived as "by far the most complex application of process models" [11]. In spite of its complexity, since the 1990's, there has been an increase in NMPC industrial applications [2], mainly in the polymers field [6–10].

2.1.1 Formulation

A general scheme of a NMPC controller is shown in figure 2.2.

The NMPC action represented in figure 2.2 can be described in the following steps, which will be described in detail in the next sections:

1. Obtain plant measurements y
2. Estimate states of the system for immeasurable variables x'
3. Calculate optimal control input
4. Implement the optimal trajectory for the first control interval u
5. Restart step 1

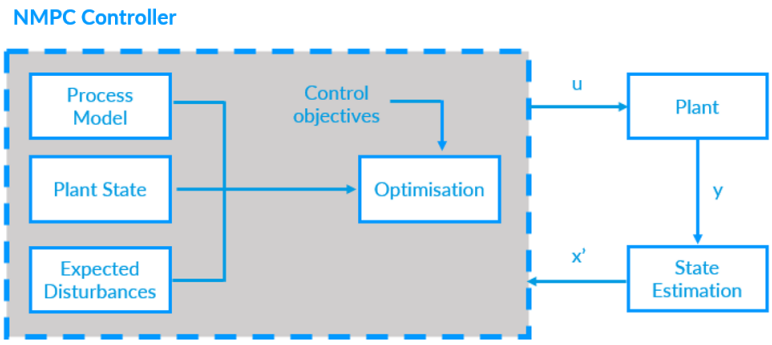

Figure 2.2: General scheme for a NMPC controller

Plant Model

The model of the system can have various forms, nonetheless, it is usually expressed by a nonlinear continuous time differential equation as follows ([3], [2], [15] and [5]):

$$\dot{x}(t) = f(x(t), u(t)), \tag{2.1}$$

And an algebraic output equation:

$$y(t) = g(x(t), u(t)), \tag{2.2}$$

Subject to a set of input and state constraints:

$$U := \{u \in \mathbb{R}^m \mid u_{min} \leq u \leq u_{max}\} \tag{2.3a}$$

$$X := \{x \in \mathbb{R}^m \mid x_{min} \leq x \leq x_{max}\} \tag{2.3b}$$

$$\tag{2.3c}$$

In which x(t) and u(t) refer to state and input vectors at time t, respectively and f and g are continuous time functions. u_{min}, u_{max}, x_{min} and x_{max} represent the constraint vectors for the input and state, respectively.

Optimal Control Problem

As it was explained in the beginning of this chapter, in order to reach its control objectives, the controller performs an optimisation to calculate which control action is able to steer the CVs into their target set points. This optimal control problem is usually expressed by a cost function, typically represented by an expression of the following form [14–17]:

$$\min_{u(t)} \int_{t_k}^{t_{k+n_p}} J(u(t), x(t))dt + J_f(u(t_{k+n_p}), x(t_{k+n_p})) \tag{2.4}$$

Subject to the following set of constraints:

$$\dot{x}(t) = f(x(t), u(t)) \tag{2.5}$$

$$x(t_k) = x_k \tag{2.6}$$

$$y(t) = g(x(t), u(t)) \tag{2.7}$$

$$\underline{u}(t) \leq u(t) \leq \bar{u}(t) \tag{2.8}$$

$$\Delta u_{min} < \Delta u(t) < \Delta u_{max} \tag{2.9}$$

$$\Delta y_{min} < \Delta y(t) < \Delta y_{max} \tag{2.10}$$

$$other\ constraints \tag{2.11}$$

Where equation 2.5 refers to the predicted future input $\dot{x}(t)$, as a function of the past output x(t) and past control moves u(t). Equation 2.6 refers to the system state at time k. Equation 2.7 refers to controller output, which is also a function of the past output x(t) and past control moves u(t) and equation 2.8 refers to the input control constraints. Equations 2.9 and 2.10 denote penalties on the value changes of the variables, usually to account for actuator and system's delays.

As the optimal control problem is non-convex, it is possible to have multiple minima, making the task of finding the optimal solution more burdensome. Hence, many formulations include all the states, instead of just the process outputs [18].

Parametrization

Despite being depicted as a continuous function of time in 2.1, the open-loop is often subjected to parameterization methods, by turning an infinite dimensional problem into a finite dimensional one [15], to allow for a solution. The most commonly implemented strategies are the following:

- Sequential approach: Model simulation and optimisation are performed sequentially. The system's ordinary differential equations are solved numerically in the simulation first, eliminating the constraints and cost functions, at each iteration [14]. In spite of being more straightforward than the remaining strategies, this strategy has a higher computational burden [18].

- Simultaneous approach: Model simulation and optimisation are performed simultaneously. The ODEs are discretized in time and embedded in the optimisation problem as constraints. Although this approach increases the number of constraint variables, the computational burden is lower as it is easier to implement the constraints in the cost function [18].

- Direct multiple shooting approach: The optimisation horizon is divided into intervals and the ordinary differential equations of the model and the cost function are solved and optimised independently for each interval [14, 15]. This method provides a better structure for the optimisation. However, it also increases the computational burden as there is a need to create new sets of constraints to ensure continuity between subintervals.

2.1.2 Controller Stability

Stability is of high importance in MPC formulation. In control, stability refers to whether the CVs are under control or not. In linear MPC, setting an infinite prediction horizon is usually the most practical choice with guaranteed stability [1, 12]. Nonetheless, for nonlinear problems it is almost impossible to obtain a solution using an infinite horizon, due to computational reasons, hence, it is only perceived by authors as a theoretical concept [3, 15, 19] .The strategies that have been employed to address

this problem are not yet fully developed as they do not guarantee closed-loop stability [15]. The most common strategies used are:

- Infinite horizon: Setting the prediction horizon to infinity.
- Finite horizon: Adding a penalty to the cost function so that the system is forced to reach its initial state at the end of the prediction horizon (*zero terminal equality constraint*) [3]. This is called a *stability constraint* as it has no physical meaning and it is not applicable to all systems: just the ones that have a solution at initial point t=0 [15].
- Quasi-infinite horizon: Similarly to the finite horizon strategy, this approach employs a terminal state penalty. However, the penalty is quadratic [3]. Additionally, a terminal inequality regional constraint is included to ensure that the final state reaches a certain area that approximates an infinite horizon, instead of a fixed point [15].

The main challenge when it comes to stability is to establish a reasonable horizon length without compromising performance and stability.

2.1.3 Controller Robustness

A robust NMPC formulation is one where the model used for prediction is the same as the actual system [3, 15], meaning that there is no plant/model mismatch, which is not true for real systems. Some strategies to increase NMPC robustness have been tested, such as:

- Min-max problem: Formulating the cost function to be able to bear the worst case scenario [15]. Quite a conservative option and unreliable as it does not guarantee that the controller will perform well in more likely and less conservative scenarios.
- Constraint tightening: Enlargement of state constraints directly in the cost function, often referred as a *contraction stability constraint* [3]. This will increase the penalties' weight in the objective function.
- Optimising the input from a feedback controller between samples: this option requires the implementation of a feedback controller that handles minor disturbances, between sampling time, thus decreasing some computational burden from the NMPC controller.

2.2 Current NMPC applications

There are some processes for which nonlinear model predictive control seems attractive. Some characteristics of such processes include batch reactors, frequent product requirements changes, infrequent measurements of product quality and raw-material composition fluctuations [3, 11].

The main industrial applications of NMPC are in the polymerization sector [6, 8, 9, 20–22]. Polymers have highly nonlinear dynamics, specially in the interactive reactions between the chains. Moreover, the lack of quality measurements, due to sampling problems, large dead times and high noise level also motivates the use of a model that makes use of state estimation features. Finally, given the existence of unmeasurable properties such as the chain length distribution and the average molecular mass, there is no possible way to have output measurements at every sampling intervals.

Not as developed as the polymers processes, but still with a growing implementation at research level, is the crystallization sector [23–27]. Similarly to polymers, crystals have quite complex mechanisms such as agglomeration, growth and nucleation, with kinetics that are not easily modelled.

Likewise, crystals have immeasurable properties in real time, namely the crystal mass and the fine size distribution. In addition to that, factors like sensor limitations in taking reliable measurements and inherent process uncertainties [28, 29] all provide suitable reasons to implement a nonlinear advanced control strategy.

2.3 Crystallization

Crystallization is a very common practice in the pharmaceutical industry as a separation and purification process [23].

2.3.1 Basic Crystallization Concepts

Crystallization is a very common practice in the pharmaceutical industry as a separation and purification process [23]. Its driving force lays on the difference between the chemical potential of the supersaturated solution and the solid crystal phase [23, 28, 30].

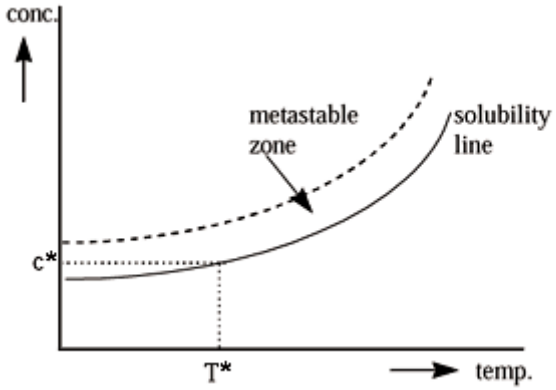

Figure 2.3: Solubility diagram [31]

Figure 2.3 shows the solubility curve for a typical API (Active Pharmaceutical Ingredient) [32]. Below the curve, it is said that the system is under saturated, as its concentration is lower than its solubility. In this case, crystals will dissolve [17]. Above the curve, the system is said to be supersaturated, given its concentration is higher than the equilibrium one. In between these two regions (solubility and dashed curves) lays the ”metastable zone”, where already formed crystals can grow, but it is quite unlikely to form new ones [17, 33]. In this area, the system is already supersaturated, but it is not yet able to respond to spontaneous nucleation [34]. Supersaturation can be induced by the following mechanisms [23, 28, 35–37]:

- Cooling
- Anti-solvent addition
- Evaporation
- pH change (acid or base addition)

Cooling allows the system to reach supersaturation, maintaining the same concentration - this is clear in figure 2.3. Although it is only efficient to use when the solubility of the compound greatly decreases with temperature [38, 39]. Adding anti-solvent reduces the solubility of the compound,

making it easier to reach supersaturation. Furthermore, anti-solvent addition has been claimed as the most efficient strategy to reach supersaturation as it is quicker and able to run at low temperatures [39, 40]. Solvent evaporation is used when the solubility curve is quite flat, making it unfeasible to achieve supersaturation by cooling [38], despite being a less common alternative [41]. Lastly, another method to induce supersaturation is by pH change, an option used in protein crystallization [42].

After reaching supersaturation, the solid phase can be created in either two mechanisms: primary or secondary nucleation. The first, also defined as "spontaneous" nucleation, can be homogeneous, if crystals nucleate due to high levels of supersaturation alone or heterogeneous, if the presence of insoluble impurities enables said nucleation [17, 33]. The latter, more common in industrial practice [23,33], occurs when suspended crystals of solute are present. It can occur by several mechanisms such as attrition, surface or dendritic breeding [17], the first of them being the most common industrially [43]. Secondary nucleation is commonly defined in mathematical terms empirically by the following Arrhenius-type expression [17]:

$$J_{sec} = k_b \, exp(-E_b/T) \, S^b \, \mu_k^j \tag{2.12}$$

Where k_b is the pre-expontential term, b the supersaturation order, E_b the activation energy and j a constant - all empirical constants. μ_k is the k^{th} moment of the crystal size distribution and S the relative supersaturation, defined as:

$$S = \frac{C - C_{sat}}{C_{sat}} \tag{2.13}$$

In which C represents the solute concentration and C_{sat} the saturated solute concentration. After having nucleated, the crystals can either grow and agglomerate or dissolve. The most accepted mechanism regarding growth argues that crystals grow at a rate proportional to the concentration difference between the solution bulk and deposition point [33, 43]. Mathematically, this mechanism can be expressed by the following empirical expression [44, 45] :

$$G = k_1 \, exp(-\frac{k_2}{T}) \, (C - C_{sat})^{k_3} \tag{2.14}$$

Where k_1 is the growth rate constant, k_2 the activation energy and k_3 the supersaturation dependency of the surface integration rate - all empiric parameters.

Usually, it is preferable for the crystals to grow in the metastable region, as it ensures proper growth, avoiding unwanted impurities, liquid inclusion and higher attrition rates [44, 46]. Operating in this region is the compromise between unrestrained nucleation , where new nuclei can be form, and longer batch times.

If a crystal in a solution displays a solubility value below its concentration in solution, it will dissolve. Dissolution may also be seen as a pure diffusion mechanism, and if so, in equilibrium, its rate would be the same as crystal growth [43]. Nonetheless, in reality, crystals dissolve faster than they grow, given that different faces of the crystal grow at different rates. Although for purpose of simplicity , authors usually describe dissolution rate as the opposite of growth rate [17, 44].

Another typical mechanism in this process is agglomeration which can be defined as the collision and subsequent bound between two particles. Particle size affects the type of collision, which in turn will affect the kinetics. Generally, agglomeration rate can be described as [34]:

$$-A = \alpha \, \beta \, N^2 \tag{2.15}$$

Where α is the collision efficiency, β is a particle-size dependent parameter and N is the particle density.

Some authors choose to neglect this mechanism, due to its complexity [17, 32, 36, 44].

The above mentioned mechanisms result in a population balance model that is usually solved by the method of moments [45].

2.3.2 Crystals Specifications

Achieving the desired crystal properties is of high importance, in industry. The most often used method is by their crystal size distribution, which can be expressed as a function of their number, mass or volume, and by means of a density or cumulative distribution, depicted in the following figure [47]:

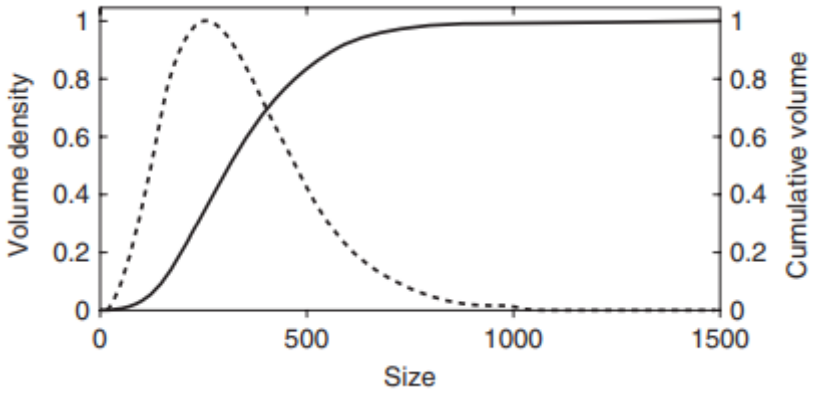

Figure 2.4: Density (dotted line) and cumulative (continuous line) volume crystal size distribution [47]

The distribution can divided into moments, which are useful to define some of its properties such as:

- Mean
- Median
- Mode
- Width

The mean is usually defined as either arithmetic ($D_{1,0}$), volume over surface ($D_{3,2}$) or diameter over volume ($D_{4,3}$), in which the indexes refer to the moment of the distribution [47]. For example, the diameter over volume is obtained by:

$$D_{4,3} = \frac{m_4}{m_3} \tag{2.16}$$

The median is simply the value at which half the population has size above and the other half below, and it is often designated as D_{50}. The mode is the highest peak of the distribution. Lastly, the width can be described by its span or its coefficient of variation, expressed as:

$$Span = \frac{L_9 - L_1}{L_9} \tag{2.17}$$

$$CV = \sqrt{\frac{m_3\, m_5}{m_3^2} - 1} \tag{2.18}$$

These properties are used to characterize the obtained crystals, and to define the objectives of the crystallization, essential to the control scheme definition. Quality wise, crystals with large mean size and narrow particle size distribution are the desired goal of most crystallization procedures [29].

2.3.3 Crystallization Process Control

Crystallization operations can be operated in either continuous or batch mode. Continuous crystallizers are often used in large scale operations [45]. Moreover, they are easier to control and provide advantages such quality consistency and process efficiency [36, 48, 49] which results in economic benefits [50]. On the other hand, batch crystallizers, widely used, have been the preferred option for small operations, as they confer flexibility in terms of volume [45, 51]. Nonetheless, the main drawback of this mode is the variability from batch-to-batch in product requirements, a subject worthy of attention by several authors [25, 51–53].

As it has been mentioned before, crystallization processes are difficult to control [17, 29], as the present dynamics are quite complex. Common approaches to control crystallization mechanisms include temperature and or concentration or supersaturation control [17, 29, 46, 52], which comprises in measuring these two variables at each time step, and using feedback control to ensure that the solution is maintained within the metastable region [35]. This strategy is often unfeasible as it is not always possible to take frequent measurements, due to sampling problems, or large dead times or high noise level. Usually, new measurements are not fast enough to go along with the system's dynamics. Hence, nonlinear model predictive control has started to gather some attention.

Since the desirable product consists of crystals with large mean size and narrow particle size distribution [29], objective functions typically include mean size of product crystals, its ratio deviation, the nucleated crystal mass to seed crystal mass at the end of the operation ratio, number-average crystal size, coefficient of variation, weight-mean crystal size and the particle size distribution shape [17, 25, 28, 35, 52]. In these cases, the controlled variables are often the seed mass, the mean size of seed crystals, the width of the particle size distribution, solution concentration and temperature. The manipulated variables usually include anti-solvent addition, heat input, temperature and evaporation rate [17, 35, 52]. In terms of constraints, the most commonly used are [35]:

- Temperature rate of change
- Cooling rate
- Maximum crystal volume
- Rate of anti-solvent addition
- Solution concentration at the end of the batch

Another example of a nonlinear control application available in literature is the control of the batch polymorphic transformation of L-glutamic acid [17]. The author used the Unscented Kalman Filter for the state estimation. He defined the optimal control problem comprising two objectives: maximization of crystals' yield and minimization of the ratio between nucleated crystals and crystal seeds. The objective function also includes an inequality constraint in the batch time and yield and an end-point constraint on concentration. The available measurements were solute and crystal concentrations, first and second order moments of both crystals and solution temperature. Concentration and temperature were considered manipulated variables and kinetic parameters disturbances. For the state estimation, Unscented Kalman Filter was used. In this work, NMPC yielded desirable results, as it satisfied control constraints, within the batch time specified [17].

Another example includes a hierarchical control structure embracing a lower-level with a super saturation control approach and a higher-level model-optimisation [52]. The objective function was minimizing the desired crystal size distribution shape at the end of the batch. Constraints included maximum and minimum temperature rate of changes and concentration. Another implicit constraint

was the yield, as the upper concentration bound was the maximum required for the desired crystal yield. As previously mentioned, the metastable region was taken into account, by inputting a certain degree of uncertainty in the nucleation parameters, by using Monte Carlo simulations.

The available measurements used were solution concentration, temperature and crystal size distribution and the system's disturbance was done by introducing fine particles in the system to cause a change in the nucleation curve. The manipulated variables are the temperature and supersaturation (via concentration). The higher-level controller NMPC was used to give an optimal temperature trajectory, which served as input for the lower-level supersaturation controller. This optimisation routine was able to achieve the desired control objective, being able to steer the system to the metastable region, as intended.

NMPC was also applied [36] in an aspirin continuous crystallizer. The objective function was minimizing crystal size and yield deviation from the desired. For that, the manipulated variables included temperature and anti-solvent addition, controlled variables were crystal size and yield and disturbances were feed solution flow rate and concentration. Coefficient of variation, although not a controlled variable, was also monitored.

In the objective function formulation, both CVs have the same weight penalty, for empirical reasons, that penalizes CVs' values from the set-point one. Furthermore, it was added an input penalty term, to ensure that the MVs do not change instantaneously their values, allowing for a smooth response. Constraints included the operation limits for both MVss. Another interesting feature of this study was the fact that the authors defined the attainable region of operation, as a function of both controlled variables, in order to evaluate what were the possible combinations of solutions. The controller was thus tuned to maintain the system inside this region, guaranteeing the desired CVs values. Authors claim the importance of defining such region to that fact that if the set-point is out of it, the NMPC optimization problem will be unfeasible [36]. Given that disturbance can shift the system out of the attainable region, the controller capacity to reject them was also tested. Authors found that the controller was able to keep its CVs within their desired value, thus confirming its robustness. Overall, implementing NMPC yielded satisfying results. The authors point to a limitation regarding sensor noise and error which was not added.

An example of a NMPC strategy was also implemented in the sugar industry [25]. Due to variability in feed characteristics and nucleation and evaporation rates, the conditions that create supersaturation are not always the same, thus affecting crystal growth. Hence, a NMPC strategy was implemented, to meet the process' requirements. Given hardware limitations, the authors proposed the execution of NMPC solely when the tracking error is outside a certain bound, thus decreasing the computational burden.

The objective function formulated is composed of two terms: the first one penalizing the CVs reference trajectory and the second one penalizing the MVs' moves. Constraints include MVs' and CVs' bounds and rate of change, due to actuator and operational limitations [25]. To enable the controller activation in certain conditions, the authors added an error function constraint: if, in the neighborhood of the reference, the tracking error reaches a certain arbitrary value, the controller is switched on. This error function is defined as the mean of errors between references and predicted outputs. The magnitude of the penalties in both terms of the objective function were determined empirically, as well as the control and optimization horizons.

MVs included feed and steam (for evaporation) flow rate The CVs were the final mass average size of crystals, its final size distribution (measured by its coefficient of variation), fraction of crystals and supersaturation. Given the existence of real plant measurements, they served as natural source of noise and disturbance. Results showed the NMPC strategy lead to shorter batch times (although time was not explicitly optimized), when compared to simple feedback control strategies. Furthermore, the addition of the error tracking constraint helped reducing computational time. Quality wise, NMPC also

yielded satisfying results. The authors point to the quality of the variables estimation as one of the key aspects to the obtained results.

Another documented industrial implementation of NMPC was done on sucrose continuous crystallization [54]. The main objective was to ensure the desired product quality, in terms of crystal size distribution at the end of the operation. The secondary objective was the mass of crystals. Similarly to remaining authors, maintaining the desired supersaturation levels was the chosen control strategy. Nonetheless, its variability with experimental conditions, such as level of impurities, make its measurement unreliable. Hence, the CV of this paper was crystal mass. The objective function included two terms: a penalization for the CV reference trajectory and another for the MV control moves. In this case, the MV was the mass flow rate of the feed. Moreover, white Gaussian noise of 1% was added to the estimated variable of crystal mass, to simulate a more industrial-like scenario. Like the previous article described [25], NMPC strategy leaded to time saving results as well as satisfying setpoint tracking and disturbance rejection.

2.3.4 Batch time Control

All the examples described in the previous section did not entail batch time as a concern - most of them assumed a fixed batch time [17, 27, 52]. Industrially, optimising batch time is attractive as it results in economic savings. However, in crystallization, when time is of a concern, it is usually regarded as secondary goal [55]. Some strategies to deal with minimising time have been found in other sectors, such as the polymerization one, both using nonlinear and linear model predictive control [55–57]. A more conservative option done was assuming fixed batch time options, whenever plant measurements were made [57]. Thus, an optimisation was performed on the fixed batch time possibilities. Another way found to deal with this subject was to stop the batch operation when a control objective was met [55]. Alternatively, fixing as an end-point constraint a specification desired for the product was yet another option found [56].

Chapter 3

Materials and Methods

Process Systems Enterprise (PSE) provides the advanced modelling software package gPROMS, which includes three major environments: gPROMS ProcessBuilder, gPROMS FormulatedProducts and gPROMS ModelBuilder [58]. Parallel to that, gPROMS also includes a general software plaform for building and testing digital applications: gPROMS Digital Applications Platform.

3.1 gPROMS FormulatedProducts

One of the environments used in this work was the gPROMS FormulatedProducts, a platform which integrates formulated products with their manufacturing process, from pharmaceutical products, to agrochemicals and food products. It includes several libraries; the one in the current project is named gCRYSTAL. This library provided the model to which the control strategy was used.

3.2 gPROMS Model Builder

The model used was validated in gPROMS Model Builder software, a platform which enables the development, validation and execution of custom models, contained inside project files. Each project contains several sections:

- Variable: definition of variable type, its units and limits
- Models: canvas for custom modelling of flowsheets; equation-based
- Tasks: scheduling operations
- Processes: execution of simulations, using created models
- Optimisations: optimisation of processes
- Saved Variable Sets: variables values from previous ran processes
- Miscellaneous Files: imported data (.txt) from other sources

This platform was used to build the communication route between the gPROMS FormulatedProducts model and the controller platform, gNLMPC. The relation between the platforms is schematized below:

The interface built is a gPROMS Model Builder project file that provides the connection between the model and the controller. The created project file included:

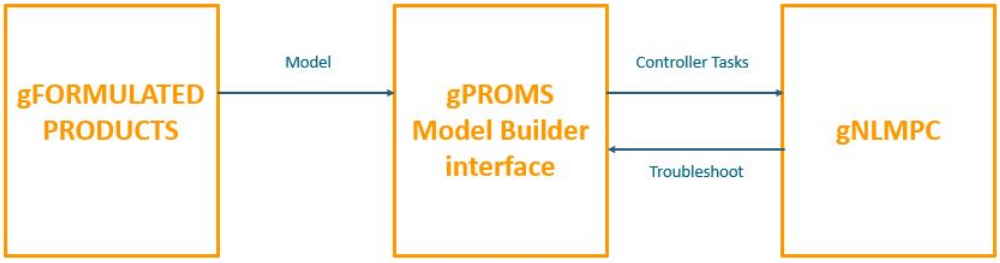

Figure 3.1: Scheme depicting the concept of interface between gPROMS and gNLMPC

- Master Model: Definition of variables, parameters and their equations
- Processes:

  - Master: Setting and assignment of variables and parameters

  - CSI: Assignment of MVs and DVs, setting of measured variables and model parameters and initializing the steady-state calculation

  - WSE: Assignment of MVs and DVs, setting of model parameters and simulating the estimation horizon

  - OP: Assignment of MVs,CVs and DVs, setting of model parameters and simulating the prediction horizon

- Tasks:

  - GetInputVariables: send MVs and DVs to gPROMS solver

  - RestoreOptimalSystemState: call a saved variable set with optimal system state

  - SendMeasured Variables: send measured variables from the gPROMS model to the gNLMPC

  - SendReportedVariables: send reported variables from the gPROMS model to the gNLMPC

  - SendUnmeasuredDisturbances: send unmeasured variables from the gPROMS model to the gNLMPC

- Saved Variable Sets

  - CurrentSystemState: text file comprising all flowsheet's variables at current time

  - OptimalSystemState: text file comprising all flowsheet's variables optimal values

3.3 gPROMS Nonlinear Model Predictive Controller

The main platform used for controller design was the gNLMPC. It is a software created for both offline and online configuration, deployment and testing of nonlinear model predictive control on a plant. It is composed of three main modules, depicted in figure 3.2.

The Manager is in charge of the management of all modules. The Data Validation (DV) checks the consistency of data from the digital control system before being sent to CMs and from the CMs to the digital control system. Finally, the Computational Modules (CMs) are the gPROMS processes and tasks that provide the controller information of what to do. Some of those processes include data reconciliation, state estimation and optimisation.

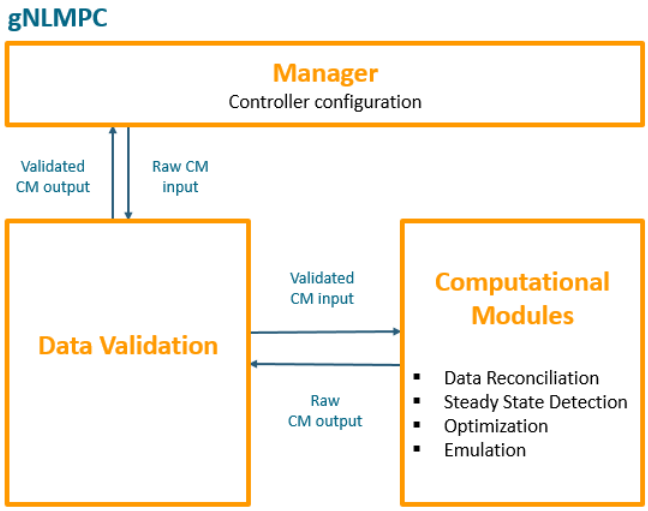

Figure 3.2: gNLMPC software scheme

There are three main operations in gNLMPC: configuration, testing and deployment of the controller. In the configuration section, the user can define the control variables, as well as their limits and properties. NMPC specific parameters such as number of control intervals, their duration and estimation and prediction horizon can also be set. In the test section, several operational scenarios (different setpoints, step tests, etc) can be created, for different plant measurements, in order to tune the controller. Available test options fall into one of the following three categories::

- Single Cycle: runs the sequence of data validation, computational module and results validation
- Run Replay: runs several single cycles
- Emulation: optimization and real time implementation of the optimal control profile of the MVs on a plant model

In the deployment section, the connection to external servers in order to operate the controller is made. Finally, troubleshooting can be executed by exporting back the case files to gPROMS Model Builder.

Chapter 4

Model Description

The model used for NMPC, which was included in gPROMS FormulatedProducts model libraries and developed based upon previous work [59], is a seeded batch crystallization of paracetamol, portrayed by the following flowsheet (figure 4.1) :

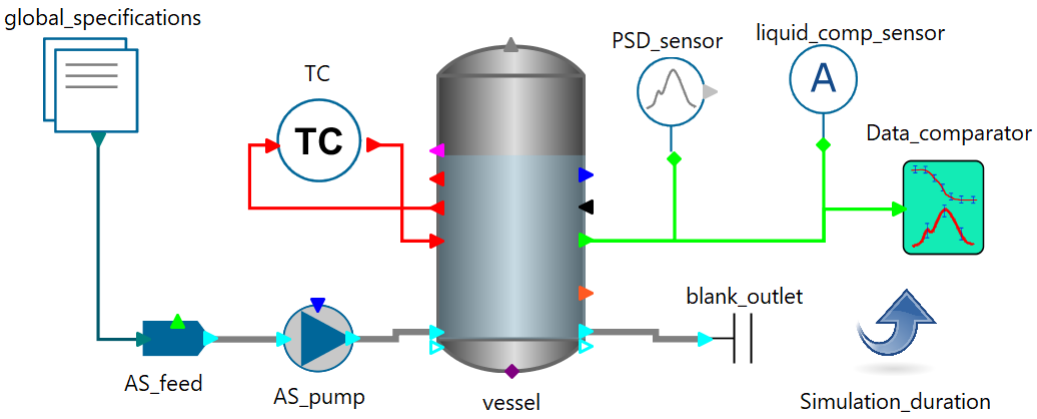

Figure 4.1: Flowsheet

It comprises the following units:

- Mixed suspension mixed product removal crystallizer (”vessel”): reactor model where crystallization specifications, such as type of operation, main mechanisms and reactions are defined.
- Anti-solvent feed (”AS_feed”): slurry feed of anti-solvent, where temperature and composition of anti-solvent are defined.
- Anti-solvent pump (”AS_pump”): pump model where anti-solvent flow rate and profile are specified.
- Temperature controller (”TC”): temperature controller unit where the control profile is specified such as setpoint and number of control intervals.
- Particle-size distribution sensor (”PSD_sensor”): unit measuring particle size distribution parameters, including quantiles, volume fractions, densities, span, coefficient of variations and moments of distribution.
- Liquid composition sensor (”liquid_comp_sensor”): unit measuring mass concentration and fraction of liquid components, solubility and supersaturation level.

- Data_comparator: unit that compares experimental and predicted particle-size distribution and solution concentration.
- global_specifications: unit that receives general model specifications such as crystal compositions and phases, thermodynamic properties and particle size distribution parameters like grid size and type.
- blank_outlet: simplifying unit representing the destiny of batch product.
- Simulation_duration: unit that receives time specification.

Paracetamol seeds are added at the beginning of the batch with the following initial conditions (table 4.1):

Table 4.1: Crystallizer initial conditions

Composition (kg/kg)	Paracetamol	0.18227
	Methanol	0.49064
	Water	0.32709
Mass (kg)		0.36687

4.1 Crystallization Mechanisms and Parameters

The main mechanisms included in the simulation are secondary nucleation, growth and dissolution and agglomeration. Only secondary nucleation by attrition was considered (as primary nucleation does not occur in industrial processes), following a custom kinetics scheme, of empirical nature given by the following expression, describing this mechanism [59]:

$$J_{sec} = k_n \, (C - C_*)^n \, \mu_2^{n_{sec}} \tag{4.1}$$

Where J_{sec} is the nucleation rate, C is the solute concentration. C_* the solubility, k the nucleation rate constant, n the nucleation order and n_{sec} is the second nucleation order.

Likewise, growth and dissolution also follow a custom kinetics scheme, described by the following rate expression, in which G represents the rate of growth and dissolution [59]:

$$G = k_g \, (C - C_*)^g \tag{4.2}$$

Where k is the growth rate constant and g the growth order.

Agglomeration is described by an empirical power law of the form [59]:

$$\beta_{agg} = a_1 G^{a_2} \varepsilon^{a_3} \tag{4.3}$$

Where β_{agg} is the rate of agglomeration, a_1, a_2 and a_3 are empirical parameters and ε is defined by:

$$\varepsilon = \frac{N_p \, d_{imp}^5 \, n_s^3}{V} \tag{4.4}$$

In which N_p is the stirrer's power number, d_{imp} the impeller diameter, n_s the stirring rate and V the reactor volume. All the empirical parameters in all three mechanisms were also based on previous work [59], and are summarized in the following table.

Table 4.2: Model Parameters

Model	**Parameter**		
Secondary Nucleation	k_n 19.81	n 1.48	n_{sec} 0.25
Growth and Dissolution	k_g 3.84E-6	g 1.12	
Agglomeration	a_1 0.27	a_2 1.34	a_3 1.34

The process entity (defined in chapter 3) provides the assignment and setting of variables and parameters of the process. After running the process, it is possible to obtain the results for the simulation. In the aforementioned conditions, the particle size distribution is depicted by the following figure 4.2:

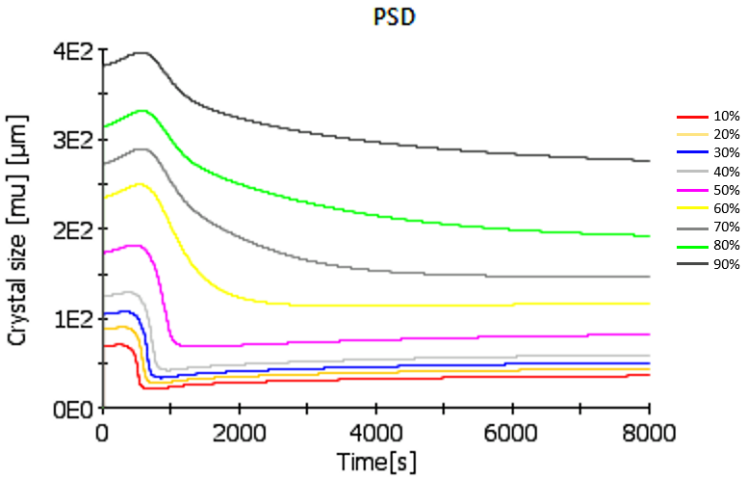

Figure 4.2: System's particle size distribution

Each color represents a quantile, going from 10% (red) to 90% (black). A 10% quantile means that 10% of the particles in the solid phase are of size equal of below the one depicted by the line. That is why bigger quantiles have higher crystal size. With time, the different particle bins reach a maximum size. This equilibrium stage is observable in the crystal's span (figure 4.3a), where the dispersion of particles' size reaches a maximum in the beginning, followed by a decrease and settlement stage, changing only slightly in the last 3000 seconds of the simulation.

Another variable worth evaluating is the volume mean size (figure 4.3b), since it is another variable that characterizes the particle size distribution. It is possible to see the system increasing its volume in the beginning of the simulation and reaching a settling stage at around 2000 seconds.

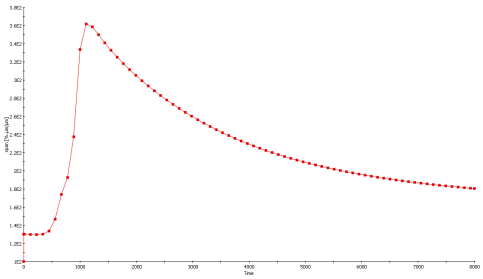

(a) Evolution of particle's span with time

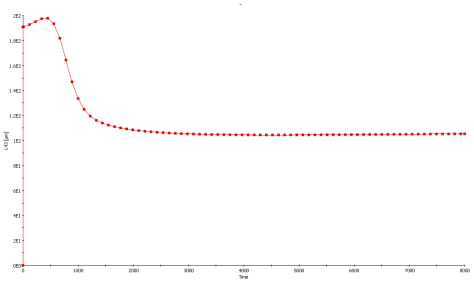

(b) Evolution of particle's volume mean size with time

4.2 Control Scheme

The system's control variables are categorized in the following table 4.3:

Table 4.3: System Variables

Variable Name	**Units**	**Variable Category**			
		Measured	Manipulated	Controlled	Disturbance
Anti-Solvent Flow	kg/s	x	x		
Temperature	°C	x	x		
Volume mean size	μm	x		x	
Supersaturation	$\mu m/\mu m$	x			
Span	$\mu m/\mu m$	x		x	
Dissolved Paracetamol	kg	x		x	
Impeller Frequency	rpm				x

Anti-Solvent flow and temperature were chosen as MV as they are the main drivers for supersaturation, and, consequently, crystallization. The range of operability for Anti-Solvent flow is between 1 and 9E-04 kg/s and for temperature is 20 and 45 °C. As discussed in section 2.3.3, typical goals for crystals include achieving maximum growth with minimum particle size dispersion. Hence, variables such as span and volume mean size were the chosen metrics for that goal. Span is defined in the model as:

$$Span = \frac{L_{90} - L_{10}}{L_{50}} \tag{4.5}$$

In which L_{90}, L_{10} and L_{50} refer to the length of crystals in the particle size distribution quantiles 90, 10 and 50% respectively. This makes it a measure of particle size dispersion. Volume mean size is defined as the mean volume of particles divided by their diameter, and it is defined in the model as:

$$Volume\,mean\,size = \frac{M_4}{M_3} \tag{4.6}$$

In which M_4 and M_3 describe the fourth and third moment of the particle size distribution. This property serves as a crystal growth metric, as it describes the mean volume over diameter of the particles.

Relative supersaturation, which in the model is defined by equation 4.7 was chosen to be a CV in

order to ensure the correct crystallization conditions are being met, as this property is the main driver for crystallization (see section 2.3 in chapter 2). The saturated solute mass concentration is temperature dependent as it is possible to observe in figure 4.4, which depicts the paracetamol solubility curve for different solvents.

$$Relative\,Supersaturation = \frac{Solute\,Mass\,Concentration - Saturated\,Solute\,Mass\,Concentration}{Saturated\,Solute\,Mass\,Concentration} \tag{4.7}$$

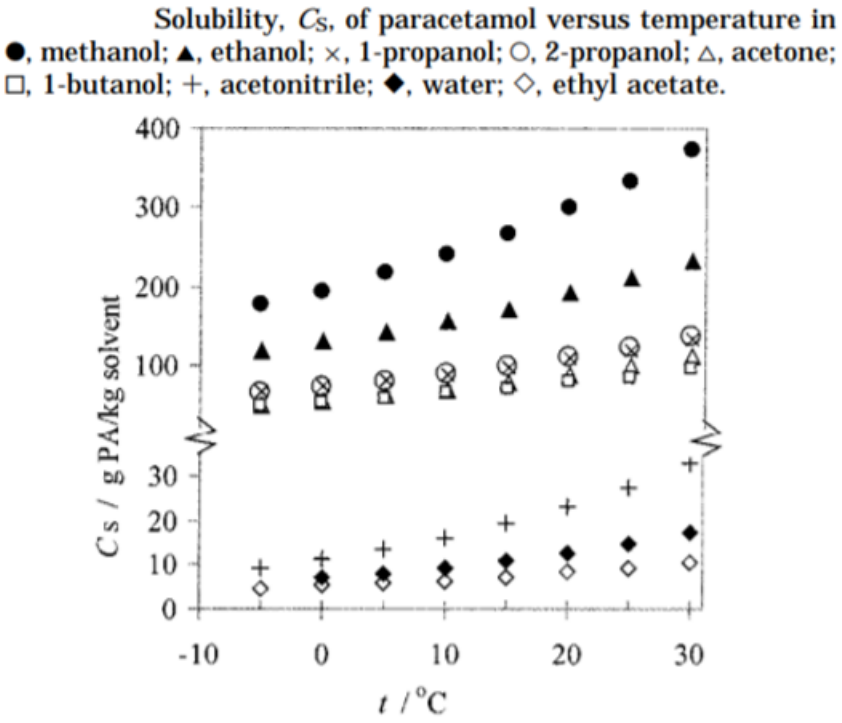

Figure 4.4: Paracetamol Solubility curve in various solvents [60]

Lastly, dissolved paracetamol was chosen as a CV to keep track of the crystallization progress and to guarantee that there is paracetamol left to react. Impeller frequency was chosen as the sole DV as it is a independent variable to the system, meeting the general criteria for this kind of variable.

4.3 Disturbances Impact on Controlled Variables

In the model, impeller frequency has an impact on the agglomeration kinetics, as the agglomeration rate constant is proportional to the logarithm of the specific power input. The power input is defined by:

$$Power\,input = \frac{Power\,number * impeller\,frequency^3 * impeller\,diameter^5}{Operating\,volume} \tag{4.8}$$

Therefore, an increase in the impeller frequency is expected to lead to a higher power input, consequently increasing the agglomeration rate. Given that both birth and death rates of crystals are exponentially dependent on this constant, it is expected to affect the CVs.

In order to establish the relation between DVs and CVs, a global system analysis was conducted. This gPROMS feature is a simple sensitivity analysis tool - from it, the impact of changes of the impeller

frequency on the CVs can be drawn.The results are depicted below (figure 4.5):

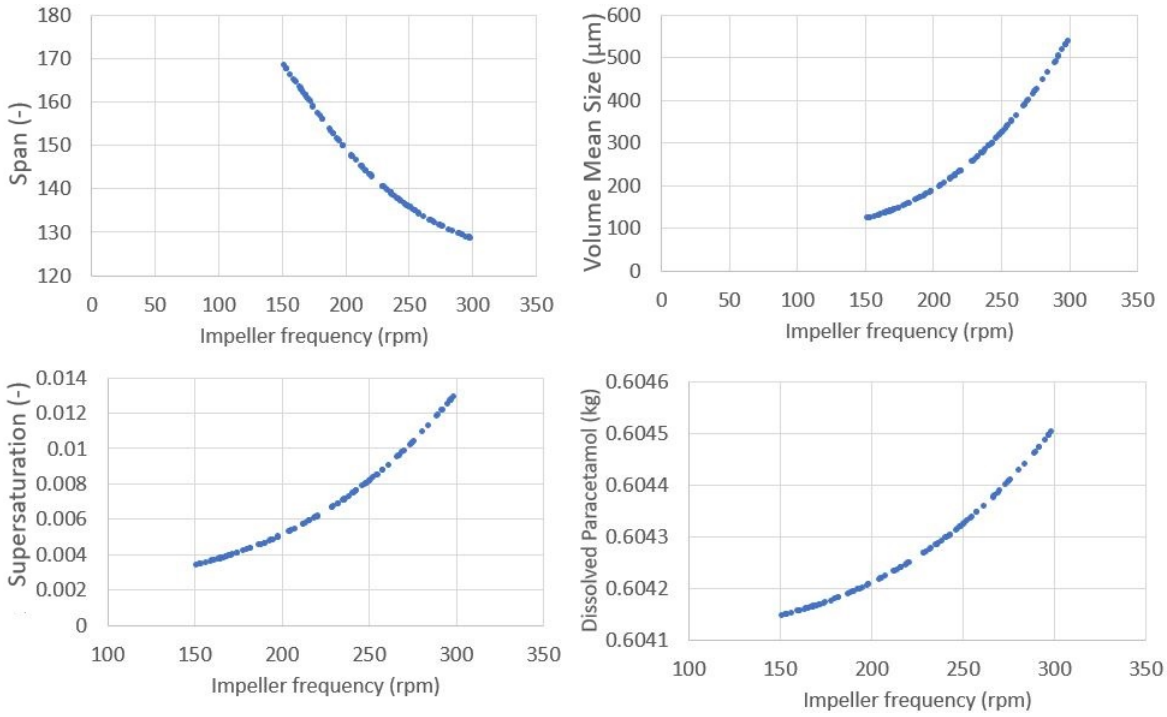

Figure 4.5: Impeller frequency impact on CVs

Increasing impeller frequency increases the stirring rate, which results in a higher number of collision between solid particles. The probability of the particles binding to each other after colliding increases as the number of collisions increases, so the agglomeration rate rises. As particles are more agglomerated, the particles' volume is higher, that is why volume mean size increases. If the particles are more agglomerated, their size disparity also decreases, which is why span assumes lower values, with the increase of the impeller frequency. The increase of agglomeration also has an impact on the solute mass, by increasing its concentration in the liquid phase. This results in an increase of relative supersaturation (see equation 4.7). Although it seems dissolved paracetamol is quite affected by the increase of impeller frequency, by taking a closer look at the magnitude of y-axis, one can conclude that its change is not as significant as the other variables.

Chapter 5

Optimisation Problem

As mentioned in chapter 2, implementing a NMPC strategy implies solving an optimisation problem, which involves minimising the difference between the current state of a given process and the desired one. The result of such an optimisation is the control action that satisfies those objectives. That control action is expressed as the optimal trajectory for the MVs. In the following chapter, how this optimisation problem is formulated is further explained.

5.1 Formulation

As mentioned in section 2.1.1, in chapter 2, the control objectives are typically expressed as the desired values for the CVs. However, a controller constructed to comply with specific values may be deemed too conservative, while also making the optimisation procedure rather burdensome, as the optimal solution would take longer to be found. In the present work, the control objectives were defined as desired intervals for the CVs, instead of values. This conferred the controller more flexibility. A typical CV trajectory is shown in figure 5.1.

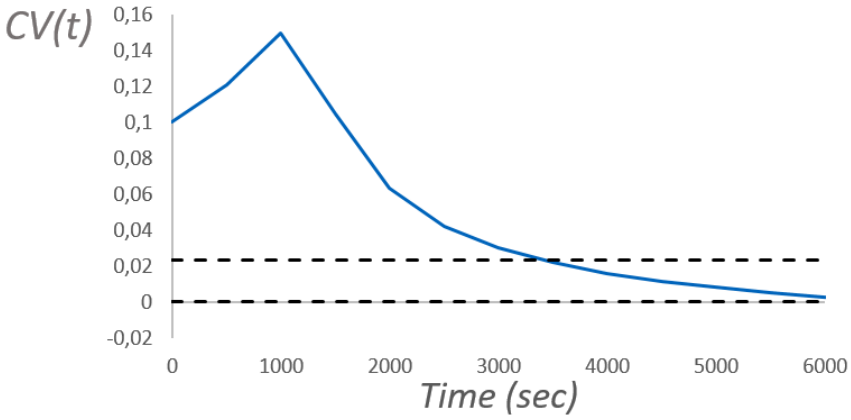

Figure 5.1: Typical CV trajectory

The objective function that describes the optimisation problem is penalty-based, which means that penalties are added whenever a CV is outside its desired interval, represented by the dashed lines in figure 5.1 (another option would have been to formulate it in a constraint-based way). The interval of values chosen are the ones intended for the CVs at the end of the batch operation. In this way, the controller ensures that these variables comply with control objectives for that batch. The penalties

added for the violation of these limits are different for each CV: this ensures the controller prioritized some objectives over others.

The objective function can also contain terms to penalize a CV heading to its desired limits too fast. The concept behind the penalty is better understood by looking at the following figure 5.2.

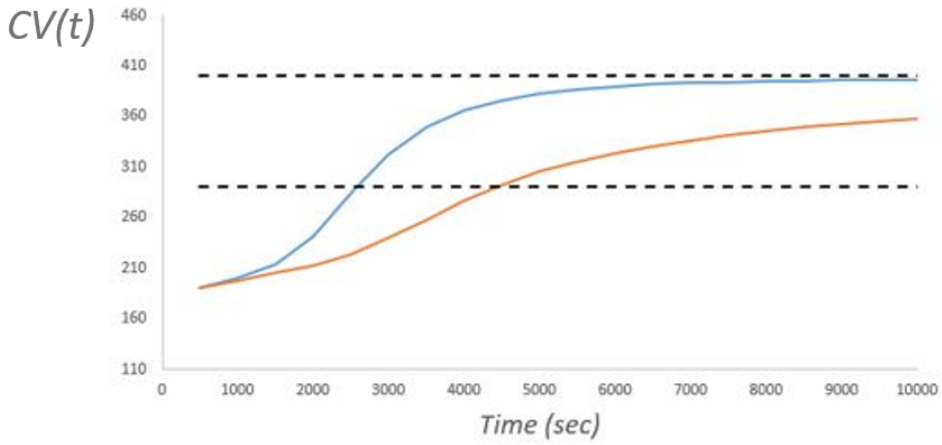

Figure 5.2: CV trajectory with (orange line) and without (blue line) a move-penalty

The blue line represents the trajectory for a CV without any penalties on its rate of change and the orange line with such penalty. In both cases the control objectives for this CV are met: both trajectories reach the intended limits. Nonetheless, the CV described by the blue line reaches those limits faster. Sometimes it is not desirable to reach the limits faster. For example, faster crystal growth is not always desired, as too rapid a growth leads to the infiltration of more impurities.

Another penalty that may be added to the objective function regards the MVs moves, more specifically it concerns MV degeneracy. Degeneracy in MVs may be due to two factors: magnitude and impact. MVs magnitude may influence the controller's willingness to move one MV rather that another. Whereas differences in impact (done by the MVs) on the system, which may result in the controller choosing always to move the same MV. These differences may thus be smoothed by the addition of penalties on the MVs moves.

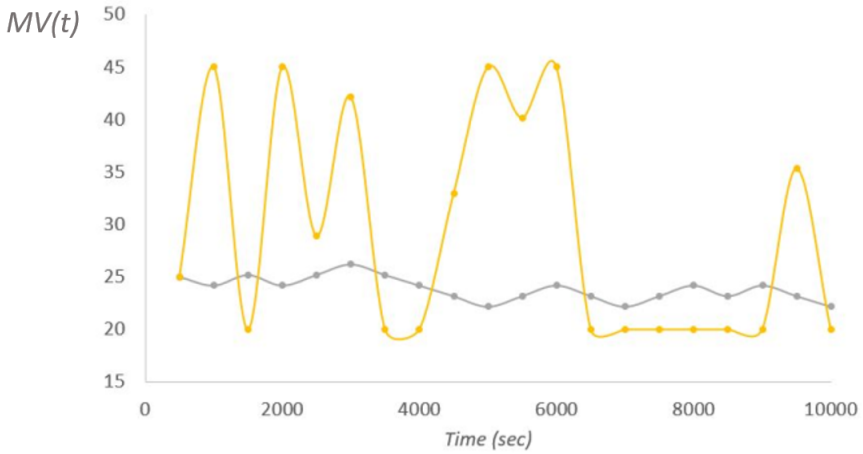

Figure 5.3: MV trajectory with (grey line) and without (yellow line) a trajectory penalty

Another penalty one can add to the optimisation concerns the MVs trajectory calculated by the controller at each cycle. Figure 5.3 shows two MV trajectories (represented by the dots). The yellow

line depicts the trajectory without a penalty. Suppose the MV depicted is temperature. It is possible to see the oscillation between the points. Despite being the optimal trajectory for this MV, such oscillation might not be feasible in practice for several reasons. For example, the actuators would have difficulty implementing a 20 °C difference from one cycle to another. Secondly, the sensors may not be able to accurately measure the temperature, as it is changing, causing the controller to not have the correct input of the system, when calculating the optimisation for the following cycle. Lastly, even if the actuator was able to implement the temperature change before the following cycle, the system itself would not have ”felt” that change long enough to actually make the impact the controller had predicted: reaching 45 °C is not the same as having being at 45 °C for an entire cycle. As such, a penalty on the trajectory change between cycles may be added, which is the option depicted by the grey line, in figure 5.3. This trajectory may be not the true optimal one, but it is more realistic and achievable.

The objective function (OF) that describes the formulation explained in the previous section can be simplified into the following expression 5.1 [61]:

$$\min OF = A + B + C \tag{5.1}$$

in which:

- Term A includes the penalties added whenever the CVs are outside their desired limits (also referred to as ”reference envelopes”).
- Term B features the penalties concerned with the controller's movement actions (whenever either a CV or a MV is changing too much),
- Term C comprises the penalties related to MVs moves between cycles

The objective function can be further formulated as follows [61]:

$$\begin{aligned}\min_{u_{i,k}|\lambda_i^u=1} OF \equiv & \sum_{j\in CV} \lambda_j^z \, C_j'^{z,lo} \int_0^{T^{opt}} \max(0, z_j^{ref,lo}(t) - \bar{z}_j(t))^2 \, dt \\ & + \sum_{j\in CV} \lambda_j^z \, C_j'^{z,hi} \int_0^{T^{opt}} \max(0, z_j^{ref,hi}(t) - \bar{z}_j(t))^2 \, dt \\ & + \sum_{j\in CV} \lambda_j^z \, C_j^z \int_0^{T^{opt}} \bar{z}_j(t) \, dt + \sum_{i\in MV} \lambda_i^u \, C_i^u \sum_{k=1} \delta_k \, u_{i,k} \\ & + \sum_{i\in MV} \lambda_i^u C_i^{\delta u} \sum_{k=1}^{K} |u_{i,k} - u_{i,k-1}|\end{aligned} \tag{5.2}$$

where:

- OF: objective function
- CV: controlled variable
- MV: manipulated variable
- T^{opt}: optimization time horizon
- K: number of control intervals
- δ_k: duration of control intervals
- $u_{i,k}$: MV value i over control interval k

- λ_i^u: binary switch (0/1) indicating whether MV i is included in the optimisation
- λ_j^z: binary switch (0/1) indicating whether CV i is included in the optimisation
- $C_j'^{z,lo}, C_j'^{z,hi}$: violation penalty applied to CV when it is below or above its reference envelope limits
- $z_j^{ref,lo}(t), z_j^{ref,hi}(t)$: lower and upper limits of reference envelopes
- $\bar{z}_j(t)$: CV trajectory
- C_j^z: CV j cost penalty
- C_i^u: MV i cost penalty
- $C_i^{\delta u}$: MV i cost penalty at control interval boundaries

In the above formulation, the optimisation time horizon T^{opt} is the sum of the control intervals K, of length δ_k.

CVs' trajectories

The initial focus stood upon term A, as it is the term that ensures the achievement of the control objectives, by steering the CVs into their reference envelopes. As such, terms B and C were turned off. This meant:

- CV binary switch λ_j^z equal to 1
- MV binary switch λ_i^u equal to 0
- Cost penalties on CVs and MVs (C_j^z and C_i^u) equal to 0
- MV i cost penalty at control interval boundaries $C_i^{\delta u}$ equal to 0

In this way, there was no controller trade-off between terms, and the obtained solution was the most optimal one.

The first goal was to ensure that the CVs displayed the desired value at the end of the simulation, within the reference envelope. The reference envelopes bounds were chosen according to the CVs' desired values at the end of the batch. The chosen values are presented in the following table:

Table 5.1: Initial values and bounds for the CVs

Variable	Units	Initial Value	Lower bound	Higher bound
Span	$\mu m/\mu m$	128.7627	134.56575	137.28425
Supersaturation	-	0.011411	0	0.023171
Volume Mean Size	μ	196.6545	290.0341	400
Dissolved Paracetamol	kg	0.066723	0	0.037686

The presented values were taken from the original model, after a 6000 seconds simulation. Some CVs have wider reference envelopes than others - that is due to their flexibility. Span, a measure of particle dispersion, is more restricted than volume mean size, which is a measure of particles' growth, given that assuring the desired particle size distribution is more important than achieving maximum size.

5.2 Optimal Control

Two scenarios under optimal control were analysed. Optimal control refers to the optimal scenario predicted by controller for the output variables. The controller parameters used for this study were:

Table 5.2: Controller Parameters

Controller Cycle Length	500 sec
Number of Control Intervals	[1,1,1,1,1,5,5]

The number of control intervals is given as an array. It was observed that the system was very dynamic in the beginning of the simulation, compared to the end. Thus, smaller cycles were chosen for the beginning of the simulation, to capture the system's interactions more accurately. Whereas in the end, shorter cycles were not necessary, so to decrease the computational burden, longer cycles were chosen.

Controller Tuning

The controller tuning under optimal control included studying how the magnitude of term A impacts the CVs and MVs. Different penalties for each of the CVs were analysed individually. The method used was to turn on only the CV to be analysed (CV binary switch λ_j^z equal to 1) and to change the violation of bound penalties ($C_j'^{z,lo}, C_j'^{z,hi}$) to 0.1, 1, 10, 100 and 1000 accordingly. The system's response to a 10% disturbance on DV impeller frequency was observed.

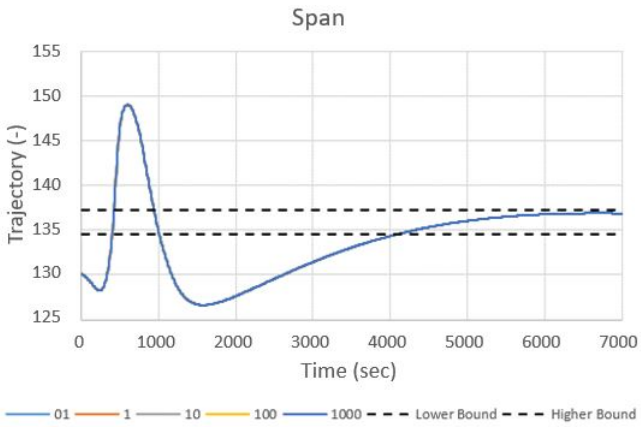

Figure 5.4: Span's optimal trajectory

Figure 5.4 shows that span is able to return to its reference envelope (in dashed lines) and that the optimal trajectory does not change with the penalty for bounds violation. Looking at the MVs trajectory (figure 5.5), one observes that Anti-Solvent Flow is the same for all cases. Whereas temperature slightly changes: with increasing penalty, the first value for temperature after initialisation is lower. Although this is only visible from penalty 100 or higher, the other cases displayed an initial value of around 25 °C. For all cases, temperature returns to 25°C at time t=500 seconds, which is the controller cycle length. This suggests that after the first cycle, the controller decided that the CV was already heading to his reference envelope as desired. The magnitude of the value after initialisation seems to be related to the magnitude of the bounds' penalties. The higher the bound, the more pressure the controller had to make

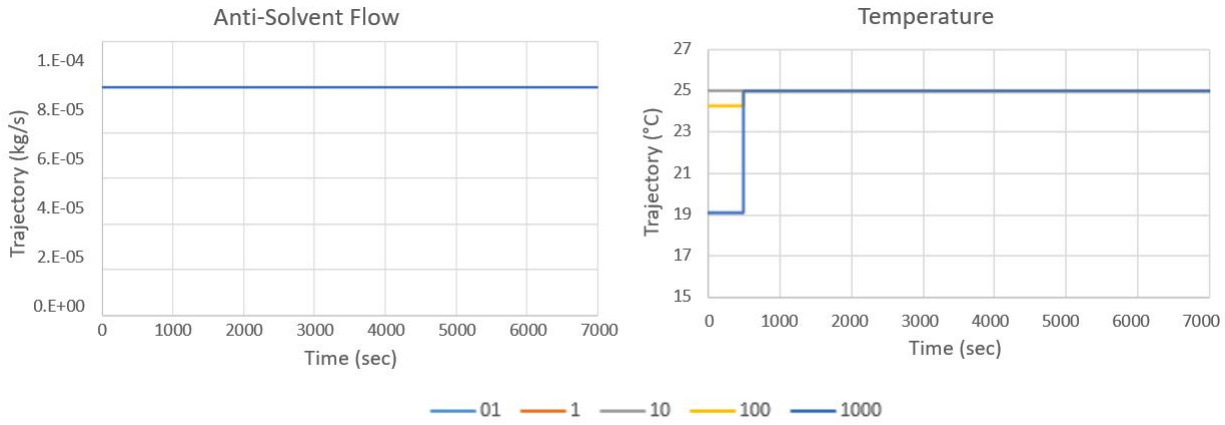

Figure 5.5: MVs optimal trajectory for different penalties on Span

sure that its CV returned to its reference envelope, hence, the bigger decrease in temperature (figure 5.5) .

The following CV to be analysed was supersaturation (figures 5.6 and 5.7).

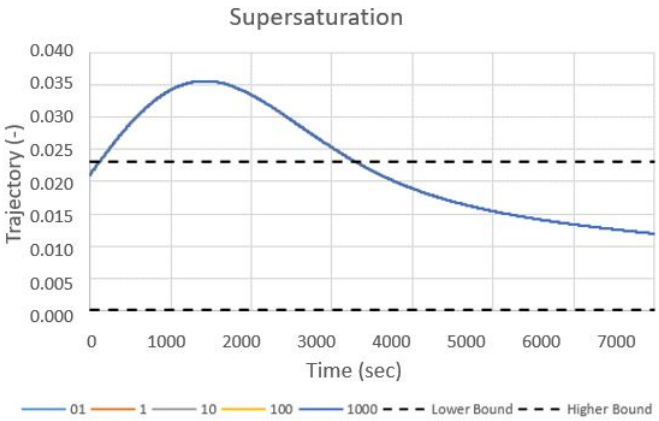

Figure 5.6: Supersaturation's optimal trajectory

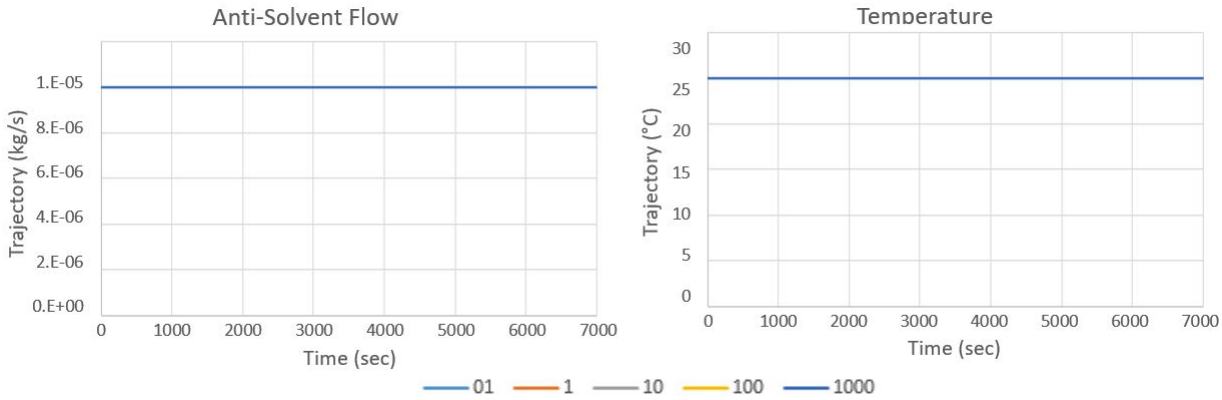

Figure 5.7: MVs optimal trajectory for different penalties on Supersaturation

As it was observed for span, supersaturation's optimal trajectory does not change with the magnitude of the reference envelope penalty (figure 5.6). Neither do the MVs (figure 5.7). Although it did return to its reference envelope as intended. Unlike span, supersaturation's initial value was already inside the

reference envelope - it only started to violate its bounds some time after time 0. This may be the reason behind the fact that temperature does not display the same initial step as it did in the previous simulation (figure 5.5).

Another CV to be analysed is the volume mean size (figures 5.8 and 5.9).

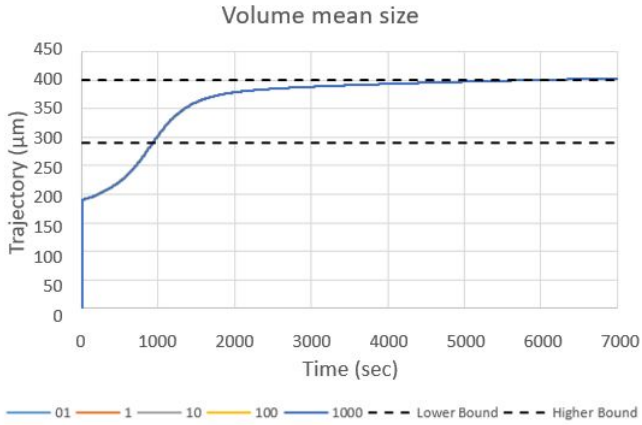

Figure 5.8: Volume mean size's optimal trajectory

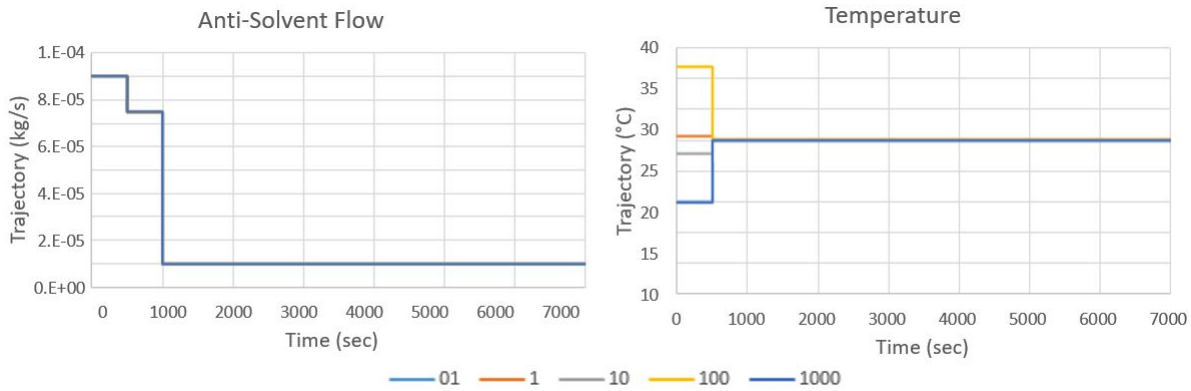

Figure 5.9: MVs optimal trajectory for different penalties on volume mean size

Similarly to the other analysed CVs, the optimal trajectory does not change with the reference envelope penalties (figure figures 5.8). The same is observed for the MV Anti-Solvent Flow (figure 5.9). Although, unlike in the other CVs case, it does not remain constant throughout the optimisation. The same goes for MV temperature which displays different values for the first 500 seconds (figure 5.9). For both penalties of 0.1 and 1000, initial temperature was 15. For penalty equal to 1, 10 and 100, the initial temperature value observed was 25.54, 22.79 and 36.90°C. The temperature value does not seem to be proportional to the magnitude of the penalty, as it was observed for span. These results seem to confirm the non-linearity of the system's response to disturbances. Nonetheless, this CV seems to be starting to violate its upper bound, and neither MVs display any change. One possible reason for that is that the violation was not severe enough (in both time and magnitude) for the controller to take any action before the simulation ended.

The last CV to be analysed is the dissolved paracetamol (figures 5.10 and 5.11).

For this CV the optimal trajectory is also independent of the bound's violation (figure 5.10). In this case, temperature does exhibit the same pattern: remaining constant (figure 5.11). However, MV Anti-Solvent Flow seems to be displaying a step behaviour, starting from its upper limit value of 9E-05 kg/s (figure 5.11). For the first step, it seems that the higher the penalty, the later and more abrupt the

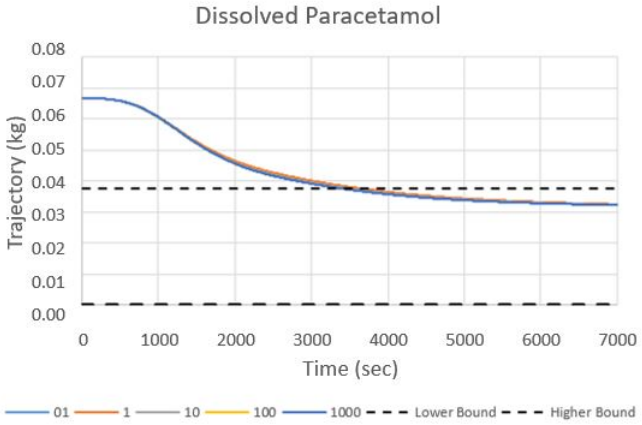

Figure 5.10: Dissolved Paracetamol optimal trajectory

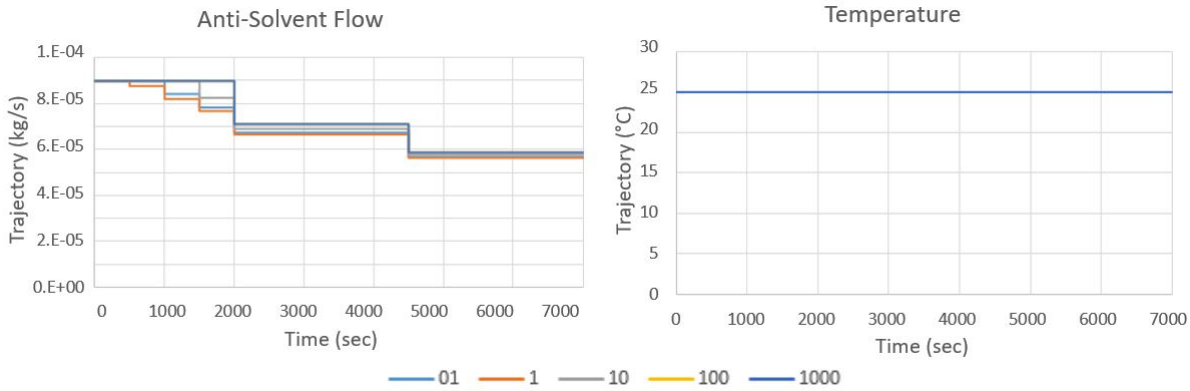

Figure 5.11: MVs optimal trajectory for different penalties on Dissolved Paracetamol

change is. For the second step, this change is barely noticeable and for the third even more. One possible reason for this is the fact that the CV is only violating its reference envelopes for the first 3000 seconds. So, the magnitude difference is only visible when there is a violation, which makes sense: when there is no violation, the controller just needs to maintain its MVs values. The magnitude of the steps are also related to the control intervals - they were defined as four cycles of 500 seconds and two cycles of 2500 seconds. Hence, each step corresponds to the new value of each cycle.

Besides the controller's behaviour, one may also see from these experiments, which MVs the controller chooses to change. CVs like volume mean size and dissolved paracetamol seem to be more dependent on the anti-solvent flow. For both cases, the MV decreases its initial value, which is related to the type of envelope violation. For dissolved paracetamol, its initial value was above its limits, which means that new crystals had to grow. That is why, for the first 2000 seconds, anti-solvent flow is at its maximum allowed value and the CV is decreasing. After 2000 seconds, there is no need to keep anti-solvent flow at its maximum as the CV is almost reaching its reference envelope. After reaching the desired area, the MV could settle at an even lower value, that allows the CV to settle inside its bounds. For span and supersaturation, their relation to MVs cannot be established so well, as they were not enough time outside their reference envelopes. Nonetheless, for volume mean size, both MVs changed, which makes the case eligible for a further analysis. The exact same scenarios were tested, although this time with only one of the MVs active at a time. In this way, it is possible to see the reason why both MVs were changed and not just one.

The initial intention of this test was to see the impact of changing the penalties added whenever the

CVs were outside their reference envelopes, in an optimal scenario. In some cases, different penalties resulted in different MVs trajectories, without impacting the CVs trajectories. These tests made it possible to confirm the penalty-based nature of the objective function, as the controller will always find an optimal solution and implement it, regardless of the magnitude of that penalty. For the subsequent scenarios, however, the exact penalty magnitude had to be specified .The final chosen penalties for the CVs are shown in table 5.3.

Table 5.3: CVs Reference Trajectory Penalties

Penalty	**Span**	**Supersaturation**	**Volume Mean Size**	**Dissolved Paracetamol**
Lower Limit	1000	1	1000	1
Upper Limit	10000	1000	100	100

As previously stated, the penalties are going to be multiplied by the square difference between the target intervals and the current values of the CVs (see equation 5.2 in chapter 5). Therefore, the choice of their magnitude had to take into account the CVs' absolute value. Not only that, but the magnitude difference between penalties help the controller to prioritize some CVs, over others. That is why span is the CV with higher penalty: it is the main indication of the crystal's quality, which is the reason why its upper limit has a higher penalty than its lower limit. On the contrary, supersaturation is not a measurement of crystal's quality, but an indication about the progress of the crystallization - if it is a positive value, there is crystallization, otherwise, there is no reason to continue with it, as crystals are starting to dissolve. The high penalty for the upper limit is to guarantee that a minimum supersaturation is achieved. The lower limit is less of a concern, hence its lower penalty. Regarding the crystal's volume mean size, a growth indicator, ensuring a minimum is more important than enforcing a maximum, thus, the difference in penalties. Lastly, for dissolved paracetamol, setting a higher upper limit violation aims to ensure a maximum liquid mass allowed in the crystallizer.

Disturbance Rejection

Disturbances of $\pm$ 5, 10 and 15 % on the DV impeller frequency (with a initial value of 250 rpm) were performed and the optimal trajectory of the CVs, as well as for the MVs are presented (figures 5.12 and 5.13). Regarding span, it is possible to verify that only for ± 5 disturbances, does the CV return to its reference envelope. One possible reason is the narrow bounds chosen to this CV. It is also worth pointing out that negative disturbances increase the trajectory, showing a reverse relation between impeller frequency and span [1], which matches the system's dynamics: a higher impeller frequency improves mixing which promotes a more uniform growth, thus decreasing the particles' span. When it comes to supersaturation, the controller is more successful as it is able to steer this CV back to its reference envelope for all cases. Also for this CV, the relation towards the disturbance is reverse as lower impeller frequencies result in higher violations in magnitude and time: a - 15% disturbance not only shows a higher initial peak but also takes longer to return to its reference envelope. This happens for the same reasons given above. Volume mean size shows a different trend comparing to the above mentioned CVs, as lower impeller frequency values yield lower volume mean size values. An explanation may lay on model itself: one can see in equation 4.3, that the agglomeration rate is proportional to the stirrer's velocity and a higher degree of agglomeration results in a higher volume size of the particles. Similarly to span, only for $\pm$ 5% disturbances is the controller able to steer this CV into its reference envelope. Violating the upper limit of the reference envelope is not of a particular concern, as crystal

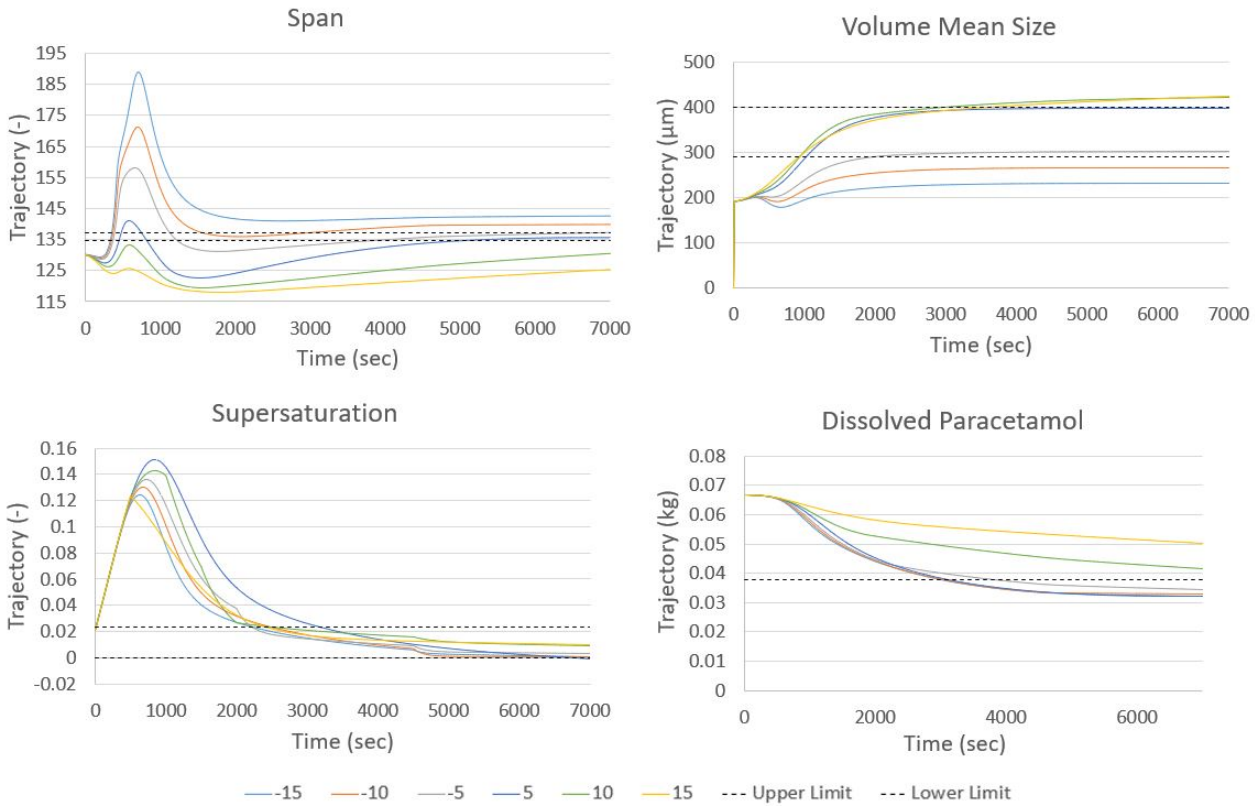

Figure 5.12: CVs trajectories

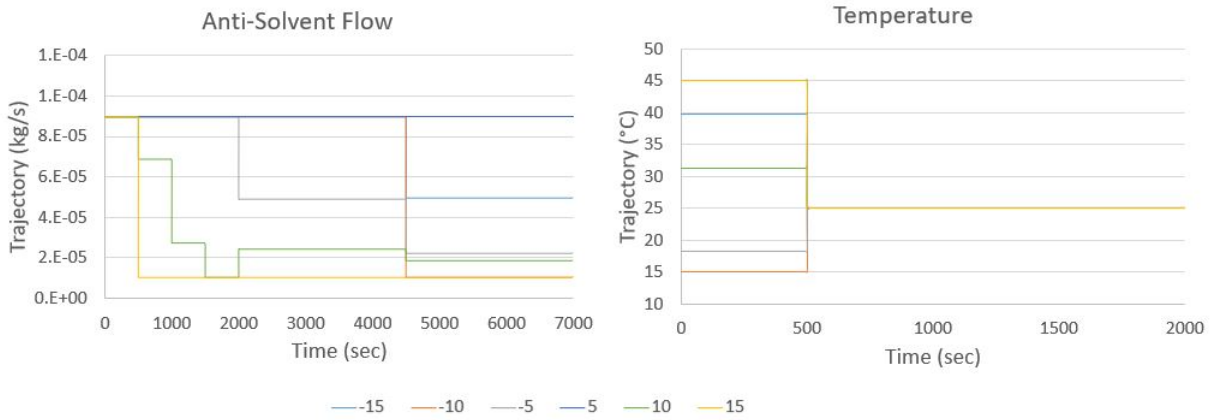

Figure 5.13: MVs trajectories

growth is one of the main goals. Lastly, except for 10 and 15% disturbances, the controller is able to steer dissolved paracetamol into its reference envelope. Similarly to volume mean size, these two cases fail to return to their reference envelopes. This means that dissolved paracetamol is slower to crystallize under higher impeller frequencies. This goes in agreement with the proposed hypothesis that stirrer rates promote a more uniform slow crystallization process.

Looking at the MV temperature (figure 5.13), one can see that the higher the impeller frequency, the higher the initial temperature. After the first control interval of 500 seconds, temperature settles at its initial point of 25 °C. On the other hand, Anti-Solvent Flow starts from its upper bound of 9E-5 in all cases. Then, the more negative the disturbance, the lower the final value is.

Chapter 6

Emulation Definition

In the following chapter, the emulation mode is further explained. As it was briefly explained in chapter 3, emulation is the real-time implementation of the controller's optimal control action on a digital twin of the model. The emulation is performed in cycles, and the controller's tasks in each cycle are explained below:

1. Cycle 1: Data Reconciliation. The optimal initial steady state conditions are calculated. The task is described by the following optimisation routine:

$$\min_{u,d} \sum_{i \in M} \lambda_i \frac{\omega - \bar{\omega_i}}{\sigma_i} \tag{6.1}$$

   Subject to :

$$f(x, 0, y, u, d, \theta) = 0 \tag{6.2}$$

$$z^{min} \leq z \leq z^{max} \tag{6.3}$$

   Where x and y are state variables, u and d are the MVs and DVs respectively, θ is a time-invariant parameter, M the group of variables to which measurements are available, ω and $\bar{\omega_i}$ denote measured variables and their measurements respectively and σ_i is the standard deviation of the measured variables (due to sensor or actuator characteristics, for example). λ_i is a binary factor, which specifies whether a measured variable should be taken into account in the optimisation. Variables whose measurements are not available will not be included. Lastly, z^{min} and z^{max} are the bounds for z, which represents variables $\{x, y, u, d\}$.

2. Cycle 1: Optimisation and Prediction. The controller performs the optimisation procedure described in chapter 5.

3. Cycle 1: Digital Twin: the gPROMS simulation of the digital twin of the model is ran with the optimal trajectory calculated in the Optimisation and Prediction procedure.

4. Cycle 2: State Estimation. The initial conditions from cycle 1 are received and used to solve the plant's current state.

5. Cycle 2: Optimisation and Prediction. Similar to procedure to optimisation in cycle 1.

6. Cycle 2: Digital Twin. Similar to cycle 1.

7. Cycle 3 - End: Similar to cycle 2. The controller will calculate the estimate of the state based on the previous cycle.

As stated in chapter 3, the gNLMPC platform offers three operation possibilities to the controller: configuration, testing and deployment. Only the deployment features of the platform were used not in the present thesis as it concerns the connection to a plant's servers. How the two other features were explored will be explained next.

6.1 Configuration of Controller Parameters

The controller tuning is done in the configuration section, where different controller parameters are specified. Three main parameters were studied: controller cycle length, number of control intervals and prediction horizon.

Controller Cycle Length

Different controller cycle lengths were tested, in order to see its impact on both CVs and MVs. Shorter cycles are expected to provide a better understating of the process, which leads to more reasonable control actions and better reference trajectory and disturbance rejection [25]. However, longer cycles duration seem to be better at identifying and dealing with measurements noise [51]. Furthermore.the smaller the length of the control cycles, the greater the computational burden of the controller, since it must run more optimisation routines to reach the same objectives [62].

Number of Control Intervals

The number of control intervals was also tested to verify whether it had any impact on the MVs and CVs. The number of control intervals multiplied by the controller cycle length results in the optimisation horizon. Hence, changing the number of control intervals is the same in principle as change the optimisation horizon.

Firstly, the computational burden is expected to increase with the increase of the number of control intervals, given that the optimal trajectory will be divided in more intervals. This may improve the efficiency of the optimisation, as it forces the controller to calculate more accurately the CVs' trajectory.

Some experiments show that the sampling intervals have little effect on the size of the terminal regional (where the estimates converge) [63]. Other experiments show that the plateau values are expected to be the same, just the path is tending progressively to a continuous profile, as the number of intervals increases [53].

Prediction Horizon

The prediction horizon's impact on the controller was also investigated. This parameter is defined in the software as an integer multiple of the controller cycle length. Its number represents the number of controller cycles to include after the optimization cycles. Essentially, the objective of this test was to determine whether the distance between T^{opt} and T^{pred} in the MV optimal trajectory (represented in figure 6.1) had any impact on CVs and MVs trajectory.

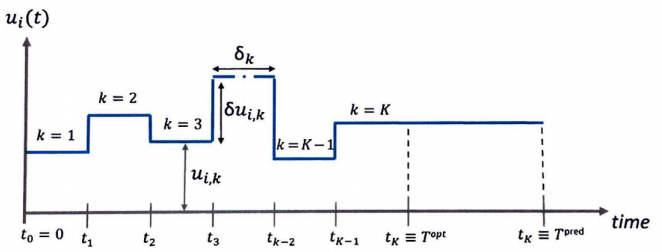

Figure 6.1: Optimization and Prediction Time Horizons

6.2 Testing

After having studied the impact of some controller parameters, it was possible to proceed to the testing phase. The testing consisted in creating disturbance scenarios to see how the controller responded, in terms of stability and robustness.

Stability

Stability tests were first performed in order to certify that the controller was able to run in ”Emulation” mode. The test included running a first cycle of a cold-start initialization to obtain the optimal steady-state values for the MVs. The following cycles were ran with a warm-start estimation routine, as explained in the previous section. This test also served to draw a baseline.

Disturbance Rejection

The controller’s ability to do disturbance rejection was tested by making step changes on the DV impeller frequency.

Measurement Noise

As sensors and actuators may not always provide a 100% accurate measurement, the ability to handle noise was tested by adding it to one of the variables. Noise was added to one measured variable, span, which is also a CV. This was done by multiplying the outputted measurement by a random number between 0.95 a 1. This meant that every measure taken after each cycle was multiplied by one random number (different from cycle to cycle).

Plant / Model Mismatch

A quite frequent problem with model-based controllers is that the model description of the process is not accurate, namely the kinetic parameters and constants are not absolutely valid. As stated in chapter 2, this makes the prediction harder for the controller, given that what it predicts for the CVs will not happen. As such, the ability of the controller to achieve its control objective in spite of plant / model mismatch was tested by changing one of the kinetic parameters, more specifically the supersaturation order. The parameter suffered a -5% deviation from its original value.

Chapter 7

Emulation Results

The results of the configuration and testing of the controller on emulation mode are demonstrated in the following chapter.

7.1 Configuration of Controller Parameters

The testing of the emulation began with studying the impact of the controllers' configuration parameters on the model.

7.1.1 Controller Cycle Length

For a base case without disturbances, different controller cycle lengths were tested: 250, 500, 750, 800, 900, 1000 and 1100. The measured values for the CVs are depicted below:

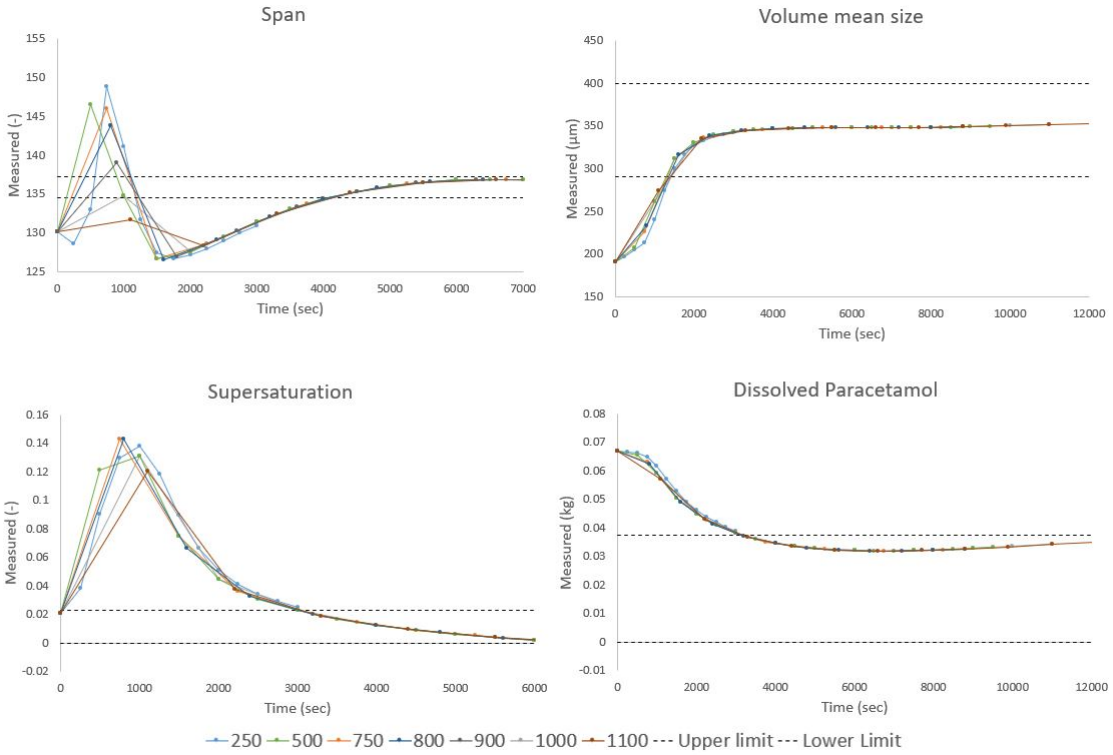

Figure 7.1: CVs measured values for different controller cycle lengths

From the figures 7.1, it is possible to observe the impact of the controller cycle length on the CVs' trajectory. In CV span, its initial peak is successively decreases, as the controller cycle length increases. For lengths above 1000, the peak does not even violate the upper limit of the reference envelope. This difference fades away as the cycles continue, given that for all hypothesis, span returns to its reference envelope in the same cycle. The same behaviour is observed for supersaturation, as it returns to its bounds within the same cycle for all cases. Although for this CV, the difference in its initial peak is not so clear as it was for span. Still, a certain delay in larger cycle lengths shows how some of the system's dynamics is affected. On the contrary, for volume mean size and for dissolved paracetamol, the change in controller cycle length does not seem to pose significant differences, as their behaviour is similar for all cases. This points to the premise that the controller cycle length has an higher impact on span and supersaturation. One possible reason for that is CVs' dynamics: the more complex the dynamics, the more behaviour the controller misses. In span's case that is quite visible as its initial peak is almost ignored for higher cycle lengths. In the case of the last two CVs, they display an almost constant behaviour throughout the emulation, rendering the computational burden of a lower cycle length meaningless.

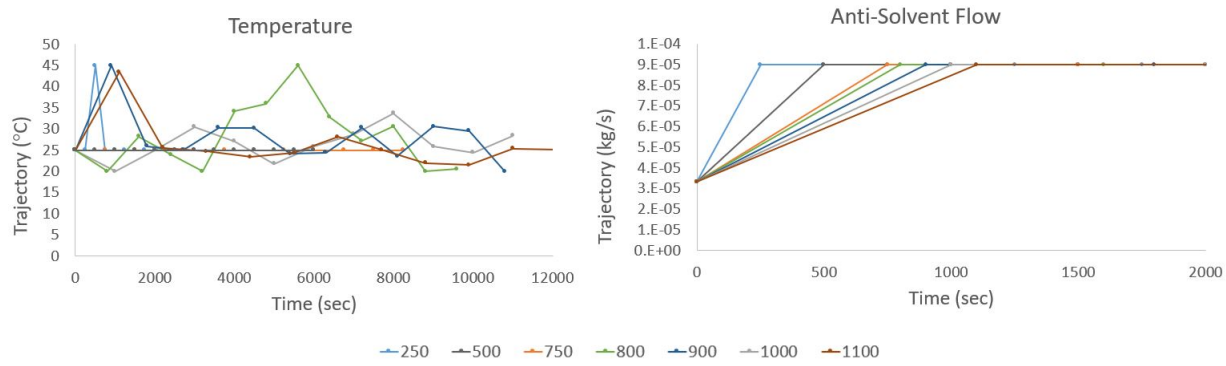

Figure 7.2: MVs measured values for different controller cycle lengths

It was not the change of the controller cycle length that directly affect the CVs trajectories. In actual fact, the controller cycle length affected the MVs trajectory, more specifically the time they were being updated, thus affecting the CVs. This is quite visible in the MVs' trajectories displayed in figure 7.2.

Regarding anti-solvent flow, the delay in reaching its optimal value is noticeable. It becomes clear that the optimal trajectory for this variable is to assume the value of 9E-05 kg/s, regardless of the cycle length. However, longer cycles take longer to implement this change, thus the system continues a larger amount of time without its optimal trajectory. This explains the CVs behaviour depicted in figure 7.1. For temperature, it is harder to retrieve some remarks as some trajectories are quite oscillatory. Lower cycle lengths seem to maintain this MV around its initial value of 25°C for most of time. Whereas for cases 800,900 and 1000 temperature displays quite some oscillating step changes. These results point to the importance of choosing the correct cycle length: in cases 800 and 900, the oscillation would not be acceptable, given that the rate of change is too fast. One would have to input some penalty on the controller for the rate of change, which would not be necessary for lower cycles. For case 1100, it returns to a more steady behaviour. This may suggest that the duration of a cycle may affect the stability of the MV trajectory.

Another interesting aspect to take into account is the execution time per cycle, which is the time the controller takes to read the measured variables, update them, calculate the CVs' optimal trajectory, implement the MVs next values and run a simulation with them.

Table 7.1 shows the average cycle time for the different cycle lengths. The cycle duration affects

Table 7.1: Average cycle time for different controller cycle lengths

Controller Cycle Length (sec)	250	500	750	800	900	1000	1100
Average Cycle Time (sec)	1314	628	3165	503	994	359	379

the optimisation procedure, and it seems that when cycles are too large, namely the last two cases, the controller finds it easier to reach a solution. Whereas shorter cycles, due to capturing more of the system's interactions, are evidence that the controller may be spending more time optimising.

This study allowed to verify the importance of choosing the right controller cycle length carefully: it has to be small enough to portray accurately the system's dynamics, but not too small as to burden the controller. The following tests were performed for a controller cycle length of 500 seconds as it is a suitable compromise between accurate trajectory and optimisation efficiency.

7.1.2 Control Intervals

Different control intervals were tested, for a -5% step change on DV impeller frequency and a controller cycle length of 500 seconds. By making a step change on DV, the impact of this configuration parameter on the controller is more visible (as opposed to no disturbance). Four different control intervals were tested: 1, 2, 5 and 15 seconds. This means that the optimisation horizon was 500, 1000, 2500 and 7500 seconds, respectively. The CVs trajectory for the different cases is shown in figure 7.3.

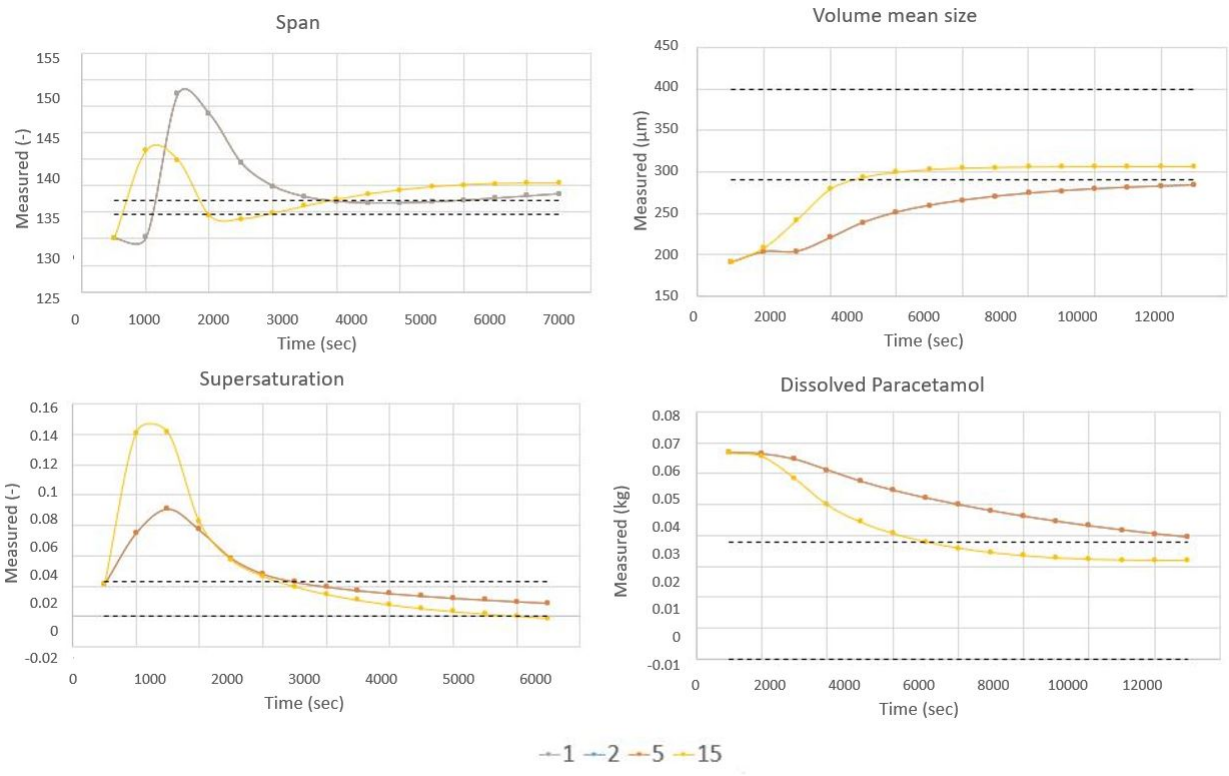

Figure 7.3: CVs measured values for different control intervals

No difference is observed between the cases of 1, 2 and 5 control intervals (they overlap), for none of the variables. One hypothesis is that the difference in horizon is not enough to allow the controller to find a better solution for the optimisation. However, for the case of 15 control intervals it is possible

to observe some changes. In span, the initial peak for a higher optimisation horizon is smaller and happens sooner. In spite of that, the end point for all cases seems to be quite similar, both outside the desired limits. When it comes to supersaturation, the opposite scenario is observed as the initial peak is higher for a higher optimisation horizon. Although a delay in this case is still present, in all cases this CV returns to its reference envelopes at the same time. For the remaining variables, the same pattern is verified as in both, the 15 control interval case not only shows a faster response, but it is the only case that complies with the control objectives. The control action responsible for the observed behaviour is depicted in figure 7.4.

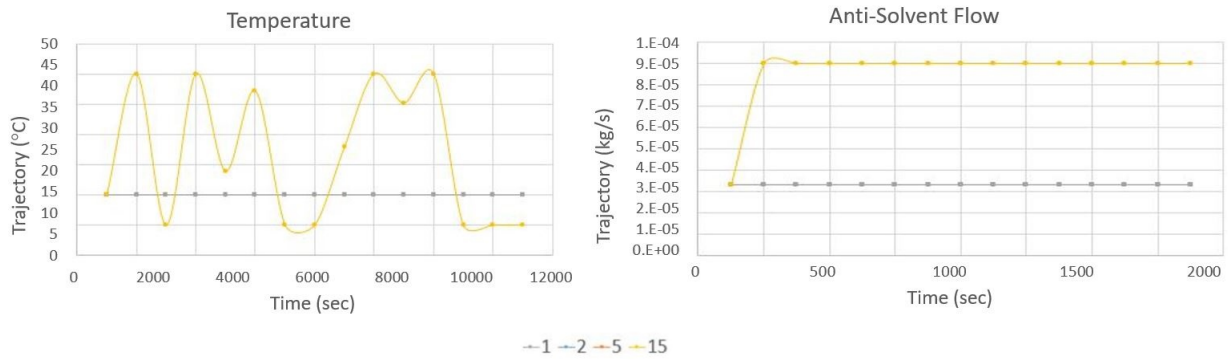

Figure 7.4: MVs for different control intervals

As expected, all cases show the same trajectory with the exception of the 15 control intervals case, in which temperature displays some oscillation in its values, whereas anti-solvent flow has a value almost three times larger than the remaining cases. In the remaining cases, both MVs remain in their initial point. It seems to be indicating that the optimisation horizon was too short for the controller to be able to find a better solution to satisfy its control objectives. Similar to the previous study, the average cycle time between cases are shown in table 7.2.

Table 7.2: Average cycle time for different control intervals

Optimisation Horizon (sec)	500	1000	2500	7500
Average Cycle Time (sec)	211	219	235	628

As expected, larger optimisation horizons take more time to run. However, the benefits of choosing a larger horizon were clear, as the controller was not able to comply with the control objectives for the shorter horizons. This study confirms what was already anticipated: the optimisation horizon should be as long as possible in terms of accuracy. One must take into account the computational burden associated with it and do a compromise, when choosing the duration of its optimisation horizon. The following scenarios were tested with a 7500 seconds optimisation horizon.

7.1.3 Prediction Horizon

In gNLMPC, prediction horizon is defined as the number of cycles ran after the optimisation horizon has finished. In other words, it is the time interval after the CVs have reached their control objectives and the controller will keep the MVs at their current value.

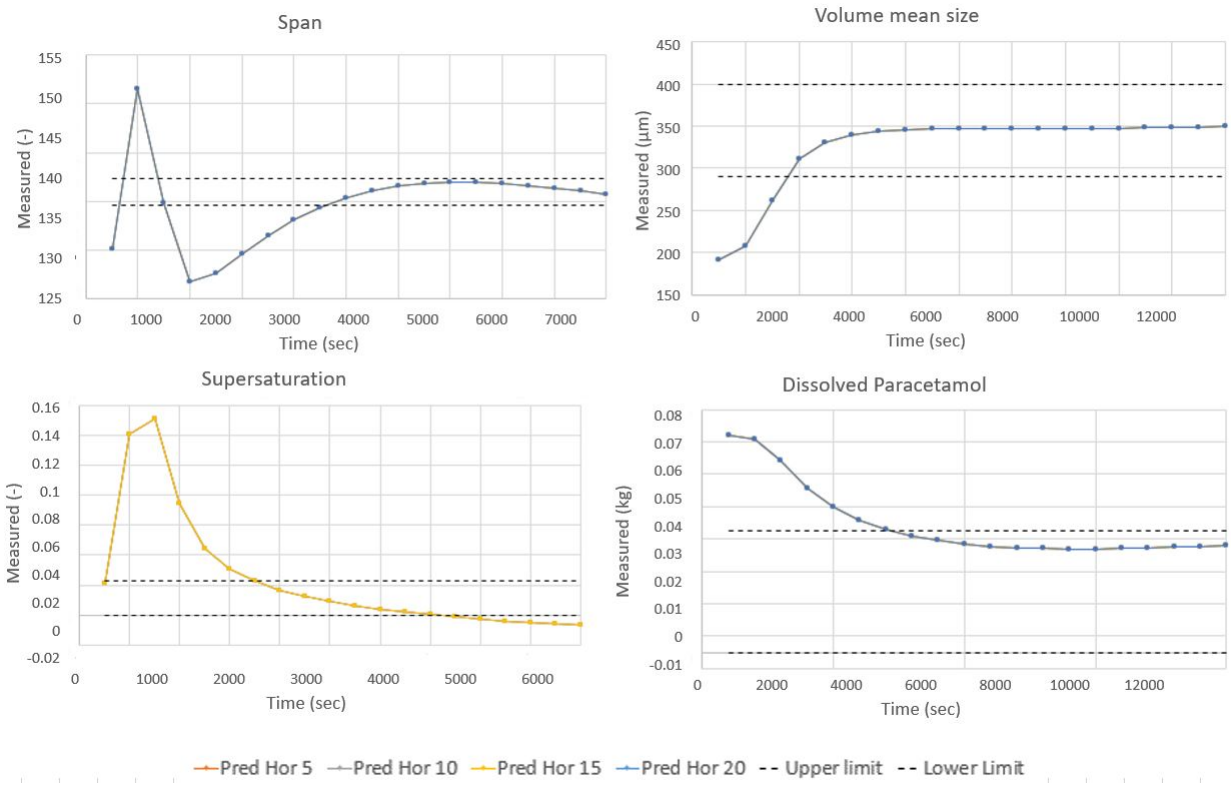

Figure 7.5: CVs measured values for different prediction horizons

For a scenario without any disturbance, different prediction horizons were tested. A prediction horizon of to 5 means 5 controller cycles were ran after the control horizon has finished. From figure 7.5, it is possible to see that the CVs are not changing with the change of prediction horizon. This may be due to two reasons. Either there is only one solution for the optimisation problem, and the controller, regardless of the prediction horizon, has only one choice of trajectory to implement, or the prediction horizon has truly no impact on the controller. Taking a closer look at the objective function 5.2 in chapter 5, one observes that only the optimisation horizon is taken into consideration. One concludes that the time interval after the optimisation horizon has no influence on the controller's optimisation. In gNLMPC, the optimisation horizon can be manipulated in two ways: either by changing the number of control intervals or the controller cycle length (both cases already discussed previously). That is the true way of altering the controller's behaviour.

7.2 Controller Testing

The controller parameters used for the testing are summarized in the following table 7.3.

Table 7.3: Controller Parameters

Controller Cycle Length	500 sec
Number of Control Intervals	15
Number of Prediction Cycles	5

The scenarios submitted to test the controller are shown next.

7.2.1 Disturbance Rejection

$\pm$ 5, + 10 and + 15% disturbance tests were performed on impeller frequency in cycle 2 of a 20-cycle emulation. The measured and optimal trajectories are presented in figure 7.6. The dotted blue line represents the closed-loop control trajectories (with the controller active), the orange one the open-loop trajectories (with the controller inactive) and the grey line the optimal trajectory (predicted by the controller). The dashed lines represent the lower and upper bounds of the reference envelopes.

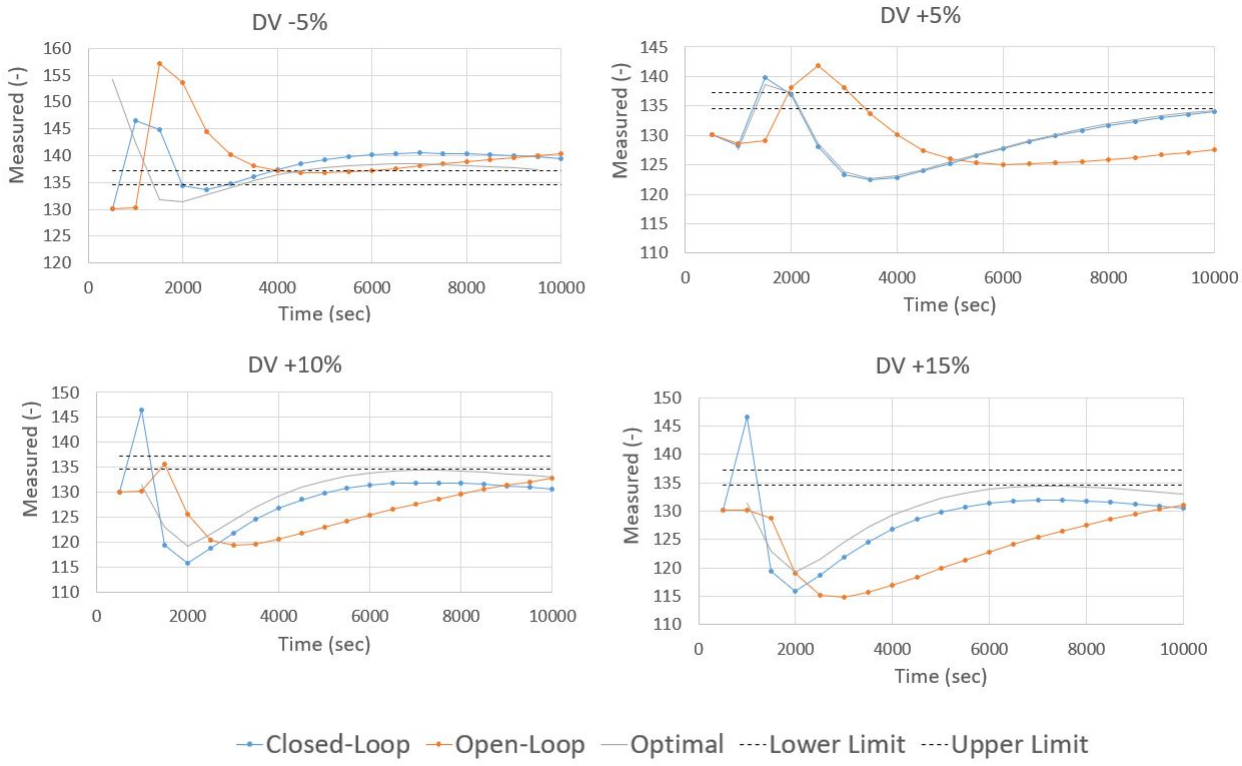

Figure 7.6: Span measured and optimal trajectories for the different disturbance rejection tests

Looking upon span's trajectories (figure 7.6), it is observed that the controller is only able to steer the CV back to its reference envelope for a + 5% disturbance, in the last cycle. For - 5% test, the measured trajectory is above the optimal one, and for the + 10 and 15% cases the measured trajectories are below the optimal ones. The possible reason for this incapacity relies on the fact that the reference envelopes are too narrow, making it harder for the controller to achieve such conservative goals. For +10 and 15% disturbances, the optimal trajectories are not able to fully return to their reference envelopes, thus confirming how restrictive the bounds are. Physically, it is more attractive for span to be as low as possible, as long as the crystals have grown. Thus, the controller's incapacity to steer this CV to its minimum bound is not worrisome.

It is possible to see that in spite of not being fully able to steer the CVs back to their reference envelopes, it is still more effective to have the controller active. With the exception of the +10% case, the closed loop response shows better results than its open loop counterpart, as the first steers the CV faster to their reference envelope.

Another aspect to notice is the mismatch between the optimal trajectory and the closed-loop one, which for a +5% disturbance is barely noticeable, but for the remaining ones, it is quite visible. This shows that the controller is not able to predict exactly the impact of the MVs on this CV, which may be due to the high degree of non-linearity associated with this particular variable.

It is possible to see in figure 7.7 that, similarly to span, supersaturation is more effectively steered

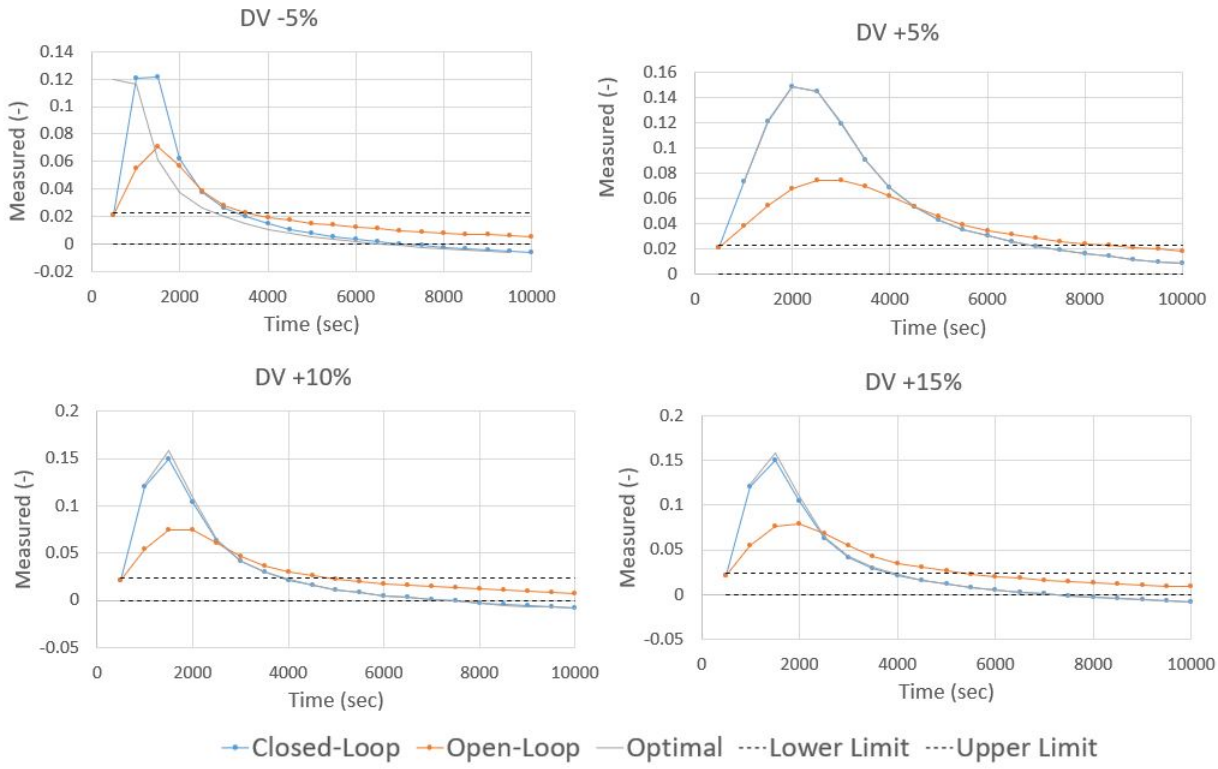

Figure 7.7: Supersaturation measured and optimal trajectories for the different disturbance rejection tests

for the + 5% step test, given that it is the only case that respects this CV's lower bound. For the rest of the cases, the measured values go below 0. When supersaturation reaches negative values, dissolution takes place of crystallization and there is no need to continue with the batch process. Hence, this lower limit violation is not only not worrisome but it is actually an advantage as the batch time can be shortened. Shortening batch time, maintaining the same control objective standards is a very attractive feature as it may result in economic savings.

Another positive result to remark is the fact that the measured trajectories are quite close to their optimal ones - they only show slight deviation in their initial peak, around 2000 seconds time. This happens because of the delay in the control actions, which is not immediately felt by the system. The match between the closed-loop and optimal trajectories is higher for this CV, when compared to the prior one, despite having less penalties associated to it. This shows that this CV is better controlled and that the control actions that lead the prior CV, span, to its reference envelopes also help this CV to reach its control objectives.

Looking upon volume mean size trajectories (in figure 7.8), one can see that the controller is able to lead this CV to its reference envelopes for both $\pm$ 5% step disturbances. Nevertheless, steepest disturbances are not as effectively controlled. In spite of being close to their optimal trajectories, measured values for the + 10 and 15% step tests are above their reference envelopes. The controller is not able to steer the CV given that it is not able to find an optimal solution inside the bounds. One possible reason for that is the fact that the penalty for this CV upper limit violation is quite low compared to other CVs, so it is not the controller's main concern to comply with this limit. In physical terms, as long as span's upper limit is not violated, it is attractive to have the highest value possible for this CV, as it translates in larger crystals.

There is a slight mismatch between the closed-loop and optimal trajectories for the -5% case, in the

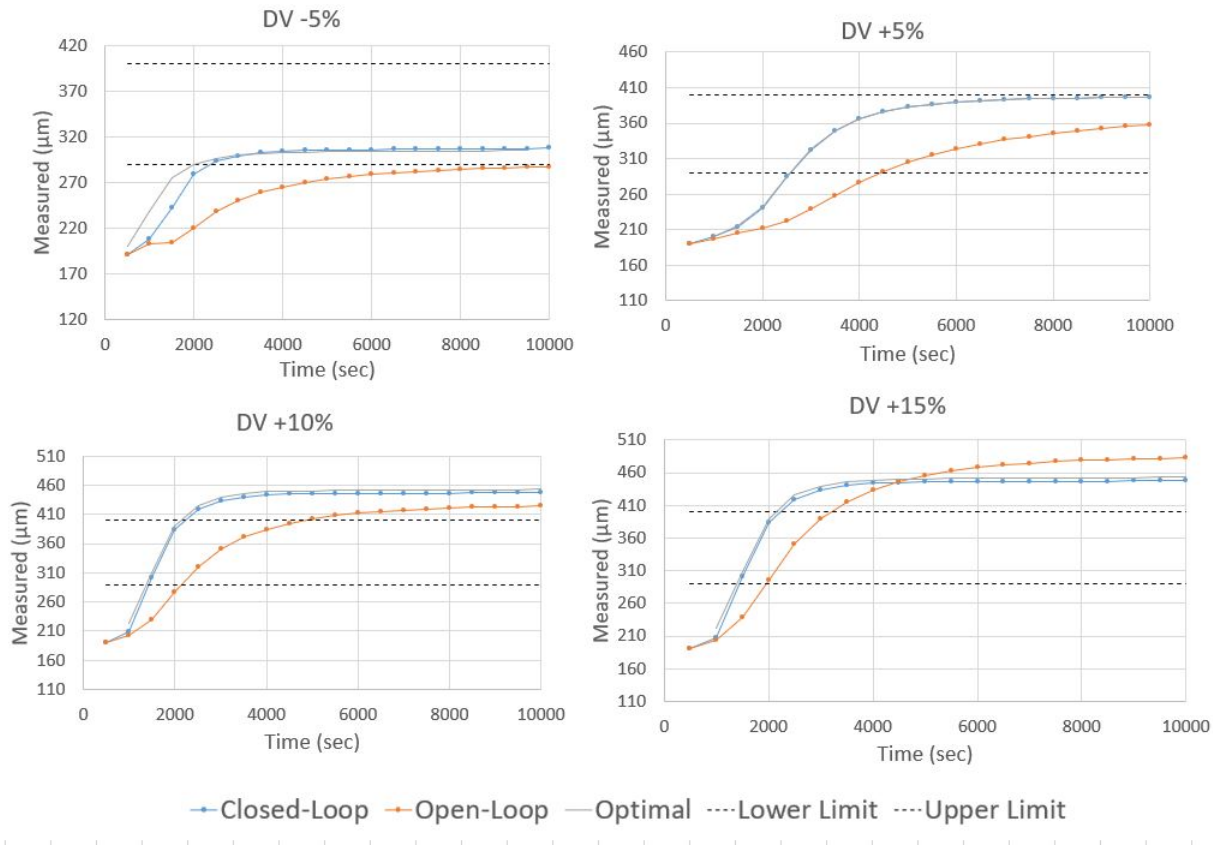

Figure 7.8: Volume mean size measured and optimal trajectories for the different disturbance rejection tests

first 2000 seconds. The reason for this has been explained in the previous sections: there is a delay in the implementation of the control action causing the initial mismatch. Nonetheless, after 2500 seconds this is no longer observed. This shows that the controller is able to predict well the impact of the MVs changes on this CV.

Additionally, regardless of the case, the closed-loop trajectory reaches the reference envelopes faster than the open-loop one, which shows the benefits of having such a control strategy implemented.

Lastly, dissolved paracetamol is able to be steered into its reference envelopes for all disturbances (figure 7.9), thus, confirming the controller's ability to meet the control objectives for this variable, despite being the lowest in terms of priority (see penalties for each CV in table 5.3 in section 5.2). This could also be due to the control actions that satisfy the more important control objectives are in agreement with the goals for this CV, which is an indication of the compatibility of control targets.

Another interesting aspect is that not only is the closed-loop trajectory faster than the open-loop one (similarly to the remaining CVs), but also for the +5% case, the open-loop trajectory does not even reach its reference envelope. This means that for this case in particular, the control objectives would not be met, if it were not for the controller. This particular CV shows clearly the benefit of having implemented such control strategy, as reaching the reference envelopes faster translates into a faster crystallization, because it means that paracetamol is transforming into crystals sooner.

Similary to the other CVs, in the -5% case, there is a mismatch between the optimal and closed-loop trajectories. However, for the remaining cases, the there is perfect match between the two. This confirms the controller's ability to predict this CV response to the control action implemented.

The MVs trajectories are depicted below in figure 7.10. As it has been seen for other disturbances, Anti-Solvent Flow heads to its upper limit and settles there for the entire emulation. One hypothesis

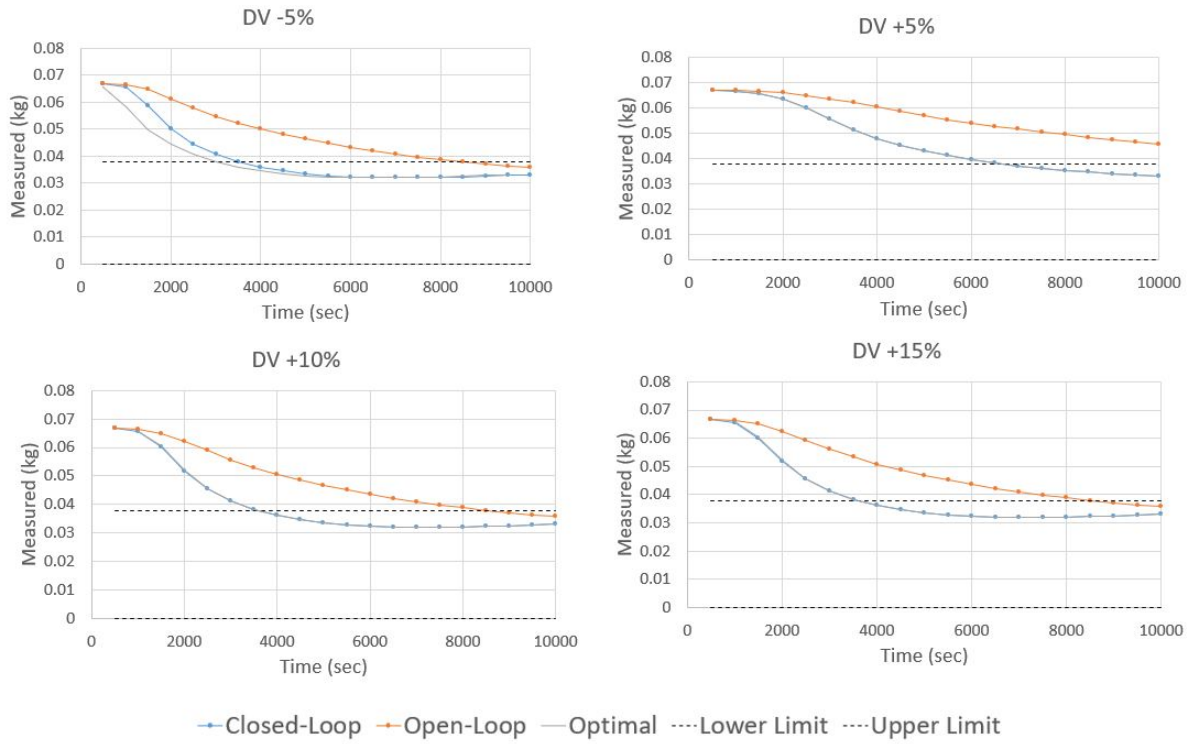

Figure 7.9: Dissolved Paracetamol measured and optimal trajectories for the different disturbance rejection tests

for this behaviour is that it is the optimal solution to maximize crystal growth, and that is achieved by promoting crystallization. This results in increasing anti-solvent flow to its maximum possible, as long as it still complies with other goals, such as particle disparity. Yet the same is not observed for temperature. A + 5 % disturbance barely changes this MV out of its initial value of 25 °C. In the rest of the cases, temperature oscillates between its bounds (from 20 to 45 °C), sometimes from one cycle to another.

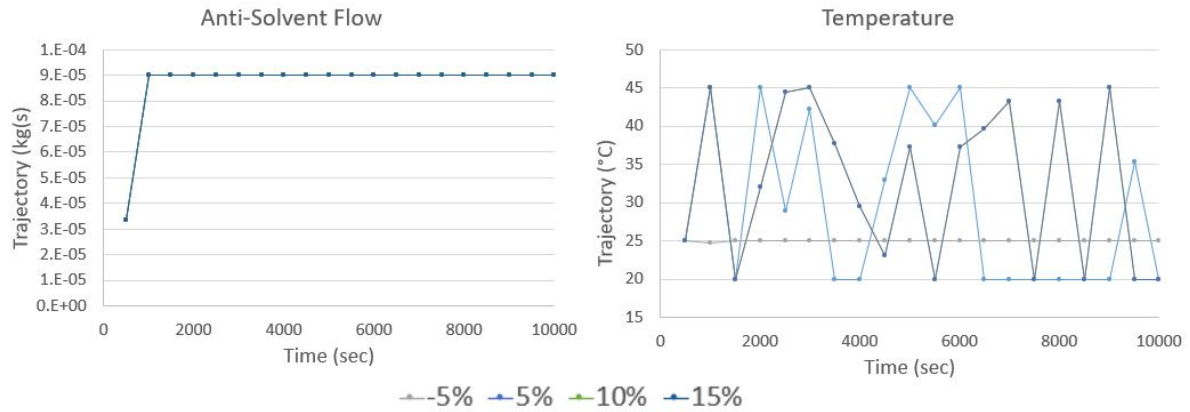

Figure 7.10: MVs trajectories to disturbance rejection tests for the different disturbance rejection tests

Another interesting aspect to notice is that trajectories for + 10 and 15 % are the same, meaning that the controller's solution to both disturbances are the same. This means that the controller may not able to cope with higher disturbance as its response would be the same.

Both MVs control actions would not be feasible in reality as the anti-solvent flow could not increase so abruptly in one single cycle, and temperature could not swing as much either. In both cases, the actuators would not be able to implement these changes so quickly, which would mean that the system

would not receive them either. This would result in increasing the plant / model mismatch, as the controller would not take into account this delay. In case of the temperature, this problem would be even more serious as the changes are not from one cycle to another, this oscillation happens throughout the emulation. So the sensors would measure a temperature, which would not be true by the time this measurement reached the controller. This would lead to the controller receiving past information, when performing its optimisation routine. In order to tackle this issue, two options were studied: adding a rate of change penalty and a control action penalty. The results for both this options will be shown below.

7.2.2 Rate of change penalty

The term C in the objective function 5.2 was activated - this meant choosing the parameters $C_i^{\delta u}$ and $|u_{i,k} - u_{i,k-1}|$, which are the penalties applied to the rate of change and the maximum rate of change allowed per cycle for the MVs. Adding a penalty to the rate of change is the way to tell the controller to find a new solution that avoids a rapid change between variables. The rate of change per cycle refers to the maximum change the controller allows for that variables, between cycles.The rates and penalties applied in each MVs are shown in table 7.4.

Table 7.4: Rate of change and penalties for both MVs

Variable	Rate of change per cycle	Penalty
Anti-Solvent Flow	1E-5 kg/s	1E5
Temperature	1 °C	1

The rate of change penalty for temperature was chosen according to literature [36]. The order of magnitude of the penalty between the variables is not due to importance but for units reasons, given that the objective function is not scaled. A -5% disturbance step was performed and the differences between the original case without rate of change penalties and the modified one with the penalty were compared. The MVs trajectories are shown in figure 7.11.

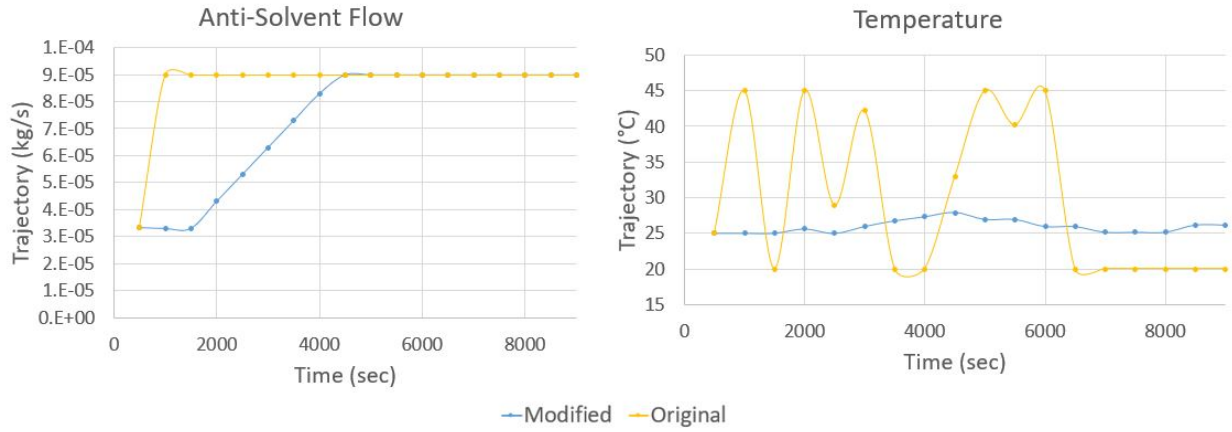

Figure 7.11: MVs trajectories with and without the rate of change penalty

It is possible to verify that the addition of a penalty was successful, as anti-solvent flow takes more time to reach its optimal value (of 9E-05 kg/s) and temperature shows a lower degree of oscillation. It is

also worth noting that whereas temperature effectively oscillates less, meaning another optimal solution was found, different from the original one, regarding anti-solvent flow, this does not hold true. Given that this variable changes its maximum allowed per cycle, one can conclude that the controller was not able to find a new optimal solution, but instead just complied with the penalties given.

The next aspect to verify was whether the controller had been able to achieve the desired control targets despite the penalties. The CVs trajectories are depicted in figure 7.12.

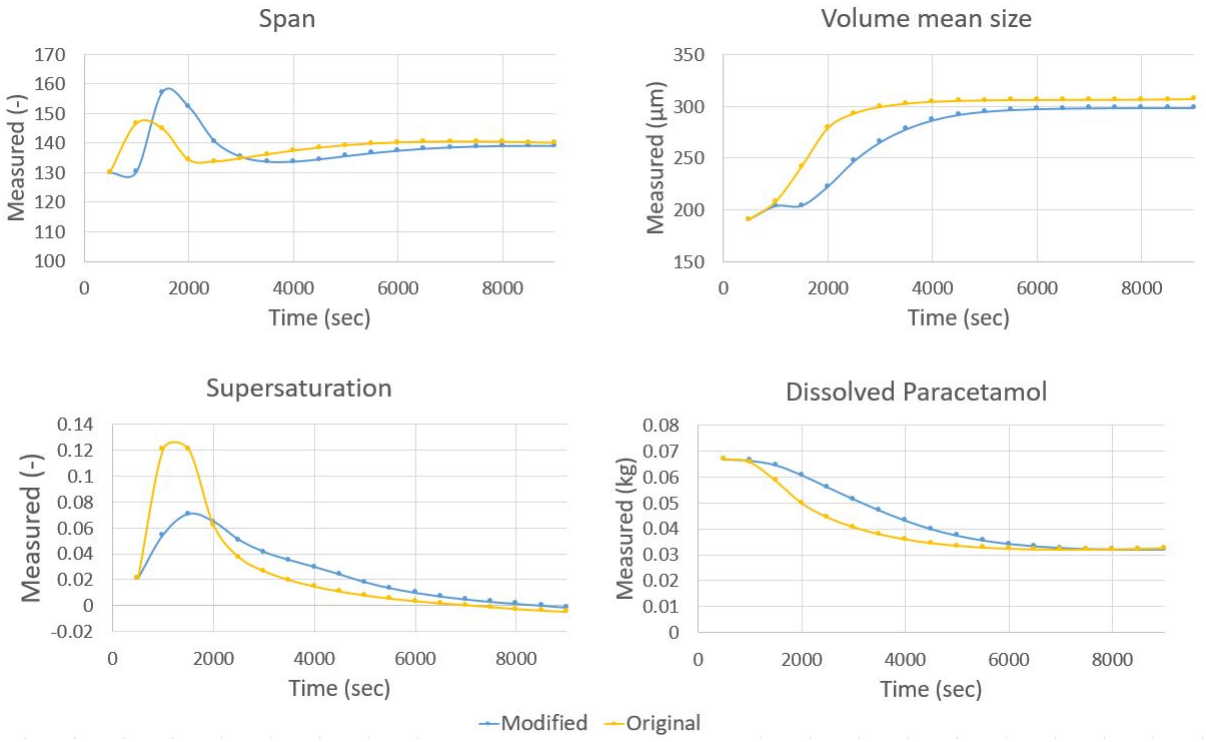

Figure 7.12: CVs trajectories with and without the rate of change penalty

As expected, the CVs were affected by the change: in the modified case, the trajectories show a slight delay when compared to the original case. Nonetheless, with the exception of volume mean size, in both cases, the end-point is similar, which seems to indicate that the penalties added did not prevent the controller from reaching its goals. The fact that the rate of change penalty made the variables rate of change slower confirms the optimality of the original solution, as it leads the CVs sooner to their reference envelopes, which is an advantage.

In the disturbance rejection test (section 7.2.1), the controller was able to find its optimal solution in the second cycle - the optimal trajectory was the same for the remaining cycles, as there was no plant / model mismatch. However, after adding a rate of change penalty, it was observed a different behaviour - the controller optimised distinct trajectories for the first 5 cycles, depicted in figure 7.13.

From figure 7.13, it is possible to see the CVs evolution throughout the emulation. With increasing the number of cycles, the optimal trajectory of the CVs, becomes faster and better at reaching the target limits. The differences between cycle 1 and cycle 6 are quite clear, particularly for dissolved paracetamol, where the last cycle takes less 3000 seconds than the first. This analysis demonstrates how the controller progressively improves its optimal trajectory to better respond to the disturbance subjected.

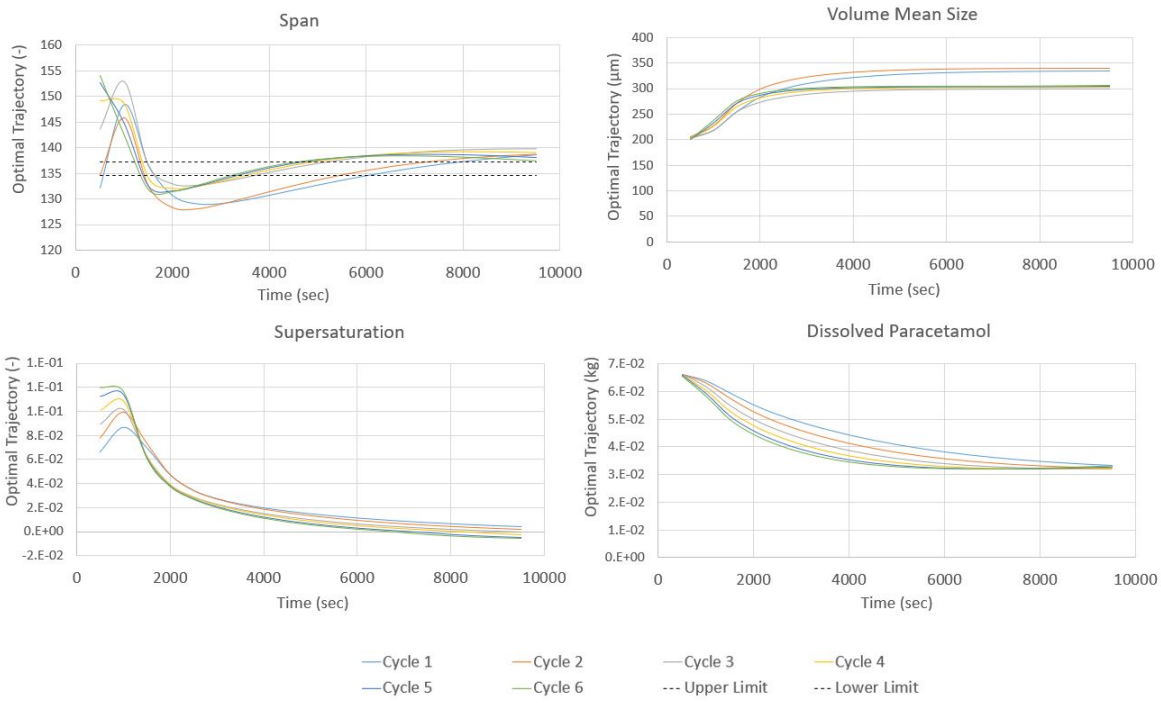

Figure 7.13: CVs optimal trajectories for different cycles

Anti-Solvent Flow rate of change

As no literature had been found with rate of change for anti-solvent flow, rates of change of the MV Anti-Solvent Flow were tested to analyse their impact on the controller actions, and conclude which one would be most suitable for the current case. Rates of change of 0.5, 1 and 2E05 kg/s were tested. The MV trajectories for the three different cases are shown next in figure 7.14.

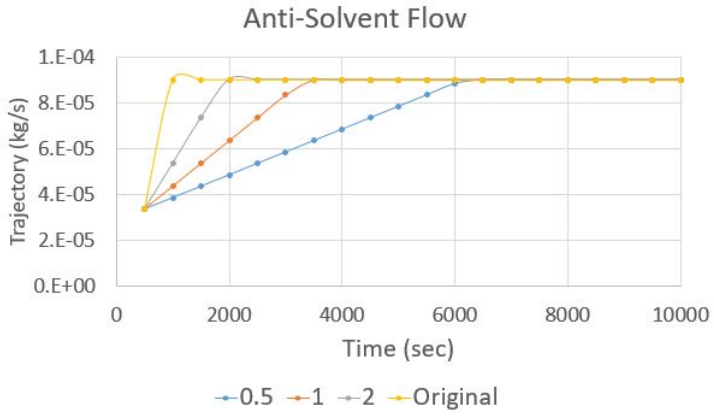

Figure 7.14: Anti-Solvent Flow trajectory for different rates of change

As expected, faster rate of change results in larger steps between cycles, and, as it was stated in the previous section, the controller is not able to find another optimal solution. It just limits itself to take longer to reach its upper limit, to comply with the penalties added.

Looking at the CVs (figure 7.15), it is possible to verify that despite the trajectories being different for all the cases, the controller is still able to steer them into their reference envelopes. This is because the rate of change was not slow enough to compromise the control objectives. Even the slower rate of change, the 0.5 case, only allows the anti-solvent flow to increase or decrease a maximum of 0.5E-5 kg/s per cycle, which results in this MV, only reaching its upper limit in cycle 12. Still, for all CVs except

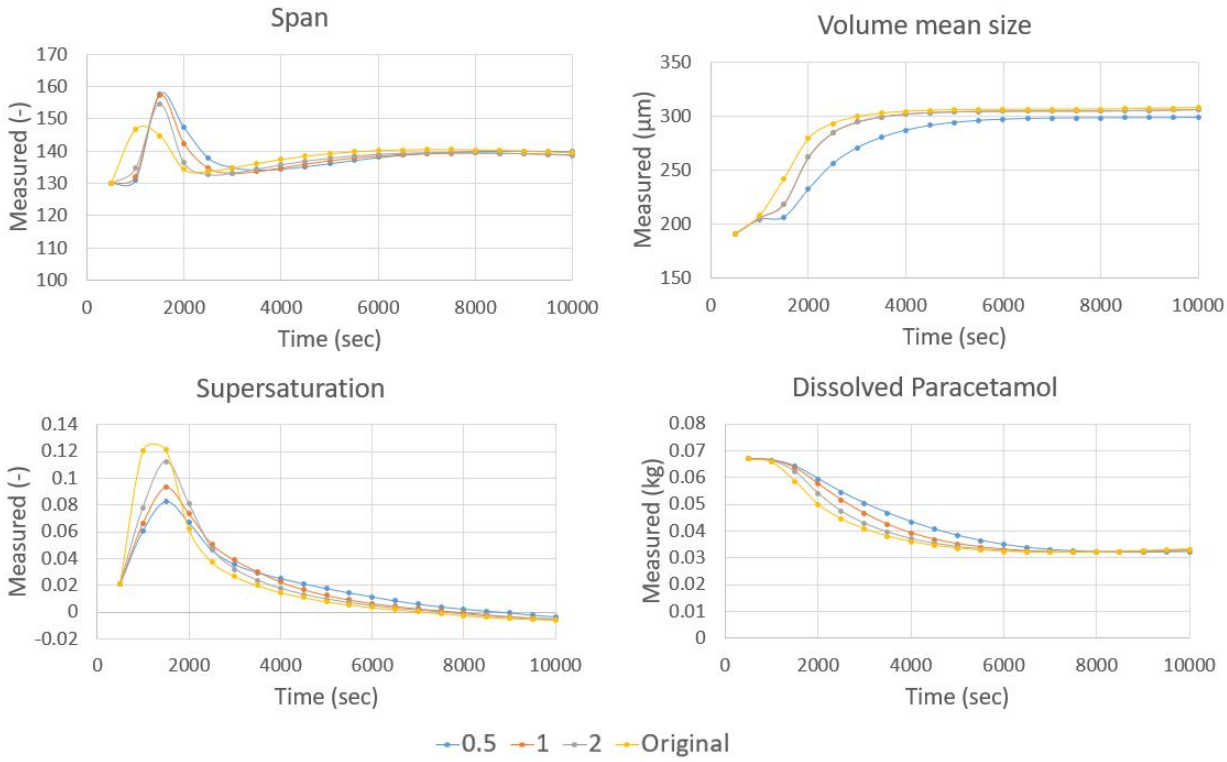

Figure 7.15: CVs measured values for different Anti-Solvent rates of change

volume mean size, in less than 4 cycles, there is no observable difference between the cases. For volume mean size, the 0.5 case is not able to lead it to the same end-point as the remaining cases. However, it still complies with its lower limit of 290, which is the main concern of the controller.

7.2.3 Control action Penalty

Another means to achieve the same end could be adding a penalty for the controller moves specifically, instead of penalizing the moves at the bounds change. This was achieved by activating term B of the objective function, equation 5.2. The activation included assigning values to the MV cost penalty, C_j^z. Penalties 10 and 100 were tested, for a -5% disturbance step test, and the results were compared with the original case, without any penalties. The MVs trajectories are shown in figure 7.16.

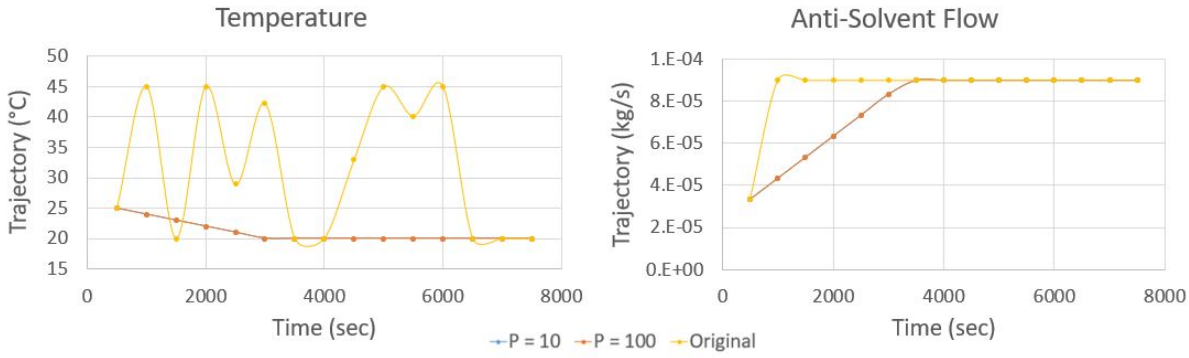

Figure 7.16: MVs trajectories under a control action penalty

Anti-Solvent Flow took longer to reach its upper bound and temperature did not show any oscillation,

but rather decrease its initial value to 20°C and remained there until the end of the cycles. The MVs trajectories were the same regardless of the penalties, indicating that the penalties had no impact on the controller. The CVs path is shown next (figure 7.17).

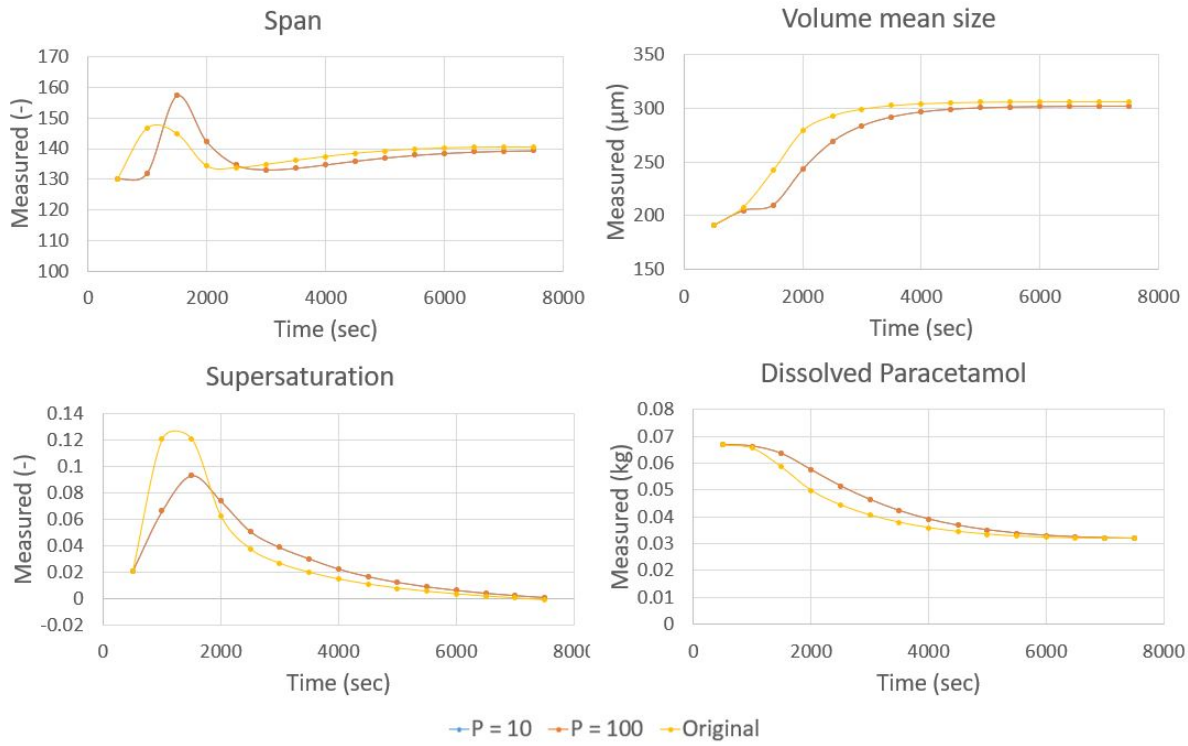

Figure 7.17: CVs setpoints under a control action penalty

Although their trajectory is slightly different, all CVs end their trajectory in the end in the same value for both cases. This shows that the changes in control action penalty did not affect the controller reaching its control objectives. This is because the delay in reaching the optimal value did not compromise the control objective of settling inside the reference envelope. The CVs trajectories were the same for both penalties given that the MVs trajectories were the same as well.

The MVs trajectories for both types of penalties were compared, to reflect on which one would be most suitable for the current case (figure 7.18).

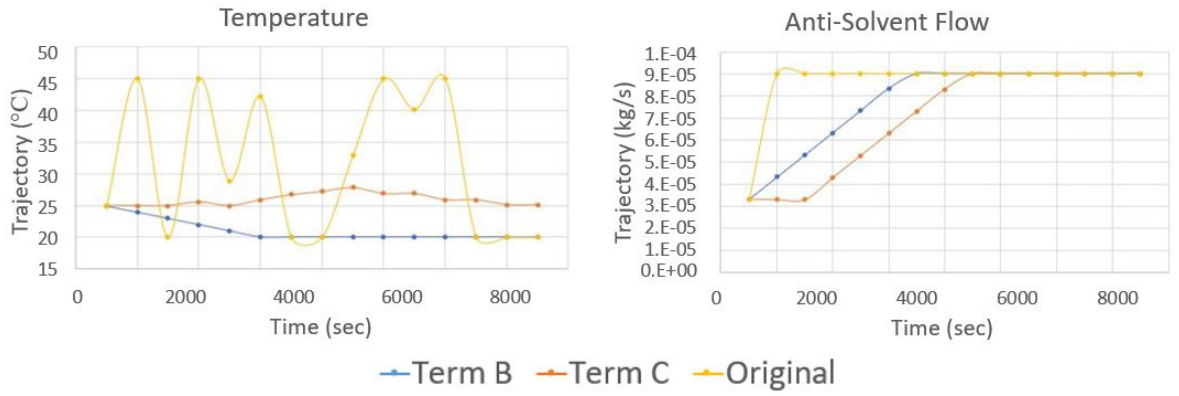

Figure 7.18: MVs trajectories for different types of penalties

Regarding temperature, both methods seem to yield feasible results, although the objective function with term B shows a more rapid decrease in values. When it comes to anti-solvent flow, the same

remarks are viable, as both terms seem to show viable solutions, however, using term C penalties is a more conservative option, given that it takes slightly more time increasing and it only starts to do so after 3 cycles.

The CVs for the original and both cases of penalties are shown in figure 7.19.

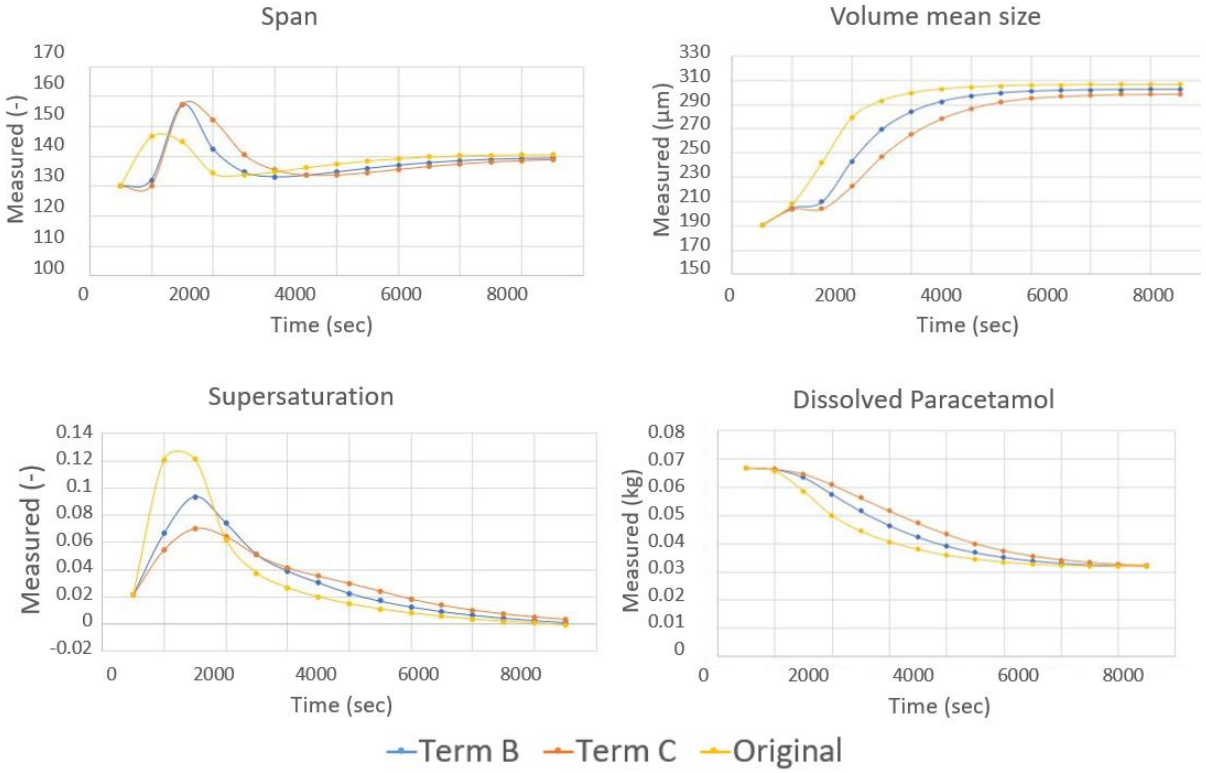

Figure 7.19: CVs setpoints for different types of penalties

From figure 7.19, it seems that the penalties using term B result in slightly faster responses than using term C. One of the reasons to that may be the fact that MV Anti-Solvent Flow shows a higher delay with term C, when compared to term B (figure 7.18). Nonetheless, both terms lead to the controller reaching its control objectives.

7.2.4 Anti-Solvent Effect

As it has been observed previously, anti-solvent flow seems to be tendentiously hitting its upper bound, in many of the scenarios tested. Thus, a global system analysis was conducted in order to find an explanation as to why the anti-solvent flow always hit its upper bound. This gPROMS feature is essentially a sensitivity analysis where the relationships between some input variables (called factors) and output variables (called responses) are analysed. The input variables are changed within some specified bounds and the impact on the responses is analysed. For this global system analysis, anti-solvent flow was chosen as a factor and the controlled variables as the responses. The results are shown in figure 7.20.

One can see that the higher anti-solvent flows values clearly maximizes volume mean size and minimizes supersaturation, which were the control objectives for these CVs. These were possibility the main factors contributing to this MV trajectories hitting its upper bound. Another CV, span, shows an oscillating relation with anti-solvent flow, inside a narrow range of values. Hence, it may not have contributed so bluntly as the previous two CVs. This nonlinear relationship between span and Anti-Solvent Flow may explain why this variable was the one the controller struggled the most in steering into

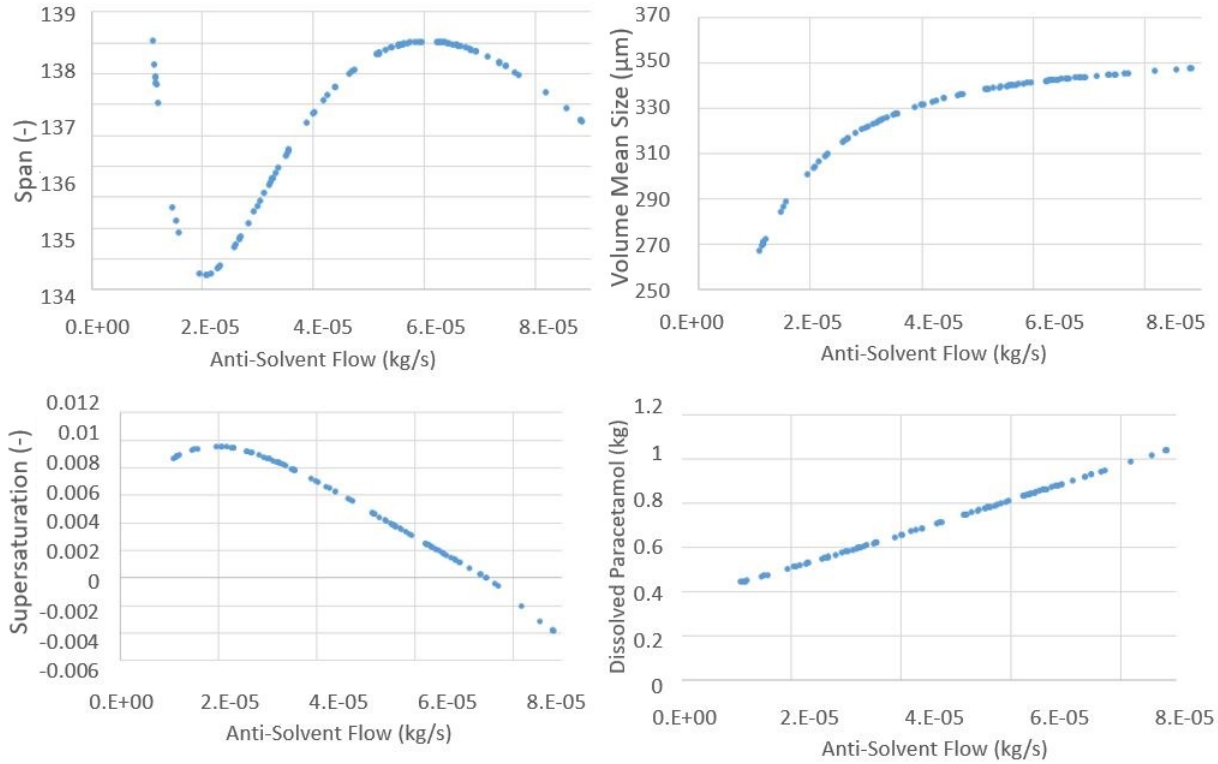

Figure 7.20: Global System Analysis Results - Responses

its bounds, despite being the one with higher penalties. In other words, due to the non linear nature of the relationship between these two variables, the controller had more difficulty in choosing the correct Anti-Solvent Flow that satisfied the span's control objectives.

Furthermore, lower anti-solvent flows led to less dissolved paracetamol at the end of the batch. Nonetheless, given this was a secondary objective (reaching Particle Size Distribution goals like volume mean size was more important - see penalties table 5.3 on section 5.2), a minor penalty was implemented, thus, the controller setpoints did not show this tendency.

The sensitivity analysis confirmed that the controller was implementing the more suitable trajectory for the anti-solvent flow, given that they are in agreement with the control objectives.

7.2.5 Noise

As referred in section 6.2, noise was added to one of the measurements, span, which is also a CV. Step changes on DV impeller frequency were performed (similarly to the ones done in section 7.2.1), and compared the original case with the case with the noise added. The CV trajectories for both cases is shown in figure 7.21.

From figure 7.21, it is possible to verify that the noise was successfully added to the CV, as its trajectory shows a higher degree of fluctuation, when compared to its original trajectory. In spite of having noise, at the end of the emulation, this CV reached the same end point as the original case. This indicates that the controller was able to accomplish the targets and perform noise rejection.

The MV anti-solvent flow trajectories is not shown as the addition of noise did not affect this variable's values (in all cases, this variable hit its upper bounds, as expected). However, temperature showed different values (figure 7.22).

In both cases (with and without added noise), temperature shows quite some oscillation. For a $\pm$ 5%

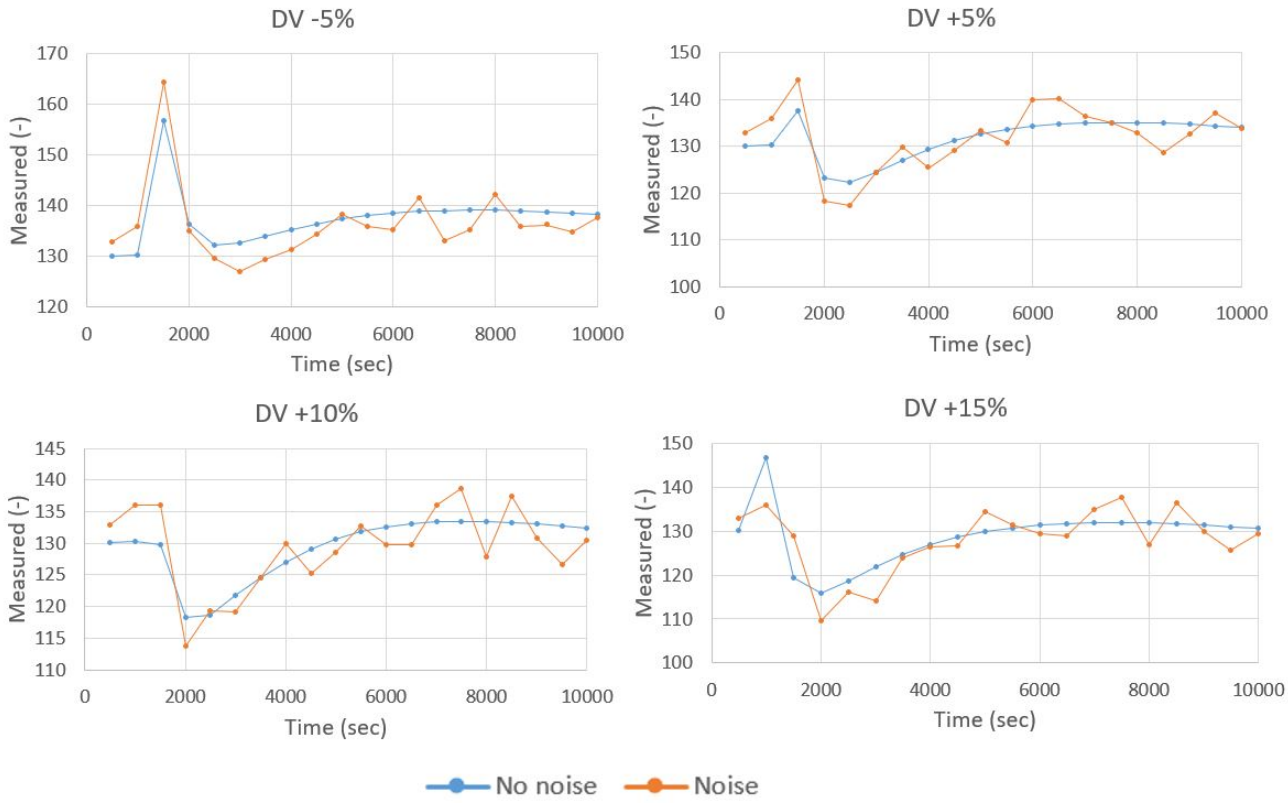

Figure 7.21: CV Span with and without noise

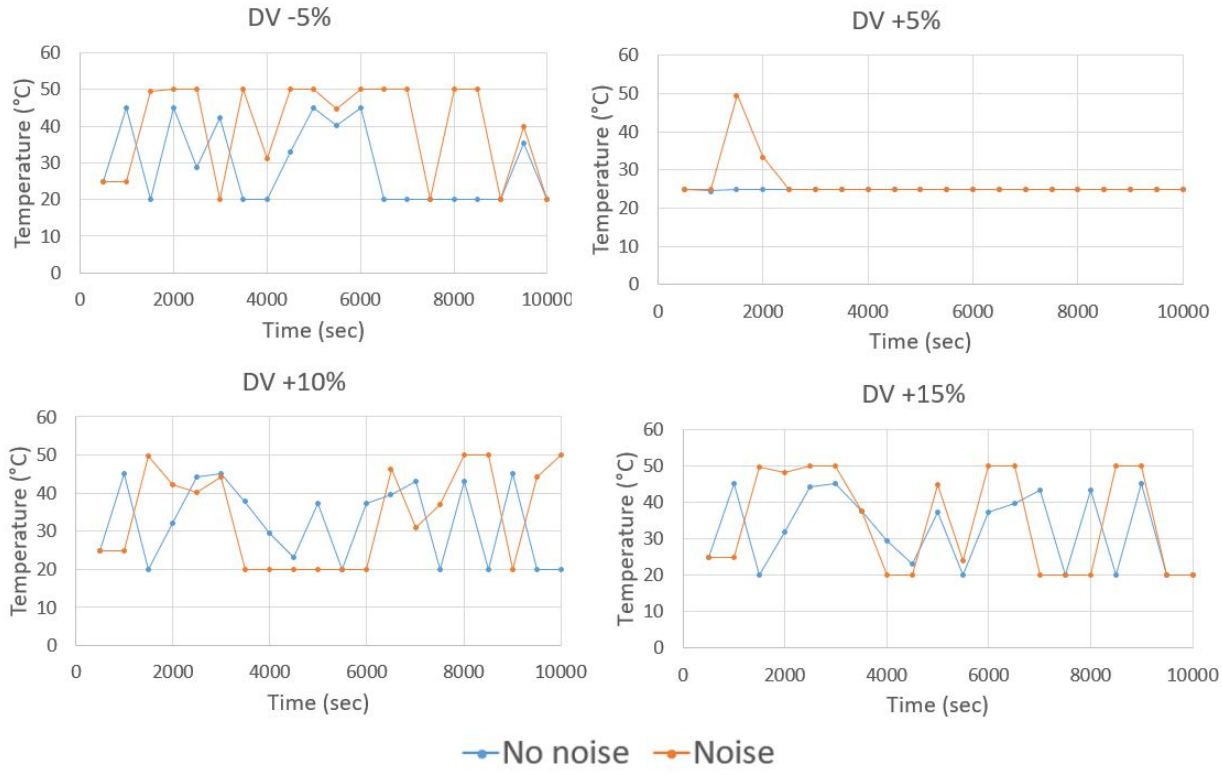

Figure 7.22: MV Temperature with and without noise

disturbance change, the case with added noise seems to have more oscillation. For the + 10 and 15% both scenarios, with and without noise, display the same degree of oscillation, without a clear pattern.

A controller able to tackle measurement noise rejection is a clear advantage. In the current case, this variable was not only a CV, but the most problematic one, as it was possible to verify throughout the several disturbance rejection tests performed (shown in 7.2.1). Span was the CV most affected by the different cycle lengths. It was also the CV that the controller struggled the most to lead to its reference envelopes in the disturbance rejection tests. These facts all point to the overall good performance of the controller in handling noise measurement rejection.

7.2.6 Plant / Model Mismatch

As explained in chapter 6, one of the kinetic parameters of the model was changed, in order to determine the robustness of the controller. This scenario is also important to analyze how accurate the kinetic parameters have to be. The wider the tolerable region of acceptance of the kinetic parameters, the more robust the controller is.

A minus 5% change in the model parameter ”supersaturation order” was conducted. This parameter is used in the nucleation rate expression, described by equation 4.1 in chapter 4.

The envisaged idea was to perform the usual disturbances of $\pm$ 5 and + 10% on the impeller frequency and see whether the controller was able to steer the CVs back to their reference envelopes as usual.

For a -5%, the CVs trajectories are shown in figure 7.23.

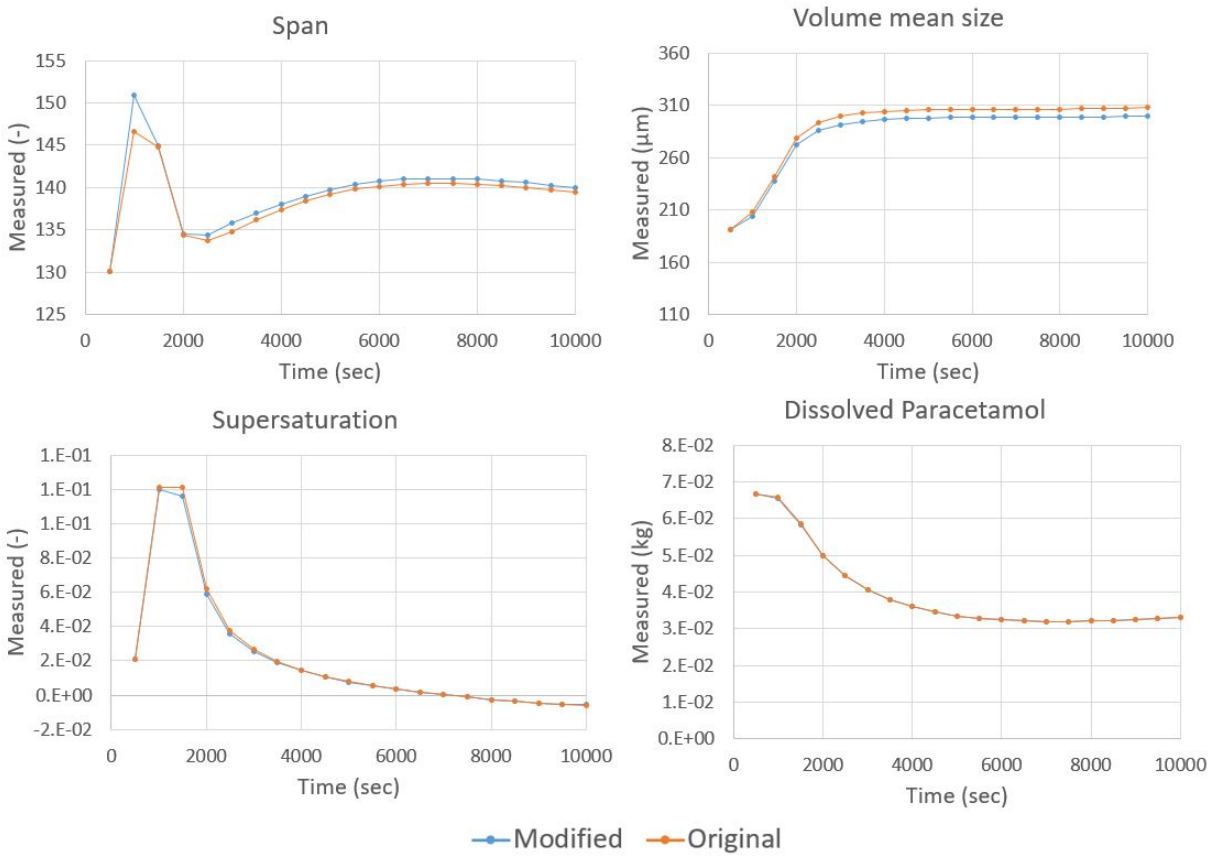

Figure 7.23: CVs measured values with and without model parameter mismatch for a minus 5% disturbance on impeller frequency

The model parameter change is barely noticeable. In CVs supersaturation and dissolved paracetamol the trajectories are the same. However, despite still being settling inside the reference

envelopes, span shows slightly higher values for the original parameter, whereas volume mean size slightly lower.

Regarding MVs, Anti-Solvent Flow exhibits the usual behaviour of settling in its upper bound of 9E-05 kg/s. Temperature is shown in figure 7.24.

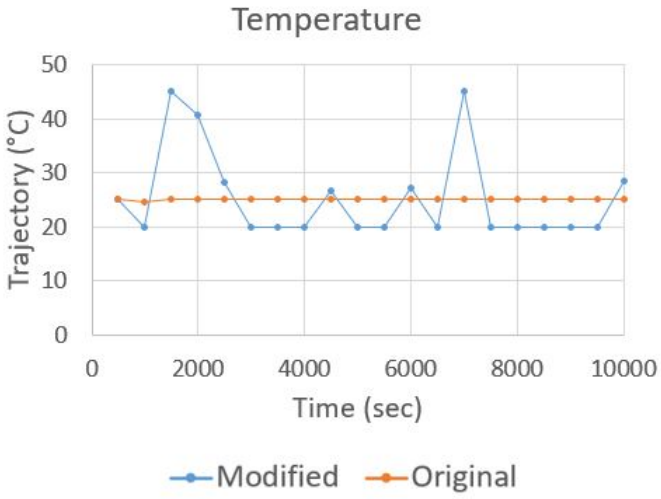

Figure 7.24: MV Temperature with and without model parameter mismatch for a minus 5% disturbance on impeller frequency

The modified case shows a more oscillating behaviour, when compared to the original case.

For a +5% step change on disturbance variable (figure 7.25), the scenario is very different from the previous case, as the trajectories for the CVs are different. Span seems to show overall lower values throughout the emulation, whereas the remaining variables display the opposite tendency. A slight delay is also observed. Nonetheless, for all cases, the end-point is very close to the original case, showing the quality of the controller.

It seems that controller continues to show its oscillating behaviour with or without the model parameter disturbance (figure 7.26). Although the modified case seems to swing less. The other MV anti-solvent flow is not shown as it shows its normal behaviour of hitting its upper bound. Lastly, for a + 10% step change on impeller frequency (figure 7.27), the differences between the CVs seem less than for the + 5% case. Supersaturation and dissolved paracetamol are practically the same. Volume mean size exhibits a slightly lower value, and Span a slightly higher value. The overall changes are less visible than expected taking into account the + 5% case.

For this case, temperature shows the same degree of oscillation for the original and the modified scenarios (figure 7.28). The observed delay in the CVs is not observed in the MVs trajectories. Anti-Solvent Flow is not shown as it displays the usual behaviour.

The overall results of this scenario are positive, as the controller was able to steer its CVs into the same end-point despite the model parameter change. It seems as if the controller is capable of handling some degree of plant/model mismatch. MV anti-solvent flow exhibits the same pattern as before. This indicates that for a mismatch of this magnitude, setting this variable to its upper bound is still enough to steer the CVs into their limits. MV temperature showed a very oscillating trajectory between cases. From these scenarios, the question as to why is temperature oscillating so much arose. In the + 10% case, temperature swings between its bounds in both the original and the modified case. The oscillation is not the same, whereas the CVs are practically the equal. This led to the following question: how much impact does temperature really have on the CVs. A study on how much this MV affected the CVs was conducted in order to determine the reason behind such an oscillating behaviour.

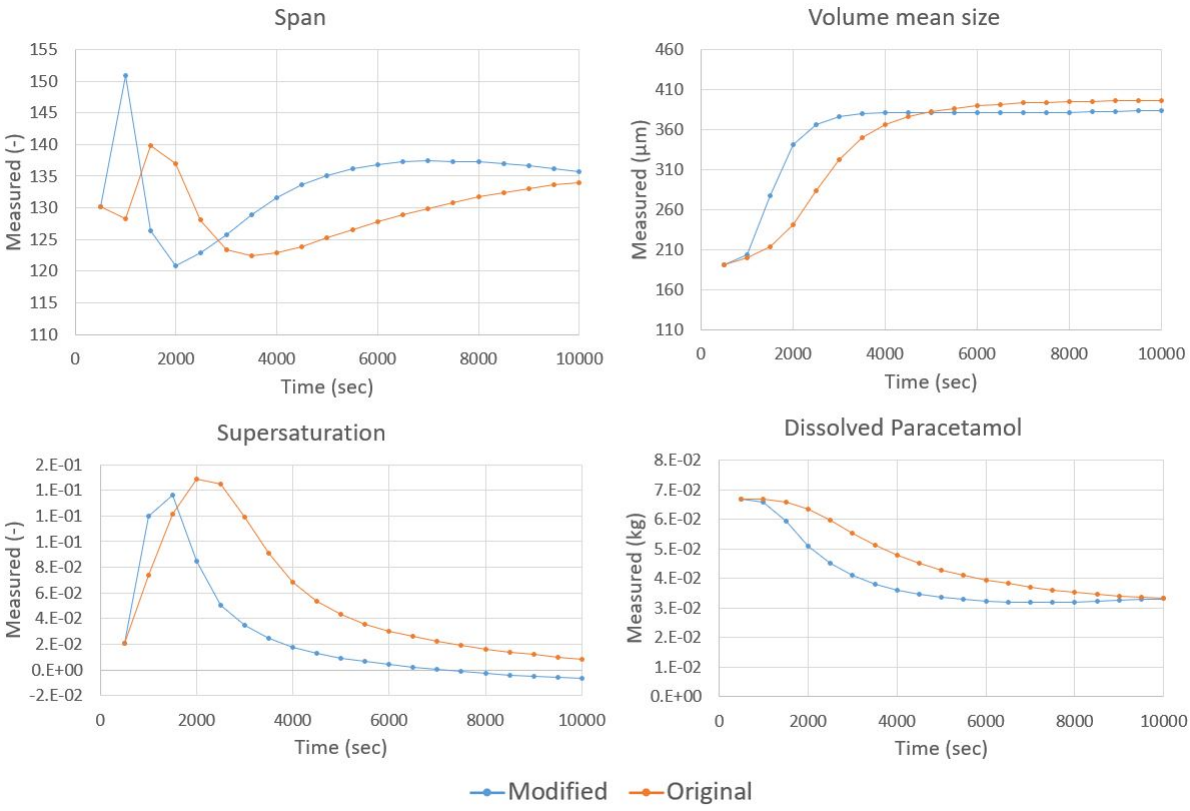

Figure 7.25: CVs measured values with and without model parameter mismatch for a plus 5% disturbance on impeller frequency

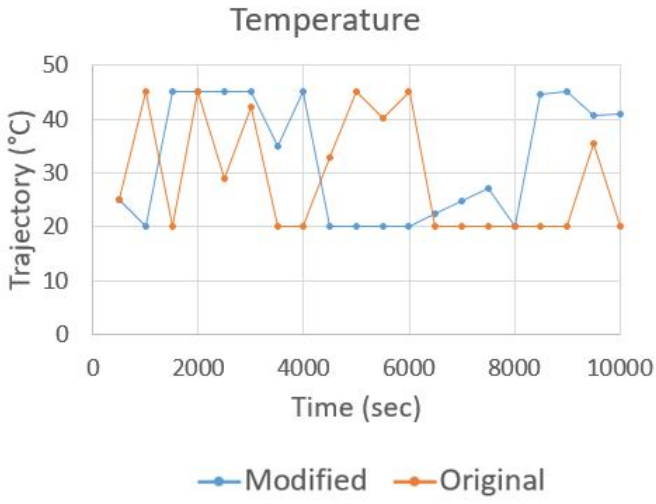

Figure 7.26: MV Temperature with and without model parameter mismatch for a plus 5% disturbance on impeller frequency

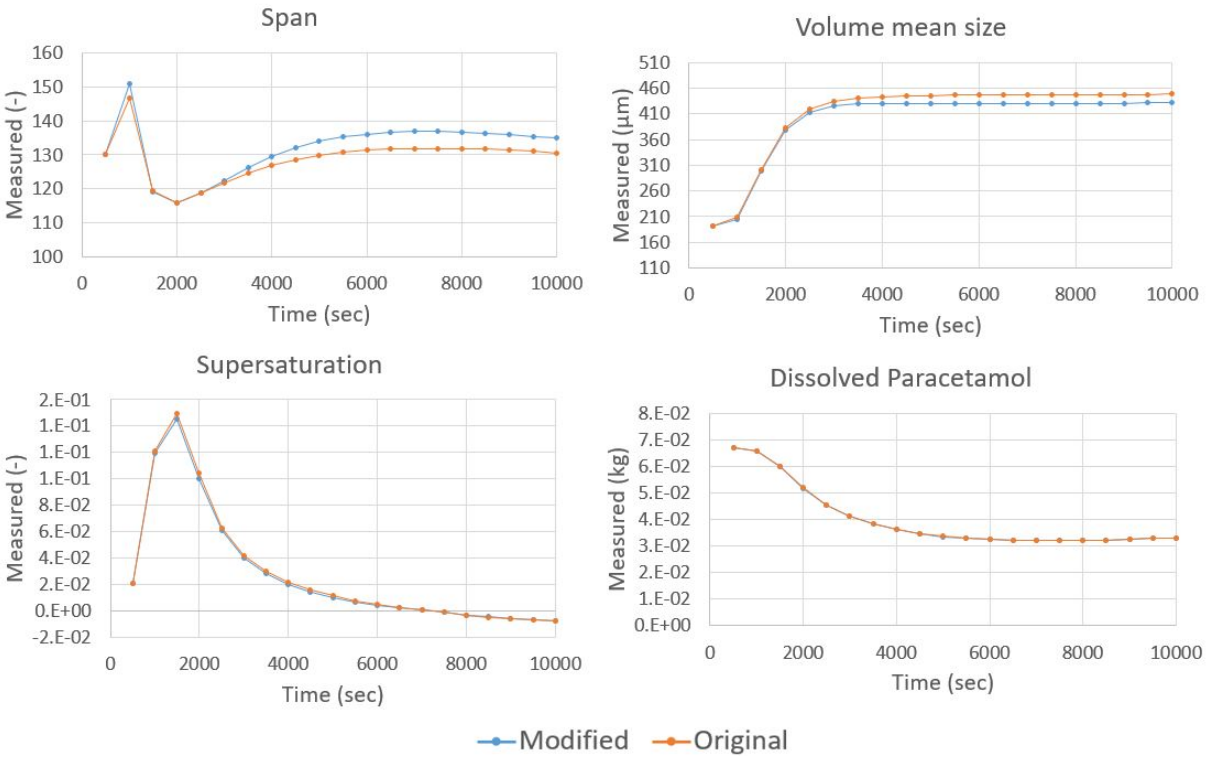

Figure 7.27: CVs measured values with and without model parameter mismatch for a plus 10% disturbance on impeller frequency

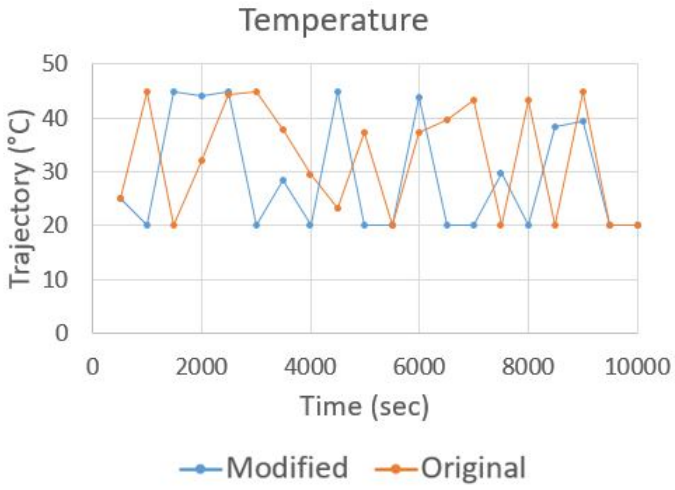

Figure 7.28: MV Temperature with and without model parameter mismatch for a plus 10% disturbance on impeller frequency

7.3 CV Trajectory Penalties

To confirm the hypothesis of the differences in the impact of the MVs, the penalties for the CVs violating their bounds (parameters $C_j'^{z,lo}, C_j'^{z,hi}$ in the objective function, equation 5.2 in chapter 5) were changed, while keeping the penalties for the rest of the CVs constant. This test was made to check whether increasing or decreasing the importance of each of the CVs changed the controller's behaviour or not. For this test, only term A of the objective function (equation 5.2 in section 5) was active.

7.3.1 Span

Span was given the following values for its reference envelope violations: 0.1,1,10,100 and 1000. For a +10% disturbance, a 20-cycle emulation was performed. The different penalties did not change neither the optimal path calculated by the controller nor the measured values. All the cases are displayed in figure 7.29.

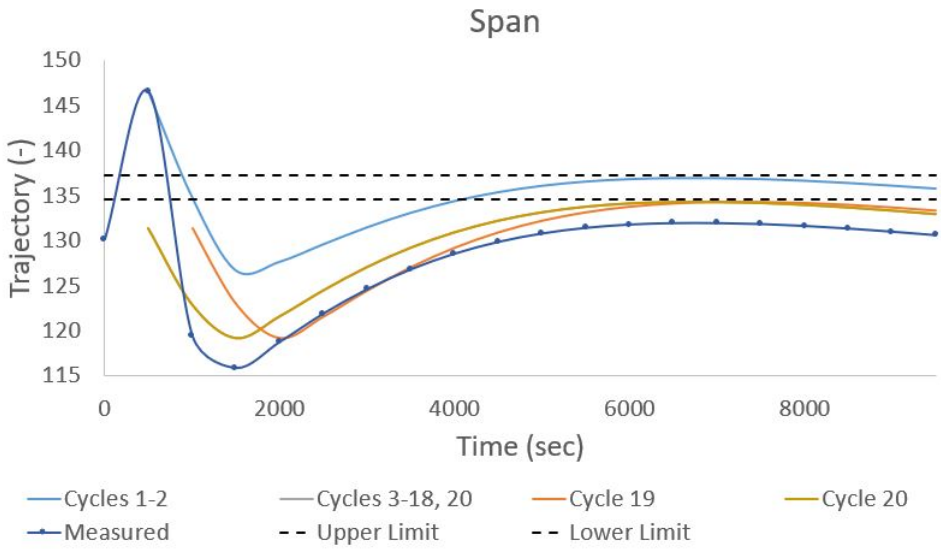

Figure 7.29: Span's Optimal and Measured Trajectory

The word "cycle" refers to the controller cycles, which is done at every 500 seconds of emulation. At each cycle, the controller produces a new optimal trajectory. Cycles 1 and 2 have different optimal trajectories from the rest because the step disturbance was only introduced in cycle 2 (and the system received it in cycle 3). It is also possible to testify the mismatch between optimal and actual trajectories, specifically in the second half of the emulation. The controller is also not able to steer the CV back to its reference envelope. One possible reason for that is the very narrow window between upper and lower envelope limits.

The different reference envelope violations have impact on MV temperature trajectories, as it is possible to observe in figure 7.30. As expected, higher envelope violations lead to higher oscillation between MVs bounds (20 to 50 °C) in the values calculated by the controller. One concern regarding oscillation is the physical constraint associated to it: the actuators would not be able to increase system's temperature in 25 °C from one cycle to another. Hence, if the most suitable option was to use higher envelope violation penalties, then one would have to add a MV movement penalty to prevent such rapid moves. MV anti-solvent flow settles at its upper limit, without changing it.

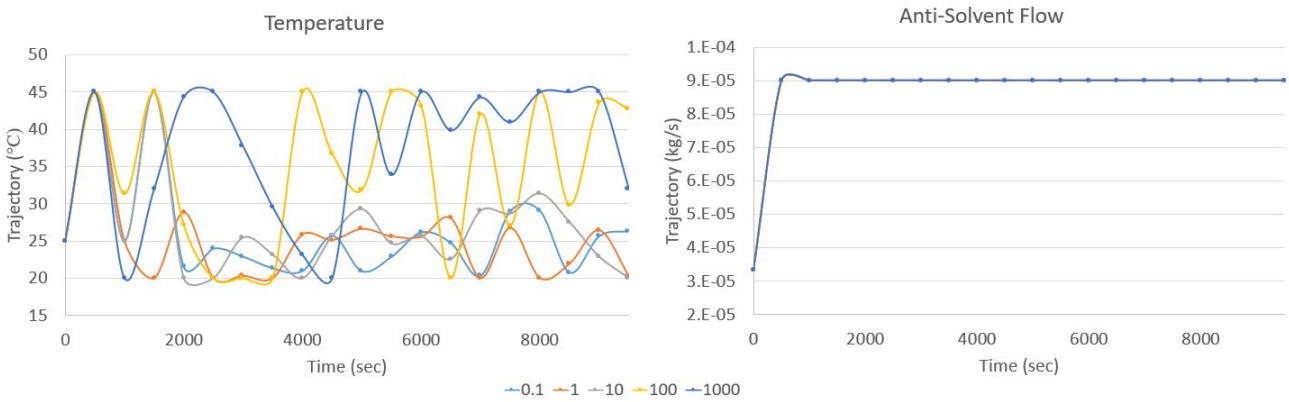

Figure 7.30: MVs trajectories

7.3.2 Supersaturation

The reference trajectory penalties were changed for the supersaturation (for the values 0.1,1,10 and 100) and the results are depicted in figure 7.31.

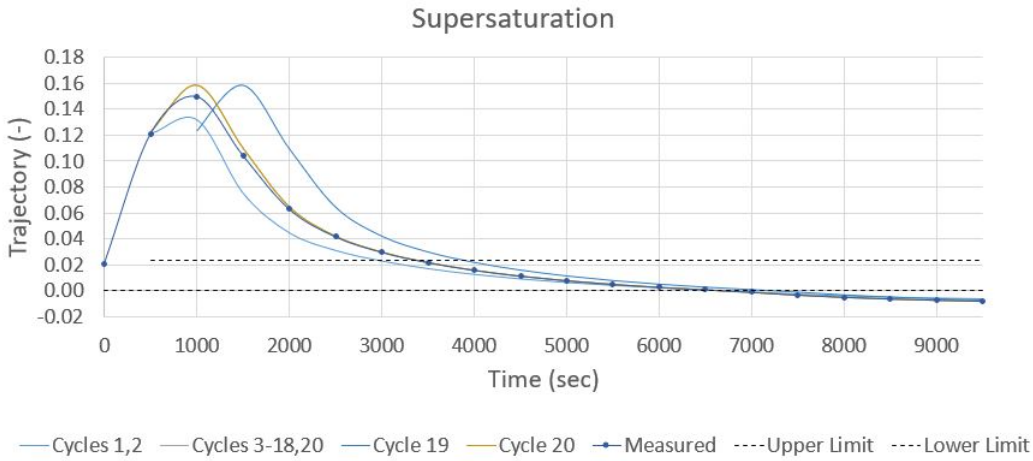

Figure 7.31: Supersaturation's Optimal and Measured Trajectory

As it was shown for span, supersaturation seems to be unaffected by penalty changes, although one of the MVs, temperature shows quite an oscillating trajectory (figure 7.32).

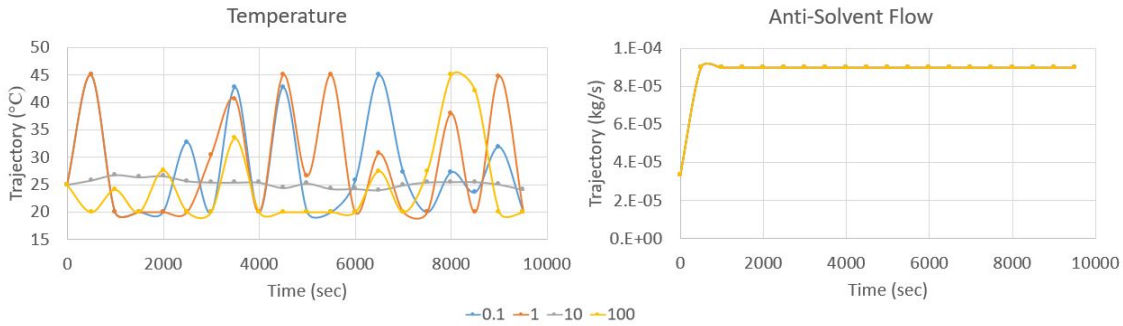

Figure 7.32: MVs trajectories

7.3.3 Volume Mean Size

Volume Mean Size reference envelope violations were given the values of 0.1, 1, 10, 100 and 1000, for a positive 10% step disturbance on impeller frequency. The optimal and measured trajectories for all this tests showed the same behaviour described previously and are displayed in figure 7.33.

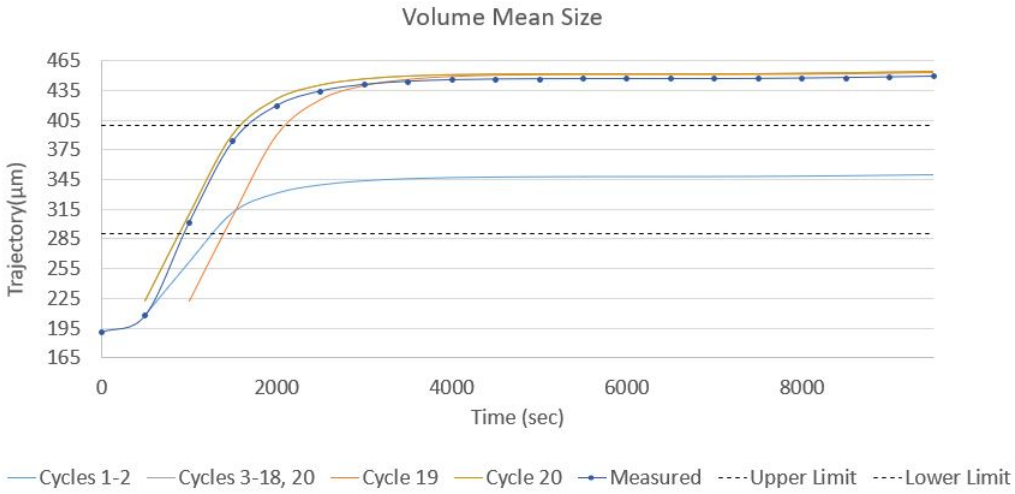

Figure 7.33: Volume Mean Size's Optimal and Measured Trajectory

For this CV, the controller is not able to steer to the reference envelope, when the disturbance is performed (that is why for the first two cycles, the CV is able to be steered into its limits). Nonetheless, the CVs' measured values are very close to its optimal trajectory, meaning there is little mismatch between the predicted behaviour and the actual one, for this variable.

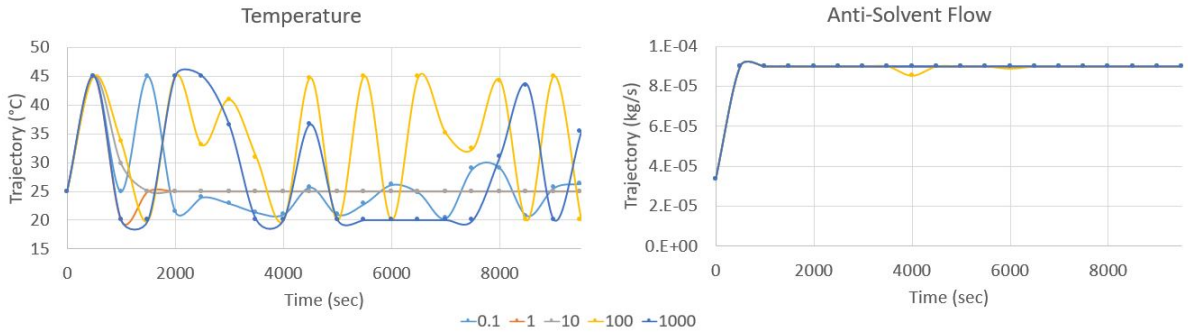

Figure 7.34: MVs trajectories

As it was observed for Span, higher penalties seem to generally lead to higher MV oscillation (figure 7.34). For this case, it also seems that too low of a violation also leads to some oscillation. Similarly to the already discussed cases, anti-solvent flow settles at its upper bound.

7.3.4 Dissolved Paracetamol

The same procedure was performed for dissolved paracetamol, whose penalties were given the values of 1, 10, 100 and 1000. The CVs trajectories are shown in figure 7.35. For this variable, the differences between cycles are barely noticeable after 4000 seconds. For all cases, this CV is able to return to its reference envelopes.

For this case, the MVs exhibit the same pattern (figure 7.36) as the rest of the MVs, previously shown.

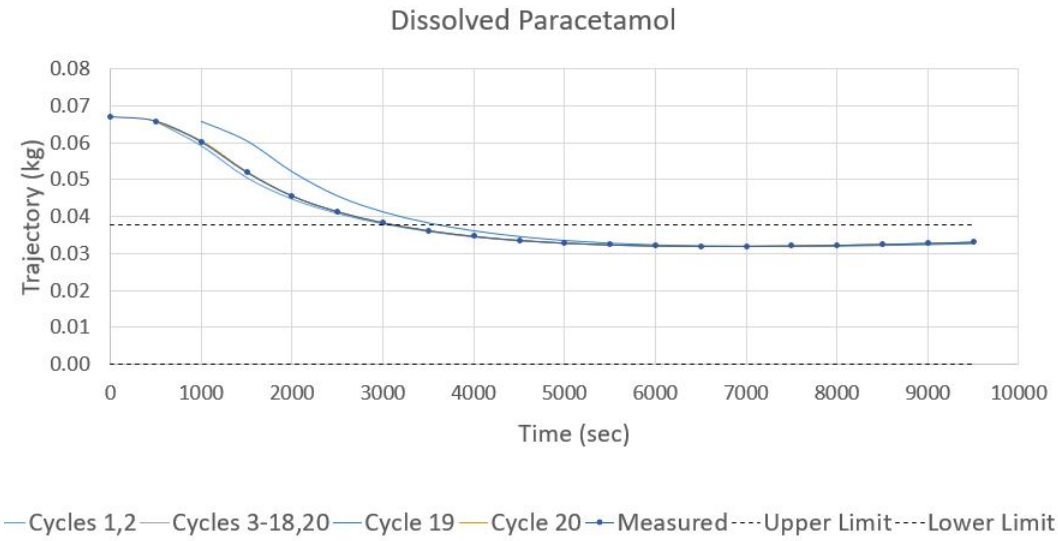

Figure 7.35: Dissolved Paracetamol Optimal and Measured Trajectory

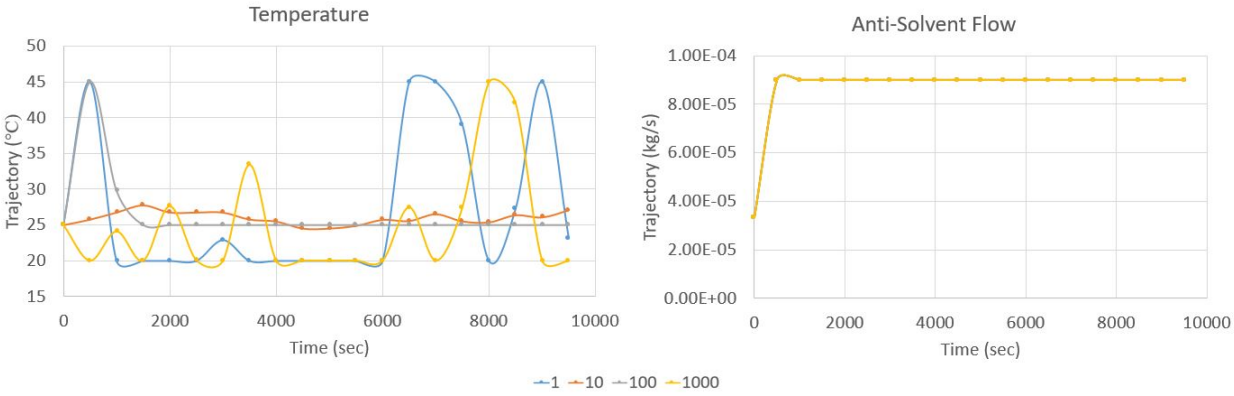

Figure 7.36: MVs trajectories

7.3.5 Reference Trajectory Penalty Change Remarks

Changing the penalties of each of the reference trajectory does not seem to influence the CVs measurements, which is odd as one of the MVs, temperature, is quite oscillating. Given that the other MV, anti-solvent flow shows the same trajectory for all simulations, an hypothesis regarding the difference in influence of these two MVs grows in relevance. Anti-Solvent Flow shows a much more significant impact on the CVs, than temperature. Hence, the CVs only change when MV anti-solvent flow changes. Temperature may be oscillating because the controller is trying to strongly find a solution (between its allowed limits of 20 to 45 °C) that changes the CVs trajectories, because regarding anti-solvent flow, it has already found the optimal solution. Some scenarios were conducted to test this hypothesis, which will be explained in the following section.

7.4 Temperature

The temperature oscillation was further investigated, as to understand why the controller outputted such an unstable action. As such, step tests were made to each of the MVs individually, to see how the system responded. For these cases only term A of the objective function 5.2 was active, without

considering any additional penalties.

With only MV Anti-Solvent Flow turned on, step tests of ± 5,10 and 15% on temperature's initial value of 25 °C were performed. The measured values for all CVs are depicted in the following figure 7.37.

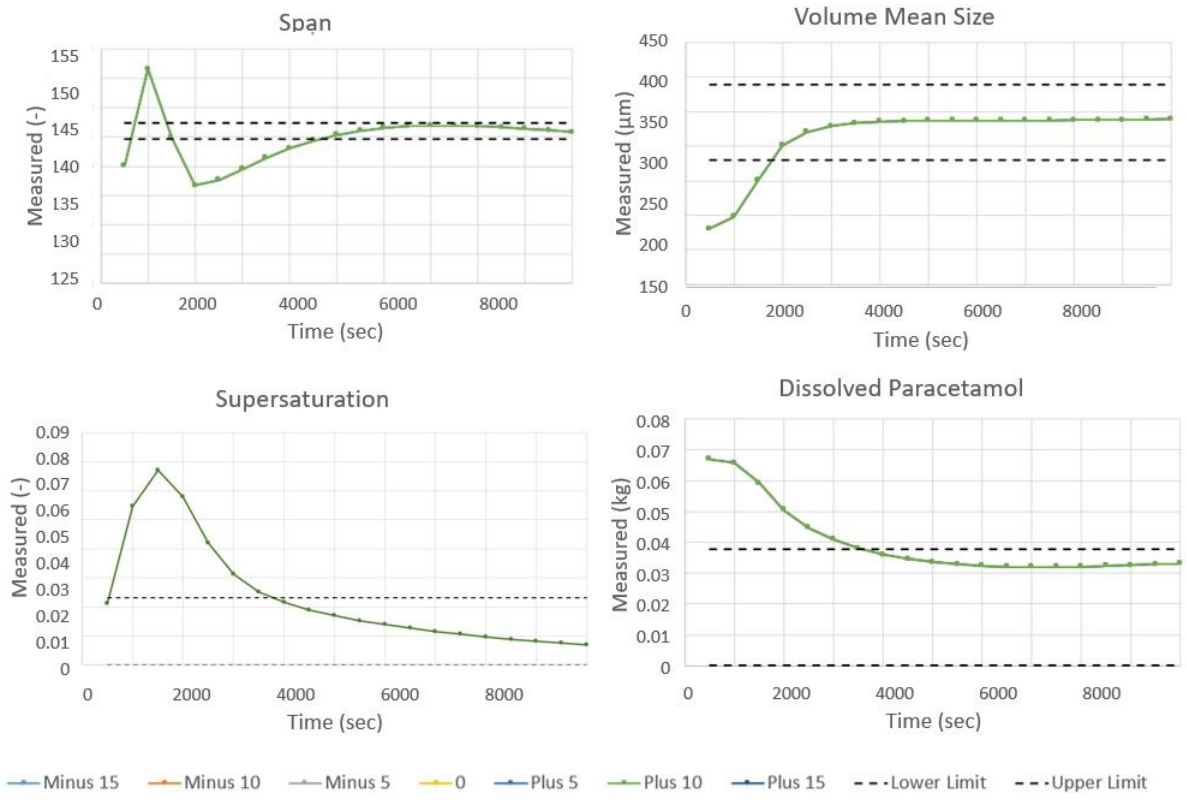

Figure 7.37: CVs measured values

As it is possible to observe, there is no difference in CVs measured values - they all follow perfectly their optimal trajectory. For all cases, the only active MV, anti-solvent flow is held at its upper bound, 9E-05 kg/s. One possible reason for this behaviour may be the fact that the magnitude steps tests may not have been large enough for the CVs to show any differences.

7.5 Anti-Solvent Flow

The same test was performed but now for the other MV, Anti-Solvent Flow, to check whether this MV yielded the same results.

In this case, a different behaviour is observed, confirming the impact this MV has on the CVs. As it is also possible to see in figure 7.38, the changes done were not enough to make the CV display a behaviour hard to control - in all cases, they return to their reference envelopes. Another interesting result to take note is how the more negative the disturbance is, the more delayed the CVs are - the longer they take to reach their reference envelopes. This result holds true for all CVs. Physically, this result is expected as increasing the Anti-Solvent addition speeds up the crystallization reaction.

These results seem to confirm the higher dependence on MV Anti-Solvent Flow, when compared to temperature. A closer look to the model revealed that this MV was not explicitly defined in the kinetics expression rate - it was taken into account indirectly through supersaturation. From the paracetamol solubility curve (figure 4.4 in chapter 4), it is possible to observe the supersaturation's dependence on temperature. In the current model, paracetamol is dissolved in water and methanol. For paracetamol

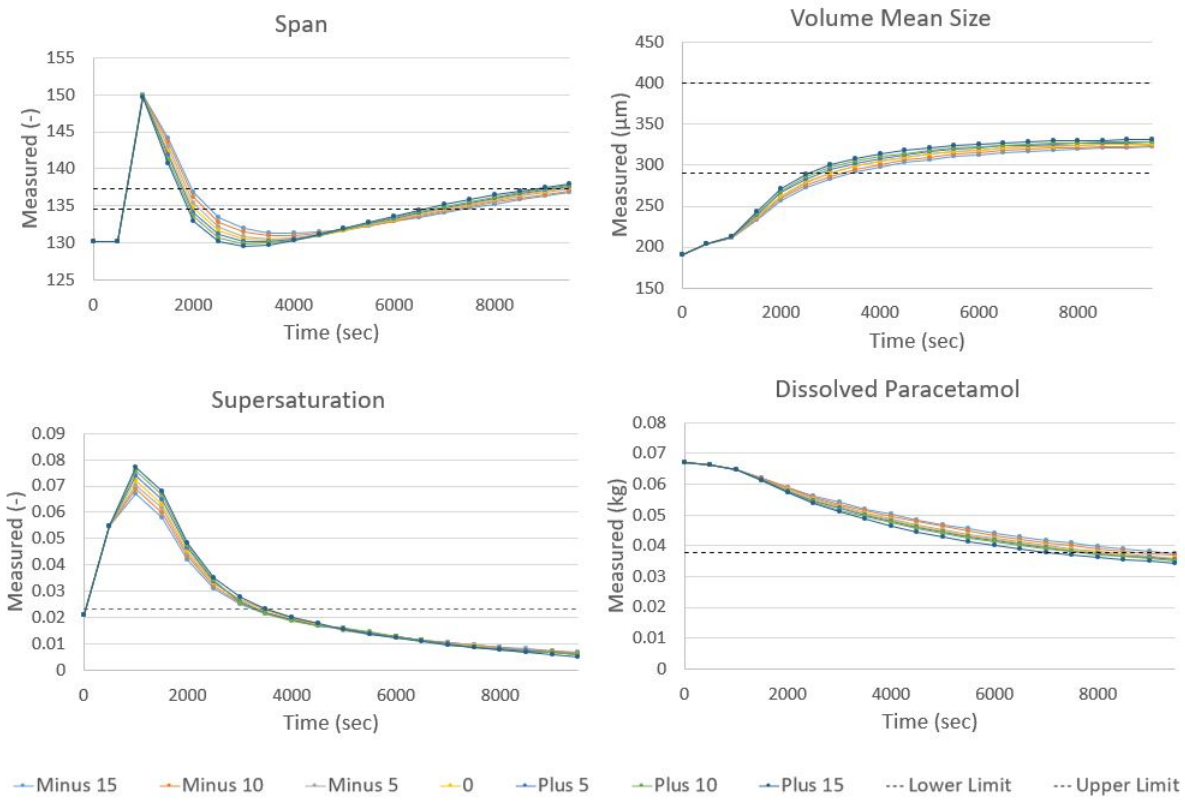

Figure 7.38: CVs measured values

dissolved in water, the solubility barely changes with temperature, whereas for paracetamol dissolved in methanol it shows some variation. It is hypothesised that for the ternary mixture in the current model, the temperature change was not significant enough to impact the solubility change. A 15% temperature change (from 25 °C to 28.75) may not have been noticeable given it was too small in scale. This inhibited the CVs of being affect by temperature changes, rendering its manipulation meaningless and leaving the burden to Anti-Solvent Flow.

Chapter 8

Conclusions and Future Work

8.1 Conclusions

The main goal of this thesis of implementing a Nonlinear Model Predictive Control application on a batch crystallization of paracetamol model was successfully achieved. The first two chapters give a theoretical background on the concept behind NMPC, and what parameters should be taken into consideration, when designing a controller of such type. Chapter 2 also gives an overview of the typical control strategies used in crystallization processes, including their advantages and disadvantages. The third chapter provides an outline on gNLMPC, the digital application platform used to configure and test the controller. In chapter 4, a description of the model is shown, including the main occurring mechanisms, such as nucleation, growth, dissolution and agglomeration. It also includes the layout of the control scheme, covering which variables are controlled, manipulated and disturbance. The chosen Manipulated Variables were anti-solvent flow and temperature as they regulate supersaturation, which is the main driving force for crystallization. Additionally, supersaturation was chosen as a Controlled Variables. Other Controlled Variables included span, volume mean size and dissolved paracetamol. The first two characterize the particle size distribution, regarding particle's dispersity size and their growth and the last one concerns the liquid mass of paracetamol in the crystallizer.

Chapter 5 provides a detailed look on the formulation of the optimisation problem, more specifically how the objective function was constructed. It shows that the objective function was written in a penalty-based way, given that penalties are added whenever the Controlled Variables are outside their target limits. This not only ensures that the controller always finds a solution, but it also allows the controller to prioritize some CVs over others. The result of such optimisation is the perfect control action that satisfies the control objectives, implemented by a set of Manipulated Variables' inputs. Furthermore, this chapter shows how different penalties were added under an optimal control scenario (without plant / model mismatch) and it was demonstrated that the CVs response did not change when their trajectory penalties were changed. This confirms the penalty-based nature of the controller, as it will always show the optimal solution regardless of the penalties.

Chapter 6 provides a definition of the emulation mode, more specifically the steps behind this real-time implementation of the controller on the model. This chapter also comprises the two main steps needed to implement the controller: the configuration of its parameters and further testing. It describes how the configuration consisted in studying the different controller parameters, such as the cycle duration and number of control intervals. Regarding the testing, it explains the main scenarios the controller was subjected to analyse its stability and robustness.

Chapter 7 delivers the main results from this thesis, obtained both from the study of the configuration

parameters and also from the scenarios tested, on emulation mode. From the configuration parameters, the impact of the duration of a cycle on the controller's response shows the importance of the choice of this parameter. It demonstrates that the cycle duration should be as short as possible for the controller not to miss the system's dynamics. Furthermore, it shows how longer cycles cause a delay on the implementation of the optimal values for the MVs. This impacts negatively the CVs as the system spends more time without the control action that will lead to its control objectives. Another impactful parameter on the controller is the optimisation horizon. It is observed that longer optimisation horizons lead to an overall better performance of the controller, as it was able to lead the CVs into the desired interval of values, whereas shorter ones were not.

The results from the different scenarios tested show the controller's ability to perform disturbance rejection, more specifically, it demonstrates how the controller is able to steer the CVs into their target limits, for most cases, for different step changes done on Disturbance Variable impeller frequency. The chosen parameters for the controller tuning also allowed to shorten the batch cycles, which is an attrractive feature. The disturbance rejection scenario also shows that the controller was able to successfully predict its CVs' trajectory, as their optimal trajectories matched their measured values. Considering that both MVs showed too fast setpoint changes (which would not be feasible in reality, increasing the plant/model mismatch), a rate of change penalty during and in between cycles was added. The results show the successful implementation of such penalty in both cases, that allows the MVs to move less abruptly, while still complying with the control objectives.

The results of the tests also show the controller's ability to handle noise, as it was able to comply with the control objectives in spite of one of the CVs, Span, had been added with measurement noise. The results for a plant / model mismatch scenario were also depicted, where one of the kinetic parameters, supersaturation order, was changed. It is demonstrated that despite having an impact on the Controlled Variable, the controller is able to steer them into the desired limits, thus confirming the controller's satisfactory performance.

In conclusion, the real-time implementation of a Nonlinear Model Predictive Control on a paracetamol batch crystallization process was possible. The controller showed good performance, yielding satisfactory results, under different scenarios. Not only was the controller able to comply with the laid out control objectives, but it also did so faster than in open loop, thus, showing its time saving capabilities. The results show the possibility of the application of such a control strategy on other crystallization models.

8.2 Future work

The results given in this work were obtained either via simulation, either via emulation (real time implementation on a simulation model). Thus, in order to truly confirm the benefits portrayed by the results shown, an application on a real model, with industrial data should be performed.

This thesis could be used as a first study of how a Nonlinear Model Predictive Control application using gNLMPC should be carried out, and how the models should be constructed. In a next step, the controller should be able to be tested against more realistic scenarios, using real plant noise and data. Furthermore, state estimation capabilities could be added, to provide the controller with the right tools to handle scenarios where measurements are not attainable at all cycles. Concerning the process itself, this thesis conveys the importance of constructing models specifically to be used for control. Models should not be built in a rigid manner, in order to provide variables with enough flexibility to impact the Controlled Variables. For example, temperature should be taken into account directly in the kinetic expressions, and not indirectly, as a function of supersaturation, otherwise the controller will tend to

provide oscillating setpoints as the change done in the CVs is not impact-full enough. This flexibility issue is also important to avoid controller's degeneracy, as it may try to move preferentially one the MVs as opposed to the other due solely to size differences. Controller's degeneracy may also be avoided by carefully choosing the correct limits for both CVs and MVs, hence, this should be taken into account as well. Furthermore, the models should be constructed with only the essential mechanisms taking place in a plant in order not to burden the controller with additional calculations, meaningless for the control objectives.

The chosen model is a batch process, which usually is not controlled with NMPC. As observed in this thesis, using such control strategy can lead into time savings, as the controller achieved faster results, than in open-loop mode. This feature could be further explored, given that saving time is an important parameter in industry.

Finally, having faster optimisation algorithms, able to provide values for the MVs in real-time is the main area where there is room for improvement, when it comes to Nonlinear Model Predictive Control, as it is the major cause for the lack of implementation in industry.

Bibliography

[1] D. A. M. Dale E. Seborg, Thomas F. Edgar, "Process dynamics and control, 2nd edition," *AIChE Journal*, vol. 54, 11 2008.

[2] S. J. Qin and T. A. Badgwell, "An overview of nonlinear model predictive control applications," in *Nonlinear Model Predictive Control* (F. Allgöwer and A. Zheng, eds.), (Basel), pp. 369–392, Birkhäuser Basel, 2000.

[3] F. Allgöwer, T. Badgwell, J. Qin, J. B. Rawlings, and S. J. Wright, *Nonlinear Predictive Control and Moving Horizon Estimation – An Introductory Overview*, pp. 391–449. 01 1999.

[4] M. Darby, M. Harmse, and M. Nikolaou, "Mpc: Current practice and challenges," *Control Engineering Practice*, vol. 20, 04 2012.

[5] T. A. Johansen, "Chapter 1 introduction to nonlinear model predictive control and moving horizon estimation," 2011.

[6] P. Kühl, M. Diehl, A. Milewska, E. Molga, and H. Bock, *Robust NMPC for a Benchmark Fed-Batch Reactor with Runaway Conditions*, vol. 358, pp. 455–464. Springer, 08 2007.

[7] K. Naidoo, J. Guiver, P. Turner, M. Keenan, and M. Harmse, *Experiences with Nonlinear MPC in Polymer Manufacturing*, vol. 358, pp. 383–398. Springer, 09 2007.

[8] R. Bindlish, "Nonlinear model predictive control of an industrial polymerization process," *Computers & Chemical Engineering*, vol. 73, pp. 43–48, 2015.

[9] S. Skålén, F. Josefsson, and J. Ihrström, "Nonlinear mpc for grade transitions in an industrial ldpe tubular reactor," *IFAC-PapersOnLine*, vol. 49, pp. 562–567, 12 2016.

[10] B. Foss and T. Schei, *Putting Nonlinear Model Predictive Control into Use*, vol. 358, pp. 407–417. 08 2007.

[11] J. Bausa, "Model based operation of polymer processes – what has to be done?," *Macromolecular Symposia*, vol. 259, no. 1, pp. 42–52, 2007.

[12] J. Rossiter, *Model-based Predictive Control-a Practical Approach*. CRC Press, 01 2003.

[13] R. Findeisen, L. Imsland, F. Allgower, and B. A. Foss, "State and output feedback nonlinear model predictive control: An overview," *European Journal of Control*, vol. 9, no. 2, pp. 190 – 206, 2003.

[14] O. Mikuláš, "A framework for nonlinear model predictive control," Master's thesis, The school of the thesis, The address of the publisher, 7 1993. An optional note.

[15] F. Allgöwer, R. Findeisen, and Z. Nagy, "Nonlinear model predictive control: From theory to application," *J. Chin. Inst. Chem. Engrs*, vol. 35, pp. 299–315, 05 2004.

[16] S. Rohani, M. Haeri, and H. Wood, “Modeling and control of a continuous crystallization process part 2. model predictive control,” *Computers & Chemical Engineering*, vol. 23, no. 3, pp. 279 – 286, 1999.

[17] M. W. Hermanto, “Modelling, simulation, and control of polymorphic crystallization,” 2009.

[18] B. Bequette, “Non-linear model predictive control: A personal retrospective,” *The Canadian Journal of Chemical Engineering*, vol. 85, pp. 408 – 415, 08 2007.

[19] R. Findeisen and F. Allgöwer, “An introduction to nonlinear model predictive control,” 01 2002.

[20] K. Naidoo, J. Guiver, P. Turner, M. Keenan, and M. Harmse, *Experiences with Nonlinear MPC in Polymer Manufacturing*, pp. 383–398. Berlin, Heidelberg: Springer Berlin Heidelberg, 2007.

[21] B. Foss and T. Schei, *Putting Nonlinear Model Predictive Control into Use*, vol. 358, pp. 407–417. 08 2007.

[22] R. D. Bartusiak and R. W. Fontaine, “Feedback method for controlling non-linear processes,” Oct 1997.

[23] M. W. Hermanto, M.-S. Chiu, and R. D. Braatz, “Nonlinear model predictive control for the polymorphic transformation of l-glutamic acid crystals,” *AIChE Journal*, vol. 55, no. 10, pp. 2631–2645, 2009.

[24] C. Damour, M. Benne, L. Boillereaux, B. Grondin-Perez, and J.-P. Chabriat, “Nmpc of an industrial crystallization process using model-based observers,” *Journal of Industrial and Engineering Chemistry - J IND ENG CHEM*, vol. 16, pp. 708–716, 09 2010.

[25] L. A. P. Suárez, P. Georgieva, and S. F. de Azevedo, “Nonlinear mpc for fed-batch multiple stages sugar crystallization,” *Chemical Engineering Research and Design*, vol. 89, no. 6, pp. 753 – 767, 2011.

[26] D. Sarabia, C. Prada, S. P. Cristea, R. Mazaeda, and W. Colmenares, *Hybrid NMPC control of a sugar house*, vol. 358, pp. 495–502. 09 2007.

[27] Y. Cao, J. Kang, Z. K. Nagy, and C. D. Laird, “Parallel solution of robust nonlinear model predictive control problems in batch crystallization,” *Processes*, vol. 4, p. 20, 06 2016.

[28] R. D. Braatz, “Advanced control of crystallization processes,” *Annual Reviews in Control*, vol. 26, no. 1, pp. 87 – 99, 2002.

[29] A. Mesbah, Z. K. Nagy, A. E. M. Huesman, H. J. M. Kramer, and P. M. J. Van den Hof, “Nonlinear model-based control of a semi-industrial batch crystallizer using a population balance modeling framework,” *IEEE Transactions on Control Systems Technology*, vol. 20, pp. 1188–1201, Sep. 2012.

[30] N. C. S. Kee, R. B. H. Tan, and R. D. Braatz, “Selective crystallization of the metastable α-form of l-glutamic acid using concentration feedback control,” *Crystal Growth & Design*, vol. 9, no. 7, pp. 3044–3051, 2009.

[31] M. Giulietti, M. Seckler, S. Derenzo, M. RÃ©, and E. Cekinski, “INDUSTRIAL CRYSTALLIZATION AND PRECIPITATION FROM SOLUTIONS: STATE OF THE TECHNIQUE,” *Brazilian Journal of Chemical Engineering*, vol. 18, pp. 423 – 440, 12 2001.

[32] N. A. Mitchell, “Numerical modelling of cooling crystallisation: process kinetics to optimisation,” 2012.

[33] A. D. RANDOLPH and M. A. LARSON, “Chapter 6 - crystallization kinetics,” in *Theory of Particulate Processes* (A. D. RANDOLPH and M. A. LARSON, eds.), pp. 101 – 110, Academic Press, 1971.

[34] W. Beckmann, *Crystallization: Basic Concepts and Industrial Applications*, pp. 173–185. 02 2013.

[35] Z. K. Nagy and R. D. Braatz, “Advances and new directions in crystallization control,” *Annual Review of Chemical and Biomolecular Engineering*, vol. 3, no. 1, pp. 55–75, 2012. PMID: 22468599.

[36] Y. Yang and Z. K. Nagy, “Advanced control approaches for combined cooling/antisolvent crystallization in continuous mixed suspension mixed product removal cascade crystallizers,” *Chemical Engineering Science*, vol. 127, p. 362–373, 05 2015.

[37] M. Kitamura, “Strategy for control of crystallization of polymorphs,” *Crystengcomm*, vol. 11, 05 2009.

[38] Baliga and J. Bantwal, “Crystal nucleation and growth kinetics in batch evaporative crystallization,” 06 2019.

[39] C. Lindenberg, M. Krattli, J. Cornel, and M. Mazzotti, “Design and optimization of a combined cooling/antisolvent crystallization process,” *Crystal Growth & Design - CRYST GROWTH DES*, vol. 9, 12 2008.

[40] C. T. Ó’Ciardhá, N. A. Mitchell, K. W. Hutton, and P. J. Frawley, “Determination of the crystal growth rate of paracetamol as a function of solvent composition,” *Industrial & Engineering Chemistry Research*, vol. 51, no. 12, pp. 4731–4740, 2012.

[41] K. Choong and R. Smith, “Novel strategies for optimization of batch, semi-batch and heating/cooling evaporative crystallization,” *Chemical Engineering Science*, vol. 59, no. 2, pp. 329 – 343, 2004.

[42] C. Ruiqing, Q.-d. Cheng, J. J. Chen, D.-S. Sun, L.-b. Ao, D.-W. Li, Q.-Q. Lu, and D.-C. Yin, “An investigation of the effects of varying ph on protein crystallization screening,” *CrystEngComm*, vol. 19, 01 2017.

[43] J. W. Mullin, “Crystallisation, 4th edition by j. w. mullin. 2001. butterworth heinemann: Oxford, uk. 600 pp. isbn 075-064-833-3.,” *Organic Process Research & Development*, vol. 6, no. 2, pp. 201–202, 2002.

[44] T. Vetter, C. Burcham, and M. F. Doherty, “Regions of attainable particle sizes in continuous and batch crystallization processes,” *Chemical Engineering Science*, vol. 106, p. 167–180, 03 2014.

[45] D. Bruce Patience, “Crystal engineering through particle size and shape monitoring, modeling, and control,” 06 2019.

[46] A. Mesbah, J. Landlust, A. Huesman, H. Kramer, P. Jansens, and P. V. den Hof, “A model-based control framework for industrial batch crystallization processes,” *Chemical Engineering Research and Design*, vol. 88, no. 9, pp. 1223 – 1233, 2010. Special Issue – 17th International Symposium on Industrial Crystallization.

[47] A. Chianese, *Characterization of Crystal Size Distribution*, ch. 1, pp. 1–6. John Wiley & Sons, Ltd, 2012.

[48] Y. Yang and Z. K. Nagy, “Application of nonlinear model predictive control in continuous crystallization systems,” *Proceedings of the American Control Conference*, vol. 2015, 07 2015.

[49] A. Mesbah, A. Ford Versypt, X. Zhu, and R. Braatz, "Nonlinear model-based control of thin-film drying for continuous pharmaceutical manufacturing," *Industrial & Engineering Chemistry Research*, vol. 53, p. 7447–7460, 12 2013.

[50] T.-T. C Lai, J. Cornevin, S. Ferguson, N. Li, B. L Trout, and A. Myerson, "Control of polymorphism in continuous crystallization via msmpr cascade design," *Crystal Growth & Design*, vol. 15, p. 150527151920003, 05 2015.

[51] J. Kwon, M. Nayhouse, G. Orkoulas, D. Ni, and P. Christofides, "A method for handling batch-to-batch parametric drift using moving horizon estimation: Application to run-to-run mpc of batch crystallization," *Chemical Engineering Science*, vol. 127, 05 2015.

[52] Z. K. Nagy, "Model based robust control approach for batch crystallization product design," *Computers & Chemical Engineering*, vol. 33, pp. 1685–1691, 10 2009.

[53] J.-P. Corriou and S. Rohani, "A new look at optimal control of a batch crystallizer," *AIChE Journal*, vol. 54, pp. 3188 – 3206, 12 2008.

[54] C. Damour, M. Benne, L. Boillereaux, B. Grondin-Perez, and J.-P. Chabriat, "Nmpc of an industrial crystallization process using model-based observers," *Journal of Industrial and Engineering Chemistry - J IND ENG CHEM*, vol. 16, pp. 708–716, 09 2010.

[55] A. Y.-D. Tsen, S. S. Jang, D. S. H. Wong, and B. Joseph, "Predictive control of quality in batch polymerization using hybrid ann models," *AIChE Journal*, vol. 42, no. 2, pp. 455–465, 1996.

[56] H. Jang, J. H. Lee, and L. Biegler, "A robust nmpc scheme for semi-batch polymerization reactors," *IFAC-PapersOnLine*, vol. 49, no. 7, pp. 37 – 42, 2016. 11th IFAC Symposium on Dynamics and Control of Process SystemsIncluding Biosystems DYCOPS-CAB 2016.

[57] J. Zhang, A. Morris, E. Martin, and C. Kiparissides, "Prediction of polymer quality in batch polymerisation reactors using robust neural networks," *Chemical Engineering Journal*, vol. 69, no. 2, pp. 135 – 143, 1998.

[58] `https://www.psenterprise.com/products/gproms`. [Online; accessed 19-May-2019].

[59] C. T. Ó'Ciardhá, K. W. Hutton, N. A. Mitchell, and P. J. Frawley, "Simultaneous parameter estimation and optimization of a seeded antisolvent crystallization," *Crystal Growth & Design*, vol. 12, no. 11, pp. 5247–5261, 2012.

[60] R. A. Granberg and A. C. Rasmuson, "Solubility of paracetamol in pure solvents," *Journal of Chemical & Engineering Data*, vol. 44, no. 6, pp. 1391–1395, 1999.

[61] R. E. Young, R. Donald Bartusiak, and R. W. Fontaine, "Evolution of an industrial nonlinear model predictive controller," *Proc. of Chem Process Control VI*, vol. 6, 01 2002.

[62] J. K. Gruber, C. Bordons, R. Bars, and R. Haber, "Nonlinear predictive control of smooth nonlinear systems based on volterra models. application to a pilot plant," *International Journal of Robust and Nonlinear Control*, vol. 20, no. 16, pp. 1817–1835, 2010.

[63] C. Rajhans, S. C. Patwardhan, and H. Pillai, "Discrete time formulation of quasi infinite horizon nonlinear model predictive control scheme with guaranteed stability," *IFAC-PapersOnLine*, vol. 50, no. 1, pp. 7181 – 7186, 2017. 20th IFAC World Congress.